Stony Brook University

Mechanism of YopJ-Induced Cell Death and Capase-1 Activation in Macrophages Infected with *Yersinia*

A Dissertation Presented

by

Ying Zheng

to

The Graduate School

in Partial Fulfillment of the

Requirements

for the Degree of

Doctor of Philosophy

in

Molecular Genetics and Microbiology

Stony Brook University

December 2011

Stony Brook University

The Graduate School

Ying Zheng

We, the dissertation committee for the above candidate for the

Doctor of Philosophy degree, hereby recommend

acceptance of this dissertation.

James B. Bliska – Dissertation Advisor
Professor, Molecular Genetics and Microbiology

Adrianus van der Velden – Chairperson of the Defense
Assistant Professor, Molecular Genetics and Microbiology

Martha B. Furie
Professor, Department of Pathology

Wei-Xing Zong
Associate Professor, Molecular Genetics and Microbiology

Yuri Lazebnik
Professor, Cold Spring Harbor Laboratory

This dissertation is accepted by the Graduate School

Lawrence Martin
Dean of the Graduate School

Abstract of the Dissertation

Mechanism of YopJ-Induced Cell Death and Capase-1 Activation in Macrophages Infected with *Yersinia*

by

Ying Zheng

Doctor of Philosophy

in

Molecular Genetics and Microbiology

Stony Brook University

2011

Pathogenic *Yersinia* species encode a Type III Secretion System (T3SS) that translocates a group of effectors termed as *Yersinia* outer proteins (Yops) into target cells to disrupt eukaryotic host signaling pathways. YopJ is an acetyltransferase, which prevents MAP Kinase Kinase (MKK) and IκB Kinase β (IKKβ) phosphorylation and activation and causes Toll like receptor 4 (TLR4)-directed apoptosis in macrophages. YopJ isoforms encoded by different *Yersinia* strains exhibit a range of cytotoxic activities. In previous work, a YopJ isoform in *Y. pestis* strain KIM5 ($YopJ^{KIM}$) was shown to cause enhanced cytotoxicity, caspase-1 activation and interleukin-1β (IL-1β) release in infected macrophages. In my study, the molecular basis for elevated activity of $YopJ^{KIM}$ was determined. In addition, the mechanism of cell death and caspase-1 activation in KIM5-infected macrophages was examined. Finally, I investigated the role of caspase-1 in a protective host response to *Yersinia* strains with normal or enhanced cytotoxicity in mice.

I determined using site directed mutagenesis that two amino acid substitutions, F177L and K206E, in YopJ^{KIM} are important for enhanced apoptosis, caspase-1 activation, and IL-1β release in *Yersinia*-infected macrophages. Despite secretion and translocation levels that were similar to other YopJ isoforms (e.g. YopJ^{CO92} (F177, K206) or YopJ^{YPTB} (F177)), YopJ^{KIM} displayed an up-regulated capacity to inhibit phosphorylation of NF-κB inhibitor α (IκBα) and a moderately raised ability to inhibit phosphorylation of mitogen-activated protein kinase (MAPK). YopJ^{KIM} also had enhanced binding to substrate IKKβ as compared to YopJ^{CO92} by pull down assay.

Previous work had established a role for IKKβ in the negative regulation of caspase-1 activation in LPS-stimulated macrophages. I demonstrated that IKKβ negatively regulates caspase-1 activation in response to a live pathogen by infection of *Ikkβ*$^{\Delta}$ or wild type macrophages with KIM5. Significantly increased caspase-1 activation was identified in *Ikkβ*$^{\Delta}$ cells, as compared to wild type macrophages by FLICA staining. A small molecule IKKβ inhibitor, TPCA-1, was adopted to mimic YopJ function. Following TLR4 activation with LPS, cell death and IL-1β release occurred in macrophages treated with TPCA-1, highlighting the importance of IKKβ in negative regulation of caspase-1.

In my studies of the mechanism of cell death in KIM5-infected macrophages, low caspase-3/-7 activity was detected by luminol assay and Poly (ADP-ribose) polymerase (PARP) cleavage. Cytotoxicity and IL-1β release were not reduced by caspase-8 inhibitor treatment or the use of *bax/bak* double knockout (DKO) macrophage infection, indicating that cell death and caspase-1 activation were independent of canonical apoptosis pathways. Alternatively, assays for High mobility group box 1 (HMGB1) release and annexin V/ propidium iodide (PI) staining suggested necrotic macrophage death during KIM5 infection. Staining for active Caspase-1/PI

uptake was performed and results showed that caspase-1 activation was associated with macrophages undergoing cell death, suggesting that caspase-1 activation may be related to necrosis. Inhibitor studies showed that reactive oxygen species (ROS) and receptor interacting protein 1 (RIP1) were not required for cytotoxicity and IL-1β production. On the other hand, cathepsin B inhibitors significantly reduced IL-1β release and caspase-1 activation, implicating cathepsin B leakage from ruptured lysosomes in caspase-1 activation. Cytotoxicity was not reduced by cathepsin B inhibitors, confirming that caspase-1 is not required for cell death in KIM5-infected macrophages.

Finally, different YopJ isoforms were ectopically expressed in *Y. pseudotuberculosis* and YopP was determined to have the highest capacity to cause cytotoxicity and activate caspase-1 in infected macrophages. *Y. pseudotuberculosis* strains ectopically expressing $YopJ^{YPTB}$ or YopP were used to infect wild type or caspase-1 deficient mice to study the protective role of caspase-1. Results show that caspase-1 is dispensable for the protective innate immune response against *Yersinia* with normal ($YopJ^{YPTB}$) or enhanced (YopP) cytotoxicity.

In summary, my results demonstrate that enhanced cytotoxicity and caspase-1 activation in KIM5-infected macrophages result from two amino acid replacements in YopJ, which intensifies its ability to inhibit nuclear factor κB (NF-κB) and mitogen-activated protein kinase (MAPK) signaling pathways. The enhanced necrotic cell death is apparently sensed by the inflammasome leading to caspase-1 activation and IL-1β release in macrophages. However, caspase-1 is not required for a protective innate immune response to *Yersinia* with normal or enhanced cytotoxicity in mice.

Table of Contents

List of Figures

List of Tables

List of Abbreviations

APC	Antigen Presenting Cell
ASC	Apoptotic Speck–Containing Protein
Bcl-2	B-Cell Lymphoma 2
BAK	Bcl-2 Homologous Antagonist/Killer
BAX	Bcl-2–Associated X Protein
BMDM	Bone Marrow Derived Macrophage
CARD	Caspase Recruitment Domain
CGD	Chronic Granulomatous Disease
COP	CARD-Only Protein
DC	Dendritic Cell
DD	Death Domain
DED	Death Effector Domain
DKO	Double Knockout
DAMP	Danger-Associated Molecular Pattern
FADD	Fas-Associated Protein with Death Domain
FMF	Familial Mediterranean Fever
GAPDH	Glyceraldehyde 3-Phosphate Dehydrogenase
HI Broth	Heart Infusion Broth
HMGB1	High Mobility Group Box 1

IAP	Inhibitor of Apoptosis Protein
ICAD	Inhibitor of Caspase-Activated DNase
ICE	IL-1-Converting Enzyme
IFN	Interferon
IκBα	Inhibitor of NF-κB α
IKKβ	IκB Kinase β
IL	Interleukin
LDH	Lactate Dehydrogenase
LT	Lethal Toxin
Mal	MyD88-Adapter-Like
MAPK	Mitogen-Activated Protein Kinase
MDP	Muramyl Dipeptide
MHC	Major Histocompatibility Complex
MKK	MAP Kinase Kinase
MOI	Multiplicity of Infection
Mtb	*Mycobacterium tuberculosis*
NF-κB	Nuclear Factor κB
NLR	Nod-Like Receptor
OD	Optical Density
PAI-2	Plasminogen Activator Inhibitor 2
PAMP	Pathogen-Associated Molecular Pattern
PARP	Poly (ADP-Ribose) Polymerase
PI	Propidium Iodide

POP	Pyrin-Only Protein
RAGE	Advanced Glycation End Products
RIP	Receptor Interacting Protein
ROS	Reactive Oxygen Species
SLO	*Streptococcus pyrogenes* Streptolysin O
SREBP	Sterol regulatory Element Binding Protein
STAT	Signal Transducers and Activators of Transcription
T3SS	Type III Secretion System
TCA	Trichloroacetic Acid
TGF-β	Transforming Growth Factor-β
TIM	Triose-Phosphate Isomerase
TLR	Toll Like Receptor
TNF-α	Tumor Necrotic Factor-α
TXNIP	Thioredoxin-Interacting Protein
Yop	*Yersinia* Outer Protein

Acknowledgements

I would like to thank Bliska lab members who set up an excellent environment to work with and have been very supportive in the whole journey of my Ph.D. study. I thank Professor Jim Bliska, my advisor, from bottom of my heart, for his patience, support and advice. In addition, his enthusiasm, loyalty and honesty on research touch my soul and show me that being a good scientist does not only mean to research, but also to possess good virtues. I thank Yue Zhang, who always gives helpful suggestions for my lab work, papers and personal life. I acknowledge Sarit Lilo, who supervised me during my rotation, and later became by good friend, sharing a lot of experimental results and ideas with me; and Hana Fukuto for revising my papers and dissertation. I want to thank Galina Romanov for preparing macrophages and Maya Ivanov for maintaining the lab.

I want to thank my committee members, Martha Furie, Wei-Xing Zong, Ando van der Velden and Yuri Lazebnik for inspiring comments and very helpful suggestions in my progress meetings.

I would like to express my gratitude to Igor Brodsky for testing my samples and troubleshooting my experiments; and Patricio Mena for maintaining mouse colonies and handling infections. I am grateful to Kate Bell and Janet Hearing for helping me settled in the department, arranging my course work and seminars and quick responses to my urgent inquiries.

I made a lot of friends in this department sharing the sweet and the bitter with me during my graduate study, Will, Kai, Qinyuan, Huaixin, Amy, Cindy, Annie, Kenny, Indra, Joe and Vinaya, who have made my time at Stony Brook most enjoyable.

I'd like to thank my dear husband, Meilong Jiang for years of encouragement and support. He puts more house work and pressures on himself and never lets me worry. I really appreciate

that for years, he commutes hours at each weekend to reunion and is always ready to help me and listen to my complain 24/7. He builds a happy life for me.

Last but not least, I would like to deeply thank my parents, who have been giving me greatest support, encouragement and endless love.

Chapter 1: Introduction

1.1 *Yersinia* pathogenesis

1.1.1 *Yersinia* species classification

The genus *Yersinia* has three human- and animal-pathogenic species: *Yersinia pestis*, *Yersinia enterocolitica* and *Yersinia pseudotuberculosis*. *Yersinia pestis* causes bubonic plague through a bite of an infected flea. Inhalation of the bacteria causes pneumonic plague (152, 206). *Y. pestis* will further replicate and spread to bloodstream and visceral organs causing systemic disease, called septicemic plague (92). *Yersinia enterocolitica* and *Yersinia pseudotuberculosis* are enteropathogens. They are transmitted via contaminated food and water and typically cause a self-healing enteritis (228).

1.1.2 *Y. pestis* pathogenesis

Y. pestis infections (bubonic and pneumonic) display a bi-phasic property: initiated with a non-detectable immune response in the first two days followed by a profound inflammatory stage with phagocyte infiltration, inflammatory cytokine production and tissue necrosis (81, 107, 177). At an early stage of infection, very few extracellular *Y. pestis* are detected. They may be efficiently engulfed by $CD11b^+$ macrophages and $Ly\text{-}6G^+$ neutrophils around infection sites (120). *Y. pestis* are killed by neutrophils and infection is temporarily controlled within 2 days. However, macrophages cannot successfully eliminate intracellular *Y. pestis* by phagosomal acidification, which leads to resident bacterial survival and replication (120, 158). Intracellular growth of bacteria induces macrophage apoptosis, which releases a large number of bacteria,

overwhelming the neutrophil-based killing (110, 120). It seems that macrophages provide a niche that protects *Y. pestis* from neutrophil killing and may also transport the bacteria to local draining lymph nodes causing systemic infection (110, 228).

1.1.3 Anti-host functions of the pCD1-encoded type III secretion system

Y. pestis harbors a 70kb virulence plasmid called pCD1 (a similar plasmid is called pYV in *Y. pseudotuberculosis* and *Y. enterocolitica*). The virulence plasmid pCD1 encodes the T3SS, Yop effectors and translocators (YopB, YopD and LcrV). Once entering host tissue, *Y. pestis* quickly and selectively target immune cells, such as macrophages, dendritic cells (DCs) and neutrophils to microinject Yops (126). The T3SS forms pores, upon docking on the host cell, translocates Yops into the target cell cytoplasm. Once inside host cells, seven effector Yops, YopE, YopH, YopJ, YopM, YopO, YopK and YopT, interfere with various host cell signaling pathways. Three general anti-host immune strategies are Yop-dependent:

1) Antiphagocytosis: Four Yops, YopO, YopT, YopE and YopH, work synergistically to disrupt the target cell cytoskeleton organization and confer the bacterium resistant to phagocytosis. YopE is a RhoGTPase activating protein, blocking Rac-regulated actin structures and resulting in de-polymerization of actin microfilaments and cell rounding up (5). YopT is a cysteine protease, which cleaves membrane anchored small G proteins and results in mislocation of these proteins, disrupting actin assembly (180). YopO is a multidomain protein, containing an N-terminal region homologous to serine/threonine kinases, a RhoGTPase binding part at the middle and a C-terminal actin binding domain (196). YopO causes a disorganized actin cytoskeleton conferring anti-phagocytosis (196). YopH is a potent tyrosine phosphatase which leads to global tyrosine dephosphorylation and loss of focal adhesion, and thus inhibits phagocytosis (196).

2) Inhibition of cytokine production: During *Yersinia* infection, NF-κB pathway and MAPK pathways are induced and then rapidly repressed (138, 144, 168). The TLR4, NF-κB, and MAPK signaling networks play an important role in controlling the host immune response to pathogens. TLRs sense a variety of pathogen associated molecular patterns (PAMPs) and stimulate, via adaptor proteins such as MyD88, cascades leading to NF-κB and MAPK pathway activation. The NF-κB and MAPK pathways increase transcription of genes encoding proinflammatory cytokines (e.g. tumor necrotic factor-α (TNF-α), interleukin-1 (IL-1)), chemokines (e.g. interleukin-8 (IL-8)) and cell survival genes (e.g. *B-cell lymphoma 2* (Bcl-2)). NF-κB is sequestered by the IκBα in the cytoplasm until IκBα is phosphorylated by IκB kinase β (IKKβ) and undergoes ubiquitin dependent degradation. NF-κB is released and translocated into the nucleus to upregulate gene transcription. By inhibiting the NF-κB and MAPK pathways, YopJ action decreases production of proinflammatory cytokines such as TNF-α, which is critical for protective immunity against *Y. pestis* challenge (109, 139).

3) Dysfunction of antigen presenting cells (APCs): YopJ-mediated killing of macrophages and dendritic cells and blockage of dendritic cell differentiation may hamper adaptive immune response (116, 126). As mentioned above, *Y. pestis* targets immune cells and translocates YopJ into the eukaryotic cytoplasm. By blocking NF-κB and MAPK pathways, YopJ inhibits transcription of survival genes, and *Yersinia* infection initiates a cell death response (126, 223). Both NF-κB and MAPK signaling pathways also have key roles in dendritic cell differentiation (116). Furthermore, inhibition of both pathways by YopJ prevents up-regulation of co-stimulatory molecules, dampening the ability of dendritic cells to cause T cell proliferation (116).

1.1.4 Molecular function of YopJ/P

YopJ is an acetyltransferase that acetylates MKK6, MKK2 and IKKβ, masking phosphorylation sites to inhibit activation of these proteins *in vitro* and in mammalian cell lines (133, 137, 138). YopJ activity thus decreases TNF-α secretion from macrophages, inhibits IL-8 release from epithelial and endothelial cells, and induces macrophages and dendritic cell to die (44, 77, 147, 219).

YopJ/P activity in host cells is controlled by how much of the protein is translocated into host cells and the affinity of the protein for interaction with substrates. Amino acid polymorphisms among different YopJ/P isoforms are responsible for differences in these aforementioned activities. The *Y. pseudotuberculosis* YopJ isoform was translocated at a lower level than the *Y. enterocolitica* strain 8081 YopP isoform, due to two amino acid substitutions at positions 10 and 11. Exchanging these two amino acids from YopP into YopJ caused YopJ to translocate more efficiently and be more cytotoxic (21). In *Y. enterocolitica*, highly virulent strains such as 8081 have an arginine at residue 143 in YopP, while low virulent strains have a YopP isoform with a serine at this position (172). The R143S substitution does not decrease the translocation of YopP, but it impairs its ability to bind to and phosphorylate IKKβ, and therefore suppression of the NF-κB pathway and cytotoxicity is reduced (172).

YopJ is required for *Yersinia* to induce macrophage cell death with features of apoptosis, as observed by activation of apoptotic caspases-3/7, DNA fragmentation, and sensitivity to caspase inhibitors (43, 219). A recent work showed that a highly virulent *Y. enterocolitica* strain induced YopP-dependent dendritic cell death that presented with necrotic-like features (77). In this study, over-expression of the anti-apoptotic protein Bcl-2 in dendritic cells did not decrease cytotoxicity. In addition, a pan-caspase inhibitor only reduced by 50% the amount of cell death.

HMGB1, released from necrotic cells, is detected in cell media (77). It seems that *Yersinia*-infected macrophage death mediated by YopJ/P is not strictly apoptotic, as other kinds of cell death pathways (such as necrosis) may be involved.

1.2 IL-1β, IL-18, caspase-1 activation and inflammasomes

1.2.1 IL-1β and IL-18

IL-1β and interleukin-18 (IL-18) are IL-1 family cytokines, sharing similar structure and signaling pathway, but they initiate distinct functions (42, 48).

IL-1β is mainly produced by macrophages, monocytes and polymorphonuclear phagocytes after infection, injury and antigen challenges (48). It affects a broad range of cells in different tissues. It is a pleotropic cytokine, affecting many functions including cell proliferation, tissue destruction, vascular smooth muscle contraction, blood pressure, inflammation, vascular cell modulation, cytokine induction, and immune cell recruitment (47, 50, 51). Abnormal IL-1β production is involved in many acute and chronic diseases such as Familial Mediterranean fever (FMF), rheumatoid arthritis, Alzheimer's disease, diabetes, acute myelocytic leukemia and periodontitis (49, 62, 75, 163, 184, 201).

IL-18 is produced by blood and tissue macrophages, dendritic cells, epithelial cells and microglial cells (27, 59, 143, 188, 191). IL-18 is very important in controlling adaptive immune responses, especially for Th1 cell development. IL-18 works together with IL-12, mitogens or microbial elements to induce IFN-γ production (131, 195, 215, 216). In addition, IL-18 induces production of TNF-α, and CXC and CC chemokines (160). Pathogenesis resulting from abnormal IL-18 production has been determined in many diseases, such as diabetes, rheumatoid arthritis, Crohn's disease and asthma (72, 88, 136, 212).

The powerful IL-1β and IL-18 cytokines must be tightly controlled. Both cytokines are produced as pro-forms and are processed by the same enzyme, IL-1-converting enzyme (ICE or caspase-1) to yield 17kDa and 18kDa mature forms, respectively (140) (will discuss in detail later). Other ICE family members, including caspase-4 (caspase-11 homolog in mouse), -5 and -11 are also involved in IL-1β and IL-18 processing (127). Caspase-4 has been shown cleave IL-18 at the same site as caspase-1, but the efficiency is hundreds of fold lower (79). Caspase-11 has been implicated as being essential for IL-1β and IL-18 maturation. Caspase-11 knockout mice are resistant to LPS-triggered endotoxic shock and produced much less IL-1β and IL-18 (207). Similar to the way caspase-11 promotes caspase-1 activity in mouse cells, caspase-5 in human cells greatly enhances caspase-1-based cleavage of pro-IL-1β (127). In vitro experiments also determined that caspase-8 can cleave IL-1β under conditions of TLR3-, or TLR4-stimulation (122). In neutrophils, serine proteases rather than caspase-1 have been implicated in IL-1β processing, a process which is under negative regulation by the NF-κB pathway (74).

Mature IL-1β and IL-18 cytokines lack an N-terminal secretory signal sequence and are secreted via unconventional pathway that is independent of the endoplasmic reticulum and Golgi apparatus (6, 123, 167). Caspase-1 has been demonstrated to not only process IL-1β and IL-18, but also regulate their secretion and itself is secreted together with mature cytokines (103).

1.2.2 Caspase-1 activation and function

Caspase-1 is produced as an inactive zymogen and undergoes proteolysis to acquire activation. Caspase-1 knockout mice show tolerance to LPS-induced endotoxic shock as a result of reduced production of mature IL-1β (112). Caspase-1 activation depends on caspase recruitment platforms — called inflammasomes. Inflammasomes are multi-protein complexes that can sense cytosolic PAMPs and danger signals, carry on oligomerization and recruit pro-caspase-1. These

proteins belong to the Nod-like receptor (NLR) family, the intracellular sensors that contain an N-terminal caspase recruitment domain (CARD) or a pyrin domain. The central part of the NLR is an oligomerization domain and the C-terminal domain harbors a signal-sensing and auto-inhibitory leucine-rich repeat domain (will explain in Chapter 1.3) (127).

Caspase-1 has a broader role than just cytokine processing, and these roles seem to be tailored according to stimuli and cell types (14).

Pyroptosis, defined as a caspase-1-dependent cell death, primarily happens in macrophages and dendritic cells (66, 200). Caspase-1 is not required for activation of apoptotic caspases, since caspase-1 deficient cells can undergo apoptosis (14). During pyroptosis, plasma membrane rupture, DNA fragmentation and IL-1β and IL-18 release occur, but not cytochrome *c* release or loss of integrity of the mitochondrial membrane (14). As mentioned above, since IL-1β and IL-18 activate innate and adaptive effector cells, pyroptosis itself facilitates pathogen clearance. In addition, caspase-1 mediated cell death by itself is microbicidal, since bacteria released from pyroptotic macrophages could be phagocytized and eliminated by recruited neutrophils in *il-1b*$^{-/-}$/ *il-18*$^{-/-}$ double knockout mice (130).

Impaired NF-κB and p38 activation have been demonstrated in caspase-1 deficient cells following activation of TLR2 or TLR4 signaling pathways. MyD88-adapter-like (Mal) requires caspase-1 dependent cleavage to active NF-κB, revealing a level of coordination between TLRs and caspase-1 in innate responses (132).

Caspase-1 also restricts bacterial intracellular growth. In *Legionella*-infected caspase-1 knockout or inflammasome component IPAF knockout macrophages, bacteria-containing phagosomes failed to fuse with lysosomes (3). A similar phenomenon has been observed in *Mycobacterium tuberculosis* (Mtb)-infected macrophages: caspase-1 is important for directing

bacteria-containing phagosomes to fuse with lysosomes and facilitating 10-fold greater bacterial killing as compared to macrophages lacking caspase-1 (128).

Surprisingly, caspase-1 is required for cell survival in pore-forming toxin-mediated death in epithelial cells (82). Responding to K^+ efflux, caspase-1 is activated and necessary to trigger sterol regulatory element binding proteins (SREBPs) activation which is involved in cholesterol and fatty acid biosynthesis and may alternatively repair membrane (82).

1.2.3 Inflammasome activation

1.2.3.1 NLRs

NLRs sense PAMPs and endogenous danger-associated molecular patterns (DAMPs) to activate innate immune responses (37). One of the major functions of NLRs is to form inflammasomes along with the adaptor protein apoptotic speck–containing protein (ASC) and to recruit pro-caspase-1 upon signal recognition. Additionally, NLRs affect adaptive immunity by modulating expression of major histocompatibility complex (MHC) II and regulate critical signaling pathways such as NF-κB, MAPK, and type I interferon (IFN) (36, 113, 161). Many human diseases related to altered NLR function have been identified and as a result intensive attention is directed toward better understand of this protein family (37).

1.2.3.2 Inflammasomes

As mentioned above, inflammasomes contain NLRs and form multi-protein platforms with adaptor proteins, such as ASC, and pro-caspase-1. ASC is implicated in bridging NLRs and pro-caspase-1 by its own pyrin and CARD domains. ASC-deficient mice displayed the same level of protection against LPS-induced shock as did caspase-1 knockout mice (213). NLR oligomerization is a prerequisite for ASC recruitment. ASC then interacts with pro-caspase-1 through CARD-CARD binding. Two pro-caspase-1 molecules are brought into proximity and

undergo self-cleavage, yielding 20kDa (p20) and 10kDa (p10) subunits enzymatically active (186). Caspase-1 cleaves the 31kDa pro-IL-1β between Asp116 and Ala117 to yield the 17kDa mature cytokine (91).

Inflammasomes show specificity in ligand recognition: the NALP1 inflammasome responds to *Bacillus anthracis* lethal toxin (LT) (60); IPAF recognizes flagellin from *Salmonella* and *Legionella* (3, 67); NLRP3 senses a variety of PAMPs and danger signals, such as ATP plus LPS or lipoprotein or dsRNA, the potassium ionophore nigericin, uric acid crystals and Gram-positive bacteria such as *L. monocytogenes* and *S. aureus* (125, 189).

1.2.3.3 The NLRP3 inflammasome

NLRP3 (also termed as cryopyrin or NALP3) senses numerous host-derived and exogenous agonists that can be structurally distinct such as ATP, cholesterol crystals, amyloid β, UV, silica, bacterial toxins and viral RNA. It has remained unclear how NLRP3 detects these highly variable signals, and no direct binding of these activators to NLRP3 has been reported (37). A low intracellular K^+ concentration as a trigger for NLRP3 activation is accepted by different models. The normal cytoplasmic K^+ concentration of around ~140 to ~150 mM restricts NLRP3 activation (197). When the intracellular K^+ concentration drops to ~70 mM, NLRP3 can be activated. Extracellular K^+ supplementation can reduce K^+ efflux and prevent caspase-1 activation in intact cells. Furthermore, cell lysates incubated in the presence of a low concentration of KCl are permissive for caspase-1 activation (154, 227). However, K^+ efflux may not be sufficient to activate caspase-1, as unknown signal(s) may be required (150).

Three popular NLRP3 activation models have been proposed to explain the mechanism. The channel model is based on studies of ATP-mediated caspase-1 activation. Extracellular ATP, a danger signal released from injured tissue and dead cells, activates the purinergic receptor

$P2X_7$ (25) (Figure 1.1). $P2X_7$ quickly mediates K^+ efflux and recruits a second hemi-channel, pannexin-1, which forms pores for further K^+ leakage and allows for other NLRP3 activators to gain access to cytoplasmic NLRP3 (150, 197). This model is also supported by results with pore-forming toxins such as *Streptococcus pyrogenes* streptolysin O (SLO), and *Staphylococcus aureus* α-toxin, but it cannot explain how other types of stimuli activate NLRP3 (34, 85).

The lysosomal rupture model applies to particular and crystalline stimuli, such as alum, silica and amyloid β, which are taken up by phagocytosis (54, 83) (Figure 1.2). Phagosomal destruction and lysosomal rupture lead to cathepsin B release into the cytoplasm, which directly or indirectly activates NLRP3 (90). Activation of caspase-1 by this mechanism can be prevented by the use of the actin polymerization inhibitor cytochalasin D, which arrests actin-mediated phagocytosis, or cathepsin B-specific inhibitor such as CA074-Me. Furthermore, the lysosome rupture inducer Leu-Leu-OMe activates caspase-1 in LPS-primed macrophages in support of this model (54, 90). A NLRP3-dependent cell death (termed pyronecrosis) can be suppressed by CA074-Me (210). In vivo, high cathepsin activity and lysosomal rupture have been detected in tissues undergoing ischemic neuronal necrosis. In addition, the findings that cathepsin B and caspase-1 co-localize in ischemic tissue and that a cathepsin B inhibitor protects against ischemic damage indicate that cathespin B released from lysosomal rupture may play a role activating caspase-1 (11, 214). However, results obtained with cathepsin B knockout or cathepsin B knockdown cells suggest that inhibitors such as CA074-Me can have off-target effects (83, 141).

The ROS model proposes that NLRP3 can sense ROS generated from PAMPs and DAMPs (197) (Figure 1.3). Many NLRP3 activators have been implicated in ROS generation, either by directly measuring ROS levels or by ROS inhibitor treatments (28, 35). Recently, thioredoxin-interacting protein (TXNIP) has turned out to be an important regulator of this

pathway. In the absence of ROS, TXNIP associates with thioredoxin, blocking its function. When ROS is generated, thioredoxin is released from TXNIP to perform its role in preventing excessive oxidative stress. Dissociated TXNIP in turn, binds to the leucine-rich repeat of NLRP3, giving rise to a conformational change and activation of NLRP3 (229). However, this model is controversial because monocytes from humans with chronic granulomatous diseases (CGDs) that are defective in NADPH-dependent ROS production have increased caspase-1 activity and IL-1β production (199). Therefore, more work needs to be done to uncover the underlying story.

1.2.3.4 Regulation of inflammasomes

Abnormal regulation of inflammasome activation can disrupt immune responses and lead to sever disease consequences, so inflammasome activation must be tightly regulated. A complete understanding of the mechanism of inflammasome regulation is presently unclear, but some recent findings suggest that multiple control steps exist (37).

Alternative splicing of NOD2 and ASC can occur, resulting in the production of isoforms that may negatively modulate their own activities (24, 166). In human monocytes, a truncated NOD2 (NOD-2S) variant is defective for muramyl dipeptide (MDP)-induced NF-κB activation and IL-1β production upon interleukin-10 (IL-10) treatment. NOD-2S binds to RIP2 and NOD2 and disrupts the normal NOD-2/RIP2 interaction (166). An ASC isotype, ASC-c, which lacks the pyrin domain and cannot interact with NLRP3, inhibits ATP-mediated IL-1β secretion in LPS primed macrophages (24).

Human monocytes translate a series of pyrin-only proteins (POPs) and CARD-only proteins (COPs) which are encoded on chromosome 11, flanking the caspase-1 gene (186). POP1 attaches to ASC, preventing its recruitment to NLRPs, and POP2 interacts with NLRPs, dampening their recruitment to ASC (10, 187).

Bcl-2 and Bcl-xL have been demonstrated to directly associate with NLRP1 to block its interaction with ASC (23). Another anti-apoptotic protein, plasminogen activator inhibitor 2 (PAI-2), significantly reduced secretion of IL-1β, when ectopically expressed in macrophages (74).

The NF-κB pathway has been implicated in the negative modulation of inflammasome activation (74). IKKβ-deficient macrophages stimulated with LPS synthesized less pro-IL-1β, yet secreted more mature cytokine due to elevated caspase-1 activation (74). As expression of Bcl-2, Bcl-xL and PAI-2 are controlled by the NF-κB pathway, one or more of these proteins may act as negative regulators of inflammasome activation. The NF-κB pathway has also been shown to promote inflammasome activation by increasing transcription of genes encoding inflammasome components (e.g. NLRP3) and by causing a redistribution of ASC from the nucleus to the cytoplasm (9, 71). Understanding how the NF-κB pathway differentially regulates inflammasome activation will required additional comprehensive study.

Type I interferon (IFN) was reported to repress NLRP1 and NLRP3 activation and IL-1β production by IL-10 induction (80). This pathway occurs through signal transducers and activators of transcription (STAT) 1 and STAT3 in an autocrine manner (80). It may explain why patients are susceptible to secondary infection after a primary viral infection (15, 33, 38, 179).

1.3 Cell death pathways in host cell infection

Induction of host cell death is a general and a very important outcome of pathogen infection, because cell death may facilitate pathogen clearance by removal of infected tissues, destruction of a pathogenic niche or up modulation of host immune responses (53, 58, 217). On the other hand, some pathogens subvert host immune responses by killing immune cells (95). Not only the death of the infected cells impacts the consequence of the battle between host immune system

and pathogen, but also the choice of cell death pathways is important. For example, avirulent Mtb strains stimulate apoptosis in macrophages, resulting in the formation of an impermeable envelope on the cell surface to prevent intracellular bacteria from spreading (52). Furthermore, apoptotic bodies that contain bacterial proteins are taken up and processed by bystander dendritic cells which in turn, prime specific anti-Mtb T cell responses (211). However the virulent Mtb strains are able to trigger necrosis of macrophages and escape from broken cell membranes; inflammation is elicited by leakage of cell contents, which recruits more naïve macrophages to serve as bacterial residences and to contribute to tissue damage (102, 156).

There are several cell death pathways responding to microbial infections.

1.3.1 Apoptosis

Apoptosis is described as an active programmed process of cellular dismantling, leading to a series of morphological changes, including blebbing, changes to the cell membrane such as loss of membrane asymmetry and attachment, cell shrinkage, DNA fragmentation and chromatin condensation (65). The disposal of cell debris by this pathway does not result in damage to the organism. Apoptosis is mediated by apoptotic caspases, including initiators: caspase-2, -8, -9 and 10 and executioners: caspase-3, -6 and -7 (105). Under cellular stress, pro-apoptotic protein Bcl-2 homologous antagonist/killer (BAK) and Bcl-2–associated X protein (BAX) are activated and oligomerized to form permeable pores on the mitochondrial outer membrane, which leads to death via cytochrome *c* release into the cytosol. Cytochrome *c* recruits apoptosis protease activating factor-1 to activate caspase-9. Capase-9 cleaves executioner caspases which modify cellular substrates by cleavage to drive cell death forward (165). The extrinsic pathway of apoptosis is initiated from TNF-receptor family of membrane death proteins. Caspase-8 and -10 are recruited and activated by TNFR1-associated death domain proteins and executioner

caspases are consequently activated by these two caspases (153).

Apoptosis shows multifaceted properties in host protection against pathogen infection. *Helicobacter pylori* infected epithelial cells initiate apoptosis via Fas-Fas ligands interaction (96). Mice lacking functional Fas have dampened IFN-γ production and have increased probability to transit from gastritis to gastric cancers in response to *H. pylori* infection (26). TNF receptor p55 (TNFR55)-mediated T cell apoptosis suppressed overwhelming inflammation and prevented lesion formation after elimination of *Leishmania major* or *Rhodococcus equi* infection in mice (99). Phagocytosis of apoptotic cells by macrophages and dendritic cells enhances IL-10 and transforming growth factor-β (TGF-β) production, suppressing the production of proinflammatory cytokines (70, 202) without up-regulating expression of co-stimulatory molecules (73).

Pathogens modulate infection either by induction or inhibition of apoptosis. Prevention of apoptosis occurs when cell survival benefits pathogen invasion; thus pathogens can block apoptosis or activate survival responses (57). The obligate intracellular pathogen *Chlamydia trachomatis* requires living cells to maintain its life cycle (57). *C. trachomatis* produces chlamydial proteasome-like activity factor (CPAF) to cleave BH3 family pro-apoptotic proteins and up-regulates inhibitor of apoptosis proteins (IAPs) in infected epithelial cells (155, 162). *Anaplasma phagocytophilum* activates p38, ERK, PI3K/AKT and NF-κB pathways and arrests caspase-8 activation to delay neutrophil death by an uncharacterized mechanism (31, 69, 108). Conversely, *Salmonella* AvrA and *Yersinia* YopP/J counteract NF-κB and MAPK survival pathways by acetyltransferase activity, thereby promoting apoptosis (97, 133).

1.3.2 Necrosis

Unlike apoptosis, necrosis is a form of traumatic death that results from acute cellular injury.

This cell death is characterized by cell swelling, membrane breakdown, and inflammatory responses are activated by released cell contents (230). Increasing evidence supports the idea that necrosis can be well-controlled in certain contexts (63). Recent studies shed light on the molecular mechanism of programmed necrosis (also termed as necroptosis), revealing that necrosis, in many cell lines, is a back-up death for apoptosis (55, 89, 205). Fas-Associated protein with Death Domain (FADD) is a crucial adaptor protein harboring a death domain (DD) for initiating necrosis and a death effector domain (DED) for propagating apoptosis (18, 204). In FAS- or TRAIL-R-induced necrosis, the so-called complex I assembles on the plasma membrane, contains TNF-R1, TRAF2 and RIP1, and activates MAPK and NF-κB pathways to upregulate synthesis of anti-apoptotic proteins (45, 46). Endocytosis of complex I results in formation of complex II, consisting of FADD, and pro-caspase-8 or -10 (55, 193). If complex I does not induce synthesis of sufficient levels of anti-apoptotic proteins, caspase-8 is activated to augment apoptosis, but in the presence of an apoptosis inhibitor, necrosis is activated (30, 205). RIP1 determines the switch between apoptosis and necrosis on the crossroad. Active caspase-8 cleaves RIP1 to promote apoptosis and suppress necrosis (30). Inhibition of RIP1 activity obstructed Jurkat cell death in the presence of a caspase inhibitor and TNF-α (40). TLR3- or TLR4-directed necrosis in macrophages resulting from treatment with LPS or dsRNA in the presence of a caspase inhibitor is also RIP1 dependent (98, 121).

Necrosis enhances immune responses in several ways. The intracellular contents released from necrotic cells are taken up by DCs to induce DC maturation (174). HMGB1 passively secreted from necrotic DCs and macrophages, works essentially as a powerful cytokine, by binding to its receptors TLR2 or TLR4 and advanced glycation end products (RAGE), and therefore actives the NF-κB pathway to produce proinflammatory cytokines (119). Necrosis

causes release of proinflammatory cytokines, such as interleukin-6 (IL-6), TNF-α and IL-8 (56, 203). The mRNA spilled from necrotic cells is a potent stimulator of TLR3, which in turn also activates the NF-κB pathway for proinflammatory cytokine production (100).

1.3.3 Pyroptosis

Pyroptosis is defined as a caspase-1-dependent cell death, which has been discovered in microbial infections, such as those caused by *Salmonella*, *Shigella* and *Fransicella* in macrophages (66, 86, 124). In contrast to apoptosis, some substrates of apoptotic caspases, such as PARP-1 and inhibitor of caspase-activated DNase (ICAD), are not cleaved and cytochrome *c* release and loss of mitochondria integrity do not occur in pyroptosis (20, 29, 66, 94). During pyroptosis, caspase-1 dependent pore formation in the cell plasma membrane leads to increased osmotic pressure by ionic gradients, causing water influx, cell swelling, cell lysis and release of inflammatory contents (66). Cell swelling during pyroptosis has been measured by flow cytometry and can be blocked by exogenous glycine addition via an unknown mechanism (66). Chromosomal DNA fragmentation during apoptosis results in the formation of approximately 180 bp fragments, while random sized DNA fragments are formed during pyroptosis, but these fragments can still be labeled by TUNEL (66, 208). The glycolysis pathway is another target of caspase-1, as suggested by the observed *in vitro* and *in vivo* digestion of adolase, Glyceraldehyde 3-phosphate dehydrogenase (GAPDH) and Triose-phosphate isomerase (TIM) by caspase-1 (181). In addition, lower lactate production has been detected upon *Salmonella* challenge in mice, indicating decreased glycolytic function (181). Caspase-7 was found to be cleaved by caspase-1 in macrophages infected with *Salmonella*, or *Legionella* or in macrophages treated with LPS and ATP; this cleavage did not occur in inflammasome deficient cells or caspase-1 deficient cells (1, 106). It is likely that there are additional downstream effects of caspase-1 activation that remain

to be identified.

Microbes modulate host caspase-1 activation to escape from immune responses. *Salmonella* and *Legionella* down regulate flagellin expression during the intracellular phase of growth to avoid activating IPAF/caspase-1 inflammasomes (118, 134). The *Yersinia* T3SS may activate caspase-1 via pore-formation in the host cell plasma membrane, a process that can be counteracted by the Rho inhibitory activities of YopE and YopT (176, 182).

1.3.4 Pyronecrosis

An NLRP3-dependent cell death, termed pyronecrosis, not only shares necrotic morphology, but also has proinflammatory responses. It is a caspase-independent cell death, but is accompanied by caspase-1 activation (194). Pyronecrosis was observed to occur following *Shigella flexneri* infection of monocytes and in monocytes from patients with certain auto-immune diseases that are related to NLRP3 hyperactivation (2, 61, 87, 210). Cell death by pyronecrosis can be blocked by cathepsin B inhibitor treatment, or by the use of NLRP3 knockout or ASC knockout macrophages (194).

1.4 Caspase-1 activation and cell death in macrophages infected with *Yersinia*

Previous studies have examined caspase-1 activation in macrophages infected with different *Yersinia* species (13, 22, 176, 182). A *Y. enterocolitica* serogroup O:9 strain known as E40 lacking six effector Yops (YopE, H, P, T, O and M), was shown to trigger caspase-1 activation and IL-1β release in infected macrophages (182). A functional T3SS, which can permeabilize host cell plasma membranes by pore formation, was required for caspase-1 activation (182). Infection of macrophages with the wild-type E40 strain did not result in caspase-1 activation, however infection with mutant strains deficient for YopE and YopT did promote caspase-1 activation and IL-1β release. Since YopE and YopT inhibit RhoGTPase-based actin

arrangements, it is possible that these effectors abolish caspase-1 activation because they inhibit actin polymerization, allowing for repair of pores formed by T3SS translocon (129, 176). Bergsbaken et al. provided evidence that LPS-primed macrophages switch their mode of cell death from apoptosis to pyroptosis following *Y. pseudotuberculosis* infection (13). The pyroptosis and caspase-1 activation seen in LPS-primed macrophages required a functional T3SS, but was independent of any translocated Yop effectors. The authors suggested that in LPS-activated macrophages the abilities of *Yersinia* effector Yops to inhibit caspase-1 activation was bypassed (13). Brodsky et al. showed two different pathways of caspase-1 activation in macrophages following *Y. pseudotuberculosis* infection (22). The first pathway required a functional T3SS and could be suppressed by the YopK effector by an unknown mechanism (22). This pathway required ASC and involved NLRP3. The second pathway required a functional T3SS and the effector YopJ, however no specific NLR could be identified as important for caspase-1 activation (22). Recently, our group determined that the *Y. pestis* strain KIM5 encodes a highly active YopJ isoform ($YopJ^{KIM}$) which is able to activate high levels of caspase-1 in infected macrophages (114). Ectopic expression of $YopJ^{KIM}$ in *Y. pseudotuberculosis* enabled the strain to induce robust IL-1β secretion in macrophage infection (114). High-level secretion of IL-1β from macrophages infected with *Y. pestis* KIM5 required NLRP3 and ASC, and could be reduced by exogenous K^+, suggesting a role for K^+ efflux in the process of inflammasome activation. Interestingly, although caspase-1 is activated in infected macrophages undergoing YopJ- or $YopJ^{KIM}$-induced cell death, caspase-1, NLRP3 or ASC are not required for the cell death pathway (114, 227).

1.5 *Yersinia* strains engineered to be hypercytotoxic by ectopic expression of highly active YopJ/P isoforms are attenuated in mouse infection models

The role of YopJ in *in vivo* infection is not well defined. In one study, wild type *Y. pestis* or an isogenic *yopJ* mutant was evaluated in a rat bubonic model by intradermal infection (109). Deletion of *yopJ* resulted in decreased immune cell apoptosis and an increase of TNF-α production, but there was no associated decrease in virulence or establishment of systemic infection (109). Another study using *Y. pseudotuberculosis* oral infection in a mouse model with wild-type or *yopJ* mutant strains showed that the *yopJ* mutant had a 64-fold increase of LD50 and decreased ability of systemic infection (135).

Two interesting studies discovered that the level of YopJ/P-induced cytotoxicity is inversely correlated to the *in vivo* virulence (21, 220). When the highly cytotoxic YopP was overexpressed in *Y. pestis* strain Kim53, the resulting strain was avirulent following subcutaneous administration and deficient in spreading to organs and to blood as compared to a Kim53 strain expressing the native low activity YopJ isoform (identical to $YopJ^{CO92}$) (219, 220). Infection of mice with Kim53 expressing YopP stimulated a rapid and effective innate mechanism of resistance when it was co-infected with virulent Kim53 expressing YopJ. The same result was obtained when infection with Kim53 expressing YopP was followed by immediate intranasal or intravenous challenge with virulent Kim53 (220). In a second study, *Y. pseudotuberculosis* ectopically expressing YopP induced more potent cell death and greater inhibition of MAPK pathways upon infection of dendritic cell as compared to the same strain expressing the native $YopJ^{YPTB}$ isoform (19). Following orogastric infection, mice infected with *Y. pseudotuberculosis* expressing YopP had a significantly higher survival rate than mice infected with the strain expressing $YopJ^{YPTB}$. Interestingly, infection with the YopP-expressing

strain resulted in lower levels of serum IFN-γ, TNF-α, IL-12 and IL-6 in mice as compared to the mice infected with the YopJ-expressing strain (19). Both authors suggested that the attenuation of *Yersinia* strains ectopically expressing YopP may come from its high cytotoxicity, which is able to destroy infected macrophages and dendritic cells that served as bacterial refuges (21, 220).

1.6 Hypothesis and rationale

In this dissertation, studies were undertaken to understand the molecular basis for the enhanced ability of $YopJ^{KIM}$ as compared to other YopJ isoforms to cause caspase-1 activation and cytotoxicity in macrophages. In addition, the mechanism of caspase-1 activation and cell death in macrophages infected with *Y. pestis* KIM5 was investigated. Finally, an *in vivo* infection experiment was carried out to determine if caspase-1 is important for the increased resistance of mice to *Yersinia* strains with enhanced cytotoxicity. Following this introduction chapter the data resulting from my studies are organized in four chapters. Chapter 2 solves the question of why $YopJ^{KIM}$ has high biological activity in macrophages. I characterized the ability of $YopJ^{KIM}$ to be expressed, translocated, inhibit host signaling pathways and interact with the substrate IKKβ, and compared these features with other YopJ isoforms. In Chapter 3, we hypothesized that the enhanced inhibition of IKKβ by $YopJ^{KIM}$ results in enhanced cytotoxicity and caspase-1 activation in macrophages. I confirmed in Chapter 3 that IKKβ is important for negative regulation of caspase-1 (74) by infecting $Ikk\beta^{\Delta}$ deficient macrophages or macrophages treated with a small molecule IKKβ inhibitor. Chapter 4 is focused on evaluation of the mechanism of KIM5-induced macrophage death and signals recognized by the NLRP3 inflammasome. We hypothesized that KIM5-infected macrophages die in another pathway instead of apoptosis that is typically initiated by other *Yersinia* strains, because IL-1β secretion is uncharacteristic of "inflammation silent" apoptosis. Macrophages were pre-incubated with ROS or cathepsin B

inhibitors to find out if NLRP3 recognized either of these "molecular patterns" to trigger caspase-1 activation. In Chapter 5, we tried to see if caspase-1 activation was important for increased survival of mice against hypercytotoxic *Yersinia* infection. A positive correlation between YopJ cytotoxicity and caspase-1 activation was observed in Chapter 4, and even stronger IL-1β production was detected when macrophages were infected with *Y. pseudotuberculosis* ectopically expressing the most cytotoxic YopJ homolog, YopP. Previous studies demonstrated that *Y. pseudotuberculosis* or *Y. pestis* expressing YopP exhibited attenuation compared to the same strains expressing YopJ (21, 220). We proposed that the attenuation was conferred by caspase-1 protection. Caspase-1 knockout and wild type mice were infected with YopP- or YopJ- encoding *Y. pseudotuberculosis* strains and the survival was recorded (Chapter 5). Finally, Chapter 6 discusses future directions for this project. Overall, the results determined the mechanisms for caspase-1 activation and cell death by a new isoform of YopJ that had not been seen in other *Yersinia* strains before.

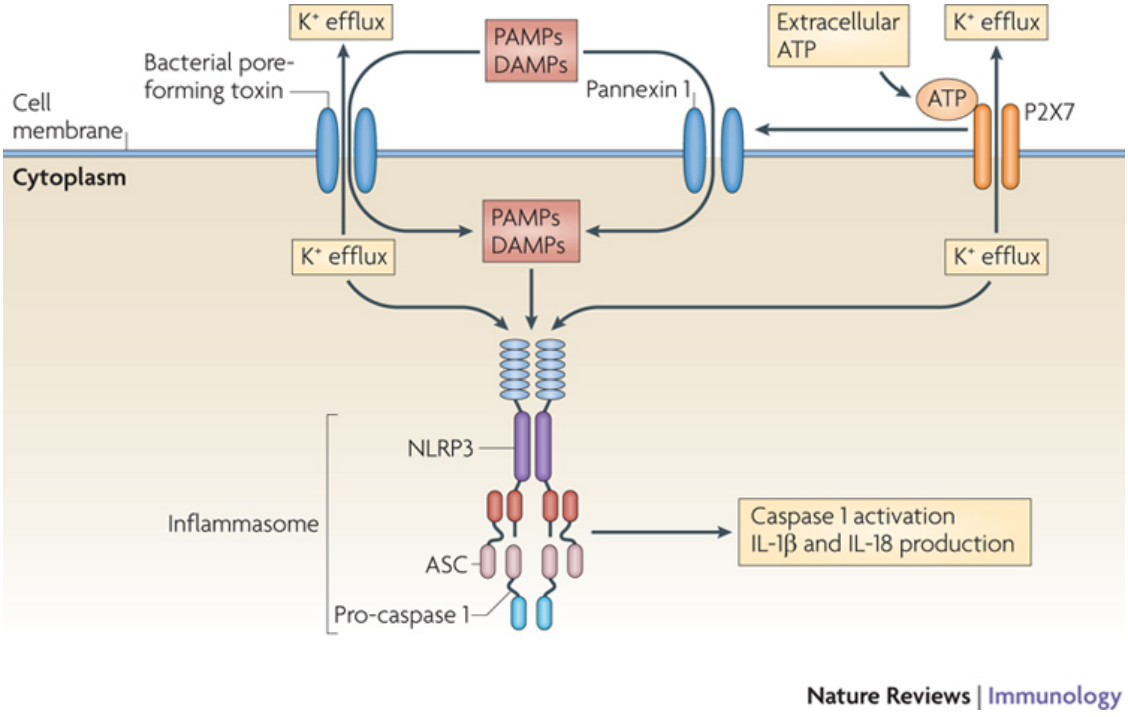

Figure 1.1 The channel model of NLRP3 inflammasome activation. Intracellular K^+ is released from purinergic channel P2X7 that is activated by extracellular ATP and hemichannel pannexin 1 is in turn recruited for further K^+ expulsion. Bacterial pore-forming toxins can also promote K^+ efflux. Low cytoplasmic K^+ concentration allows NLRP3 activation. ASC, apoptosis-associated speck-like protein containing a CARD; DAMPs, damage-associated molecular patterns; IL, interleukin; PAMPs, pathogen-associated molecular patterns. Adapted from Tschopp, 2010 (197) .

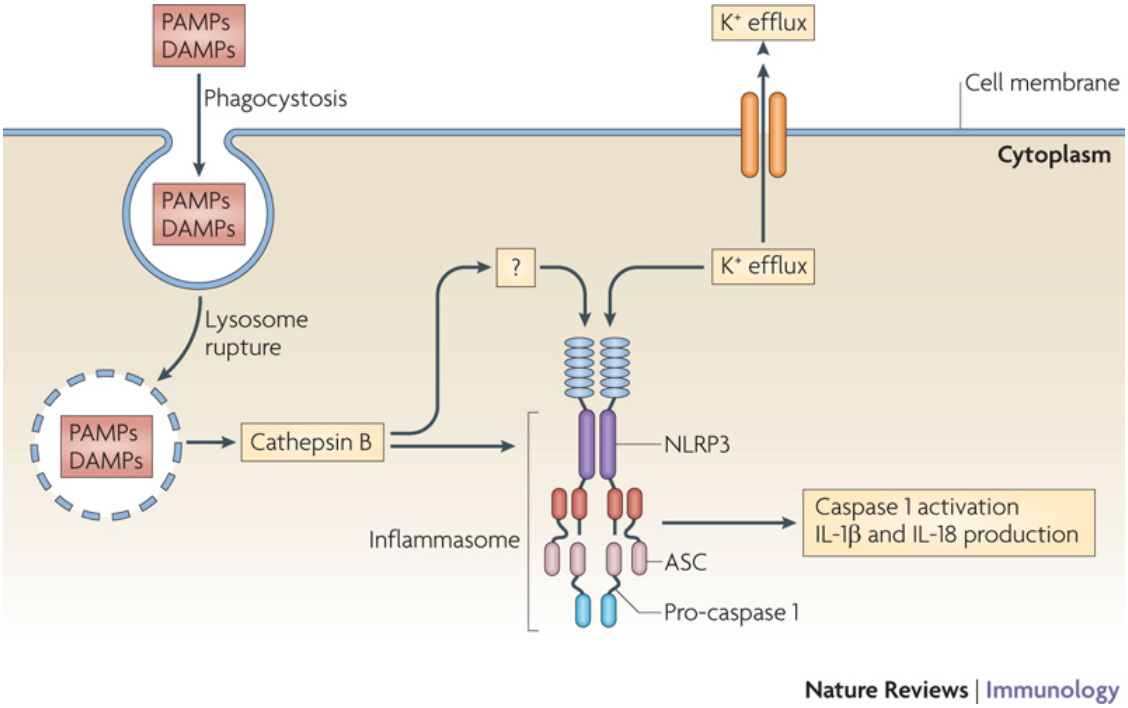

Figure 1.2 The lysosome rupture model of NLRP3 activation. Unstable lysosome breaks and releases cathepsin B which activates NLRP3 directly or indirectly. ASC, apoptosis-associated speck-like protein containing a CARD; DAMPs, damage-associated molecular patterns; IL, interleukin; PAMPs, pathogen-associated molecular patterns. Adapted from Tschopp, 2010 (197) .

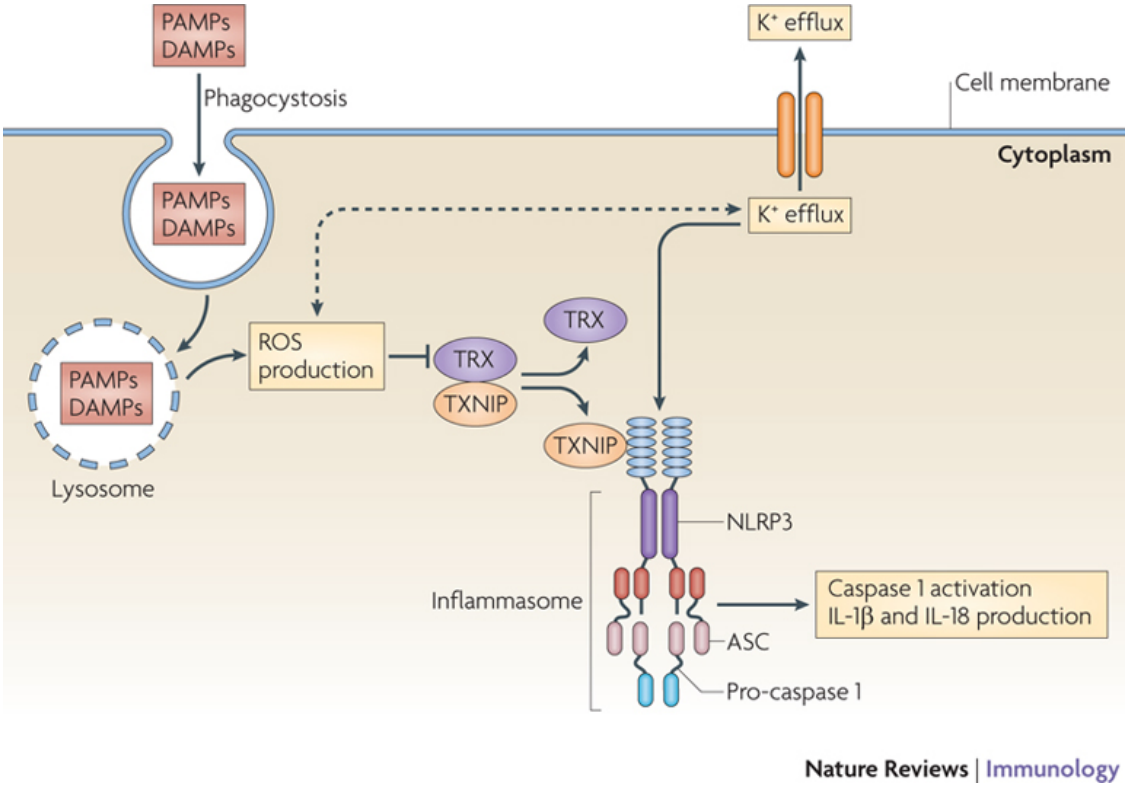

Figure 1.3 The ROS model of NLRP3 activation. ROS production leads to thioredoxin (TRX) dissociation from thioredoxin-interacting protein (TXNIP) which binds NRPL3 and triggers its conformational change. ASC, apoptosis-associated speck-like protein containing a CARD; DAMPs, damage-associated molecular patterns; IL, interleukin; PAMPs, pathogen-associated molecular patterns. Adapted from Tschopp, 2010 (197) .

Chapter 2. Amino acids 177L and 206E are crucial for the enhanced inhibitory activity of *Y. pestis* strain KIM5 effector YopJ on NF-κB pathway

2.1 Summary

It has been demonstrated that YopJ^{KIM} exhibits the unique capacity to cause enhanced caspase-1 activation and cytotoxicity in infected macrophages (114). I analyzed the YopJ^{KIM} gene and identified that two amino acids, 177L and 206E, were likely crucial for enhanced caspase-1 activation, IL-1β production and cell death. I analyzed YopJ^{KIM} in parallel with other YopJ isoforms that differ in amino acid sequence at residues 177 and 206 for expression, translocation and inhibition of NF-κB. Furthermore, the affinity of different YopJ isoforms for the substrate IKKβ was examined by GST pull down assay. The results reveal that both 177L and 206E in YopJ^{KIM} are important for amplified cytotoxicity, caspase-1 activation and negative regulation of the NF-κB pathway because these amino acids afford more effective binding to IKKβ.

2.2 Introduction

As an innate immune response against microbes, caspase-1 activation has been broadly seen in pathogen infections, such as those caused by *Salmonella*, *Legionella*, and *Shigella* (134, 190, 200). Two types of *Yersinia*-induced caspase-1 activation in macrophages were discovered, both requiring a functional T3SS but differentiating in the requirement for YopJ (13, 21, 182). In one type of caspase-1 activation pathway, it appears that T3SS introduces pores in the macrophage plasma membrane (197). YopE and YopT, which interfere with actin arrangements, are able to

block caspase-1 activation by repairing these pores formed by the T3SS (176). The presence of YopK also reduces T3SS-initiated caspase-1 activation by an unknown mechanism (22). Another kind of caspase-1 activation mechanism requires the T3SS and YopJ, but the responding inflammasome is not known (22). *Y. pestis* KIM5 not only gives rise to enhanced killing of infected macrophages, but also elicits strong caspase-1 activation in a $YopJ^{KIM}$-dependent way (114). These activities can be transferred to a *Y. pseudotuberculosis ΔyopJ* strain when $YopJ^{KIM}$ was ectopically expressed in this strain (114). As two amino acid polymorphisms were identified in $YopJ^{KIM}$ as compared to other YopJ isoforms, we hypothesized that these differences affect $YopJ^{KIM}$ activity. In this chapter, we aimed to determine if and how these two amino acids alter $YopJ^{KIM}$ activity.

2.3 Experimental Methods

***Yersinia* strains and growth conditions.** *Y. pestis* and *Y. pseudotuberculosis* strains used in this study are listed in Table 2.1. *Y. pestis* strains used in this study are derived from KIM5 (114), which lacks the pigmentation locus (*pgm*) and are exempt from select agent guidelines and conditionally attenuated. Introduction of codon changes into *yopJ* in KIM5 (Table 2.1) was performed using the suicide plasmid pSB890 and allelic exchange as described (224). The resulting plasmids were used to transform IP26 (IP2666 Δ*yopJ*) using electroporation and selection on LB agar plates containing ampicillin (100 μg/ml) (114). Bacteria were grown in heart infusion broth (HI) at 28°C overnight, then diluted 1 to 20 in HI with 2.5mM $CaCl_2$ and shifted to 37°C for two hours. Temperature shift to 37°C allowed the T3SS assembly and Yops translocation upon host cell contact. Secretion of Yops was inhibited by Ca^{2+}. IP26-derived strains were grown as above except that LB broth was used with a 1 to 40 dilution.

Construction of pBAD-yopJ mutation plasmids. The pBAD-YopJ-GSK was a gift from Dr. Gregory Plano (University of Miami). The plasmid expresses KIM5YopJ with a GSK tag under arabinose induction. The GSK tag is phosphorylated by a host cell kinase and can be differentiated from non-phospho-GSK by anti-phospho-GSK antibody. Site-directed mutagenesis was done to introduce the 177F, 206K and 177F206K mutations into pBAD-YopJ-GSK. All mutant *yopJ* genes were verified by sequencing.

Construction of KIM5 *yopJ* mutants. KIM5 *yopJ* and *yopJ* mutant genes were cloned from pBAD-YopJ-GSK plasmids and inserted into the suicide vector pSB890. This plasmid was conjugated into KIM5 by use of *Escherichia coli* strain S17*λpir* and transconjugants were selected on *Yersinia* selection medium containing tetracycline. Transconjugants were grown as overnight cultures and spread on sucrose-containing plates to force recombination and pSB890 excision. The mutant *yopJ* genes were amplified by colony PCR. To verify the presence of the codon change, the L177F mutation was detected by mismatch PCR. The forward mismatch primer was complementary to the sequence of the KIM5 *yopJ*177L, but not 177F, so the PCR was negative for *yopJ*177F and positive for KIM5 *yopJ*. The E206K codon change was detected by HphI digestion. A PCR product consisting of *yopJ* was digested by this enzyme, but not if it contains the mutation 206K. L177FE206K double mutant was constructed by introducing pSB890*yopJ*177F206K in K177. KIM5 *yopJ*^{C172A} was constructed by allelic exchange placing GCGGC (172 Ala and 173 Gly) instead of TGTGGT (172 Cys and 173 Gly) in the virulence plasmid. All mutants were verified by sequencing.

Bone marrow macrophage isolation and culture conditions. Bone marrow derived macrophages (BMDM) were isolated from the femurs of 6- to 8-week-old C57BL/6 female mice (Jackson Laboratories) and cultured as previously described (157). Briefly, isolated bone marrow

cells from two femurs were seeded in four 10 cm non-tissue culture treated plates (Nunc) at a concentration of 4×10^6 cells/plate in 20ml of Dulbecco's Modified Eagle Medium (DMEM) GlutaMax supplemented with 20% fetal bovine serum, 30% L-cell-conditioned medium and 1% 0.1M sodium pyruvate (BMM-high). After 5 days of incubation at 37°C and 5% CO_2, macrophages were harvested for infection assays.

Macrophage infections for LDH release, cytokine ELISA. Murine bone marrow derived macrophages were seeded in 24-well plates at a density of 1.5×10^5 cells/well one day before experiment in BMM low medium containing 10% fetal bovine serum, 15% L-cell-conditioned medium, and 1% 0.1M sodium pyruvate. Bacteria were grown as described above and used to infect cells at multiplicity of infection (MOI) of 10 bacteria per cell. Each infection condition was performed in duplicate. Plates were spun at 95×g for 5 minutes and incubated at 37°C with 5% CO_2 for 15 minutes to allow the bacteria to be phagocytosed by the cells. Fresh medium containing 8ug/ml gentamicin was added for 1 hour to kill extracellular bacteria. Medium with 4.5ug/ml gentamicin was maintained for the remaining time. For expression of YopJ from pBAD plasmid in *Yersinia*, 0.2% arabinose was added into cell culture medium with gentamicin for the remaining time.

Cytokine measurement. IL-1β and TNF-α secretions were measured by Quantikine Mouse IL-1β and TNF-α Immunoassay kit according to the manufacturer's instruction (R&D). IL-18 was detected by mouse IL-18 ELISA Kit (MBL). Briefly, supernatants were collected 24 hr post infection, spun down to exclude cell debris and transferred to new tubes. 50ul of each sample were tested.

Cell death assay. Lactate dehydrogenase (LDH) release assay was performed to measure cell death percentage by using the CytoTox-96 nonradioactive cytotoxicity assay following

manufacturer's instruction (Promega). Supernatants were collected 24 hr post infection, spun down and transferred to new tubes. Fifty microliters of each sample were tested. Total LDH release was measured by freezing and thawing uninfected cells. Spontaneous release was measured from uninfected cell supernatants. Blank was made by medium. The LDH content in each well was measured in triplicate. The percentage of cell death was calculated as follows: percentage of LDH release= (LDH infected- LDH spontaneous)/ (LDH total– LDH spontaneous)×100%.

Immunoblotting of *Y. pestis* lysates. *Y. pestis* strains were grown in defined TMH medium at 28°C overnight. Cultures were diluted 1 to 20 in TMH containing 2.5mM Ca^{2+}, shaken at 28°C for 2 hr and transferred to 37°C for 4 hr with shaking to induce Yop expression. Bacteria were normalized by optical density (OD) and spun down. Pellets were boiled in 1× Laemmli buffer. Samples of the lysates were resolved by 10% SDS-PAGE and processed for immunoblotting using mouse anti-YopJ monoclonal antibody (224) at a 1:1000 dilution at 4°C overnight. IRDye800 conjugated goat anti-mouse antibody (Rockland) was used as the secondary antibody. The blots were scanned by Odyssey (LI-COR) and reprobed using a mouse monoclonal anti-YopH antibody as the loading control.

Immunoblotting of secreted Yops. IP26 strains containing pBAD plasmids encoding different YopJ isoforms were grown overnight with shaking in LB broth at 28°C. The next day, the cultures were diluted 1:40 in LB containing 20 mM NaOX and 20 mM $MgCl_2$ and incubated at 28°C with shaking for 2 hr. To induce Yop expression, 0.2% arabinose was added to cultures and incubation was continued for 4 hr at 37°C with aeration. Bacteria were normalized by OD_{600} measurements and centrifuged to collect supernatants. Trichloroacetic acid (TCA) was added to supernatants to a final concentration of 10% and samples were rotated overnight at 4°C. The next

day, samples were centrifuged at maximum speed in a microcentrifuge for 30 minutes at 4°C and supernatants were discarded. Pellets were washed with cold acetone and centrifuged at maximum speed for 5 minutes at 4°C after which the acetone was discarded and samples were dried by vacuum centrifugation. Pellets were dissolved in 1X Laemmli buffer, and the resulting samples were resolved by SDS-PAGE (10% gels) and processed for immunoblotting. Immunoblots were developed with mouse anti-GSK monoclonal antibody (Cell Signaling) and goat anti-mouse IRDye800 secondary antibody (Rockland). The blots were scanned by Odyssey (LI-COR). Immunoblots were reprobed with polyclonal rabbit anti-YopE antibody (16) as a loading control.

Macrophage infections for YopJ translocation and caspase-1 cleavage assays. *Y. pseudotuberculosis* strains were grown in 2xYT at 26°C overnight and diluted 1:40 in the same medium supplemented with 20 mM NaOX, and 20 mM $MgCl_2$. Cultures were shaken at 26°C for 1 hr and shifted to 37°C for 2 hr. BMDMs were seeded into wells of 6-well plates at a density of 10^6 cells/well. Bacteria were harvested, washed with DMEM and added to BMDMs at an MOI of 20. After 1 hr of infection gentamicin was added to a final concentration of 100 μg/ml. To induce expression of YopJ-GSK proteins, arabinose (0.2%) was maintained during grown in 2xYT at 37°C and in the cell culture medium used for infection. *Y. pestis* strains were grown and used to infect macrophages as above except that HI broth was used and arabinose was omitted. Two hr post-infection, infected BMDMs were washed with PBS and lysed in buffer containing 50 mM Tris-HCl pH 8.0, 5 mM EDTA, 2% Triton X-100, and 0.02% sodium azide with protease inhibitors. In some experiments the macrophages were incubated with 50 ng/ml of LPS for 3 hr and then exposed to ATP at final concentration of 2.5 mM for 1 hr as a positive control for caspase-1 cleavage. Proteins were resolved by 10% SDS-PAGE, transferred to a PVDF membrane and probed with anti-phospho-GSK-3β primary antibody (Cell Signaling). In some

experiments the blots were stripped and re-probed with rabbit polyclonal anti-caspase-1 antibodies (Santa Cruz) or directly developed with this antibody. As a loading control blots were reprobed with an anti-actin antibody (Sigma-Aldrich, clone AC15). Goat anti-rabbit HRP conjugated secondary antibody was used. Blots were detected with ECL reagent (Perkin Elmer Life Sciences, Inc.).

Phospho-IκBα ELISA. BMDMs (10^6 cells per well) were seeded in 6-well plates. *Y. pestis* cultures were grown as above and used to infect BMDM at an MOI of 50. One hr post infection, cells were washed with ice-cold PBS and incubated in 150ul of 1X Lysis Buffer (Cell Signaling) for 5 min. Cells were scraped on ice and sonicated twice for 5 seconds each. Lysates were centrifuged at full speed at 4°C for 10 min and 100 µl of supernatant was used for ELISA. Phospho-IκBα levels were determined using a PathScan Phospho-IkappaB-alpha (Ser32) Sandwich ELISA kit according to manufacturer's protocol (Cell Signaling).

Macrophage infections for Phospho-MAPK ELISA. BMDMs (10^6 cells per well) were seeded in 6-well plates. *Y. pestis* cultures were grown in HI at 28°C overnight and diluted 1:20 next day in the same medium supplemented with 20mM NaOX and 20mM MgCl2. Cultures were shaken at 28°C for 1 hr and switched to 37°C for 2 hr. Cells were infected at an MOI of 20 and incubated for 30 or 60 min without adding gentamicin. Macrophages were harvested and lysed as above. The PathScan MAP Kinase Multi-Target Sandwich ELISA kit was used to determine phospho-ERK, -p38 and –JNK levels according to manufacturer's instruction (Cell Signaling).

GST pull down assay of $YopJ^{KIM}$-IKKβ interaction. Plasmids for expression of GST-YopJ fusion proteins were constructed from pLP16 (148). The pLP16 vector was derived from pGEX-2T and codes for $YopJ^{YPTB}$ with an N-terminal glutathione-S transferase (GST) affinity tag and a C-terminal M45 epitope tag. Quikchange mutagenesis (Invitrogen) was used to introduce codon

changes into pLP16 to generate pGEX-2T-YopJ^{KIM}, pGEX-2T-YopJ^{KIMC172A} and pGEX-2T-YopJ^{CO92}, which encode GST-YopJ^{KIM}, GST-YopJ^{C172A} and GST-YopJ^{CO92}, respectively. The plasmids pGEX-2T, pGEX-2T-YopJ^{KIM}, pGEX-2T-YopJ^{KIMC172A} and pGEX-2T-YopJ^{CO92} were used to transform *E. coli* TUNER cells (Novagen). Cultures of TUNER cells harboring the above plasmids were grown in LB at 37°C to OD600 of 0.2. IPTG was added to 0.1mM final concentration and cultures were grown at 18°C with shaking for 4 hr. The bacterial pellet obtained from 40 ml of each culture was resuspended in PBS supplemented with protease inhibitor cocktail (Roche) and sonicated on ice. The solubility of proteins in the sonication was increased by incubation in the presence of a buffer containing 10% sarkosyl at 4°C overnight (192). After centrifugation, the supernatant of the bacterial lysate was diluted 5 times with a buffer containing 4% Triton X-100 and 40 mM CHAPS at final concentrations. Thirty μl of glutathione beads (GST Bind Kit, Novagen) were added and the mixture was rotated at 4°C for 1 hr. Beads were washed 4 times with 1 ml of GST Bind Kit buffer and used for pull down assays.

Cell lysates containing overexpressed IKKβ were prepared from HEK293T cells tranfected with a retroviral construct (pCLXSN-IKKβ-IRES-GFP) (223). HEK293T cells were seeded in 10cm dishes and grown to reach 70% confluence. The culture medium was replaced with serum free DMEM and the HEK293T cells in each dish were transfected with 10 μg of pCLXSN-IKKβ-IRES-GFP using a calcium phosphate method. Six hr post transfection, the culture medium was replaced with DMEM containing 10% FBS. Cells were harvested 48 hr post transfection, sonicated in PBS and centrifuged. Supernatants were stored at -80°C until use.

Beads containing bound GST proteins were incubated with 250 μl of cell lysate supernatants from transfected HEK293T supernatant for 4 hr at 4°C with constant rotation. The beads were then washed 4 times with 1 ml of PBS each and proteins bound to the beads were

eluted in boiling 2X Laemmli sample buffer. Samples of the elutes were subjected to SDS-PAGE and immunoblotting. Rabbit polyclonal anti-IKKβ antibodies and mouse monoclonal anti-GST antibodies were purchased from Cell Signaling and Santa Cruz, respectively. Immunoblot signals representing IKKβ and GST or GST fusion proteins were quantified using an Odyssey imaging system.

Statistical analysis. Experimental data analyzed for significance (GraphPad Prism 4.0) were performed three independent times. Probability (P) values for multiple comparisons of cytokine, phospho-IκBα ELISA and LDH release data were calculated by one-way ANOVA and Tukey's multiple comparisons post-test. P values for two group comparisons of cytokine and phospho-MAPK ELISA were calculated by two-tailed paired student t test. P values were considered significant if less than 0.05.

2.4 Results

Amino acid substitutions in YopJ^{KIM} do not alter expression and secretion levels as compared to other YopJ isoforms. Sequence comparisons were made between YopJ^{KIM} and YopJ proteins from two other *Yersinia* strains that display lower apoptosis activity in macrophages, *Y. pseudotuberculosis* IP2666 and *Y. pestis* CO92. There is one amino acid difference between YopJ^{KIM} and YopJ in *Y. pseudotuberculosis* (YopJ^{YPTB}), corresponding to L177F in the predicted catalytic core (145) of the enzyme (residues 109-194; Figure 2.1). Comparison of YopJ^{KIM} with YopJ from *Y. pestis* CO92 (YopJ^{CO92}) revealed two differences, L177F and E206K, the latter of which is located just beyond the carboxy-terminal end of the predicted catalytic core (Figure 2.1). The differential ability to induce IL-1β and cell death may come from differences in YopJ expression, translocation or interaction with the NF-κB pathway. To construct *Y. pestis* KIM5 strains expressing different YopJ isoforms, a L177F codon change

was introduced into the sequence of *yopJ*^{KIM} on pCD1 by allelic exchange, converting it to *yopJ*^{YPTB}. In addition, an E206K codon change, a double L177F/E206K codon change, and a C172A codon change were introduced into pCD1, creating *yopJ*^{KIME206K}, *yopJ*^{CO92}, and *yopJ*^{C172A}, respectively**.** The resulting strains (referred to as Yp-YopJ^{YPTB}, Yp-YopJ^{KIME206K}, Yp-YopJ^{C092} and Yp-YopJ^{C172A}) (Table 2.1) were phenotypically analyzed. To measure total YopJ expression in the KIM5 strains, they were grown in Ca^{2+}- containing medium to inhibit Yop secretion. YopJ immunoblotting was done to quantify expression with YopH as the loading control. In all KIM5 strains, the different YopJ isoforms were expressed at levels similar to the wild type YopJ^{KIM} (Figure 2.2A).

To determine if the amino acid substitutions at positions 177 and 206 of YopJ^{KIM} affect secretion of the effector, expression plasmids encoding YopJ^{KIM}, YopJ^{YPTB}, YopJ^{KIME206K} or YopJ^{CO92} appended with C-terminal GSK tags were constructed. The expression plasmids were introduced into a Δ*yopJ* mutant of *Y. pseudotuberculosis* (IP26; Table 2.1). *Y. pseudotuberculosis* was used in the experiment because it lacks the Pla protease of *Y. pestis* which is known to degrade Yops secreted *in vitro* (185). The resulting strains were induced to secrete Yops under low calcium growth conditions and immunoblotting of the secreted proteins showed that YopJ^{KIM}, YopJ^{YPTB}, YopJ^{KIME206K} and YopJ^{CO92} were exported at equal levels (Figure 2.2B).

Amino acid polymorphisms at positions 177 and 206 in YopJ^{KIM} do not enhance translocation, but increase caspase-1 activation in *Y. pestis*-infected macrophages. A translocation assay was performed using the phospho-GSK reporter system (68). IP26 strains expressing the different YopJ isoforms fused to GSK were used to infect BMDMs for 2 hr. Delivery of the effector into host cells was measured by anti-phospho-GSK immunoblotting

(68). The results showed that YopJ^{KIM}, YopJ^{YPTB}, YopJ^{KIME206K} and YopJ^{CO92} isoforms were translocated at similar levels (Figure 2.3A). Samples of the same lysates analyzed in Figure 2.3A were subjected to immunoblotting with anti-caspase-1 antibody to measure the level of caspase-1 cleavage. Consistent with previous results (22), cleavage of caspase-1 was detected in BMDMs infected with *Y. pseudotuberculosis* expressing YopJ^{YPTB} (Figure 2.3B, lane 2). However, caspase-1 cleavage was comparatively higher with expression of YopJ^{KIM} (lane 1) and lower with expression of YopJ^{KIME206K} or YopJ^{CO92} isoforms (lanes 3 and 4, respectively). These results suggest that the ability of YopJ^{KIM} to trigger maximal caspase-1 activation requires both the F177L and K206E substitutions, and these codon changes impart an activity to the protein that is manifested following its delivery into the host cell.

The F177L and K206E substitutions in YopJ^{KIM} are important for enhanced cell death and cytokine secretion in *Y. pestis*-infected macrophages. The ability of *Y. pestis* strains expressing the different YopJ isoforms to induce apoptosis and cytokine secretion in BMDMs was determined after a 24 hr infection. As shown in Figure 2.4A, the amounts of lactate dehydrogenase (LDH) released (used as a marker of late apoptotic cell death) and IL-1β (Figure 2.4B) secreted were significantly lower in macrophages infected with Yp-YopJ^{YPTB}, Yp-YopJ^{KIME206K} or Yp-YopJ^{CO92} as compared to Yp-YopJ^{KIM}. A similar trend was seen for secretion of IL-18 (Figure 2.4C).

As a control, levels of TNF-α, which is secreted independent of caspase-1 activity, were measured. Macrophages infected with Yp-YopJ^{C172A} or Yp-YopJ^{CO92} secreted significantly higher levels of TNF-α as compared to Yp-YopJ^{KIM}, whereas the other mutants tested produced intermediate results (Figure 2.4D). Overall, these results indicate that amino acid substitutions at positions 177 and 206 are important for the ability of YopJ^{KIM} to induce high levels of

macrophage apoptosis, caspase-1 activation and secretion of mature IL-1β and IL-18 in *Y. pestis*-infected macrophages. Conversely, the amino acid substitutions at positions 177 and 206 are important for the ability of YopJ^{KIM} to inhibit TNF-α secretion in macrophages under the same conditions.

YopJ^{KIM} binds to IKKβ with higher affinity and more efficiently inhibits phosphorylation of IκBα as compared to YopJ^{CO92}. To determine if YopJ^{KIM} has higher affinity for IKKβ as compared to other YopJ isoforms, several different YopJ proteins were assayed for the ability to bind this kinase in cell lysates. Purified GST-YopJ fusion proteins or GST alone bound to beads were incubated in HEK293T cell lysates that contained overexpressed IKKβ. The amount of IKKβ and GST protein recovered on the beads after washing was measured by quantitative immunoblotting. IKKβ bound to beads coated with GST-YopJ^{KIM} but not to beads coated with GST alone (Figure 2.5A, compare lanes 2 and 3). There was reduced binding of IKKβ to GST-YopJ^{CO92} as compared to GST-YopJ^{KIM} (Figure 2.5A, compare lanes 3 and 5). When the amount of bound IKKβ was normalized to the amount of GST fusion protein recovered, it was estimated that 10-times less IKKβ bound to GST-YopJ^{CO92} as compared to GST-YopJ^{KIM} (Figure 2.5B). A GST fusion protein encoding YopJ^{C172A} bound ~5 times less IKKβ as compared to GST-YopJ^{KIM} (Figure 2.5A, compare lanes 3 and 4, Figure 2.5B), suggesting that the catalytic Cys residue contributes to binding between IKKβ and YopJ^{KIM}. Overall, these results suggest that YopJ^{KIM} has higher affinity for IKKβ as compared to YopJ^{CO92}.

To determine if YopJ^{KIM} is a better inhibitor of IKKβ than YopJ^{CO92}, the amount of phosphorylated IκBα (p-IκBα) in BMDMs was measured after a 1 hr infection. As shown in Figure 2.5C, significantly lower levels of p-IκBα were present in macrophages infected with Yp-

YopJ^{KIM} as compared to BMDMs infected with Yp-YopJ^{CO92}. Because IκBα is directly phosphorylated by IKKβ, these results are consistent with the idea that YopJ^{KIM} more efficiently inhibits IKKβ activity as compared to YopJ^{CO92}.

YopJ^{KIM} more efficiently inhibits activation of MAPKs as compared to YopJ^{CO92}. In addition to binding to and acetylating IKKβ, YopJ binds to and acetylates other members of the MKK superfamily including MKK1, MKK2, MKK3, MKK4, MKK5, and MKK6 (133, 138, 145). There is evidence that YopJ binds to a site conserved on members of the MKK-IKK superfamily (84). Since we had previously obtained evidence that inhibition of MAPK signaling was critical for YopJ-induced macrophage apoptosis (225), it was important to determine if YopJ^{KIM} could more efficiently inhibit MAPK phosphorylation as compared to YopJ^{CO92}. BMDMs were left uninfected or infected for 30 or 60 min with Yp-YopJ^{KIM}, Yp-YopJ^{CO92}, or Yp-YopJ^{C172A} and ELISA was used to measure phosphorylation of the MAPKs ERK (substrate of MKK1/2), p38 (substrate of MKK3/6) and SAPK/JNK (substrate of MKK4/7) (Materials and Methods). As shown in Figure 2.6A, ERK was not phosphorylated to a large degree at either time point in macrophages infected with Yp-YopJ^{C172A} and therefore it was not possible to evaluate the degree to which ERK phosphorylation was inhibited by either YopJ^{KIM} or Yp-YopJ^{CO92}. In contrast, p38 and JNK did show increased phosphorylation upon infection with Yp-YopJ^{C172A}, especially at the 30 min time point (Figure 2.6B and C, respectively). There was in general reduced phosphorylation of p38 and JNK in BMDMs infected with Yp-YopJ^{KIM} as compared to YopJ^{CO92}, especially at the 30 min time point, and the difference was statistically significant in the case of JNK (Figure 2.6B and C). These results suggest that YopJ^{KIM} more efficiently inhibits the activities of MKK3/6 and MKK4/7 as compared to YopJ^{CO92}.

2.5 Discussion

It was previously shown that caspase-1 was activated during YopJ-induced apoptosis of macrophages infected with *Y. pseudotuberculosis* (22). In addition, it was demonstrated that YopJ^{KIM} had increased capacity to cause macrophage apoptosis and activate caspase-1 as compared to other YopJ isoforms (114). However, the mechanism of YopJ-induced caspase-1 activation and the molecular basis for enhanced apoptosis and activation of caspase-1 in macrophages by YopJ^{KIM} was unknown. The results of studies reported here indicate that several of the requirements for YopJ-induced apoptosis and caspase-1 activation are the same, and therefore it is likely that these two processes are mechanistically connected. TLR4 signaling is important for YopJ-induced macrophage apoptosis (135, 171, 222) and caspase-1 activation (224). In addition, comparison of the activities of different YopJ isoforms showed a direct correlation between cell death, caspase-1 activation and inhibition of MAPK and NF-κB signaling pathways.

Inhibition of MAPK and NF-κB pathways by YopJ is thought to reduce expression of survival factors (e.g. FLIP, XIAP), thereby redirecting TLR4 signaling to trigger apoptosis (171, 222, 225). Data presented here suggest that YopJ^{KIM} triggers increased cytotoxicity and caspase-1 activation because it is a better inhibitor of macrophage survival pathways than other YopJ isoforms. YopJ^{KIM} could function as a better inhibitor of macrophage signaling pathways if it had a longer half-life in the host cell, or had higher affinity for substrates. The F177L polymorphism could increase protein stability, although it is not immediately clear why a Leu at position 177 rather than a Phe would increase protein half-life. The K206E mutation could increase half-life, which is reasonable since Lys residues can be subject to ubiquitination. Although not mutually exclusive of the preceding ideas, we favor the hypothesis that the F177L and K206E

substitutions allow YopJ^{KIM} to bind more tightly to substrates, thereby making acetylation of targets more efficient at limiting enzyme concentrations. We obtained two pieces of evidence supporting this hypothesis. First, YopJ^{KIM} had higher apparent affinity for IKKβ than YopJ^{CO92} when these interactions were measured in cell lysates by a GST pull down assay. Second, macrophages infected with Yp-YopJ^{KIM} had lower levels of phosphorylated IκBα and MAPKs as compared to macrophages infected with Yp-YopJ^{CO92}, indicating that there was increased inhibition of IKKβ and MAPK kinase activity by Yp-YopJ^{KIM}.

The results suggest a model whereby the canonical *yopJ* allele in *Y. pseudotuberculosis* (*yopJ*^{YPTB}) was inherited by an ancestral *Y. pestis* strain, from which it evolved to encode an isoform with higher apoptotic and caspase-1-activating potential, YopJ^{KIM}, by the F177L mutation. The predicted sequence of a YopJ protein in *Y. pestis* biovar 2.MED strain K1973002 (ZP_02318615) is identical to the sequence of YopJ^{KIM}, suggesting that the phenotype observed is not an artifact resulting from a mutation acquired during laboratory passage, but is associated with a unique *yopJ* genotype associated with 2.MED strains. It is also hypothesized that the *yopJ*^{CO92} allele evolved from *yopJ*^{YPTB} to encode an isoform with lower cytotoxic and caspase-1 activating potential (YopJ^{CO92}) by the E206K codon substitution. How these polymorphisms in YopJ affect *Y. pestis* virulence and or the host response is not known but is an important question to address in future studies.

Acknowledgements

I thank Igor Brodsky for contributing the YopJ translocation assay and caspase-1 immunoblotting. Thanks to Gregory Plano from University of Miami for the pBAD-YopJ-GSK plasmid. I acknowledge Bliska lab members who contributed to this study: Hana Fukuto for construction of KIM5, Galina Romanov for preparing and maintaining BMDM cultures, and Yue Zhang and Shirou Wu for construction of KIM5 *YopJ*^{C172A}.

Table 2.1. *Yersinia* strains used in this study

Strain name	Relevant Characteristics	Reference or source
Y. pestis		
Yp-YopJ^{KIM}	KIM5, Biovar 2.MED, (pCD1Ap, pMT1^{+}, pPCP1^{+}, Δ*pgm,* Ap^{r})	(114)
Yp-YopJ^{C172A}	KIM5 pCD1Ap *yopJC172A* (codon change of Cys172 to Ala172), Ap^{r}	(114)
Yp-YopJ^{CO92}	KIM5 pCD1Ap *yopJL177F E206K* (codon change of Leu177 to Phe177, Glu206 to Lys206), Ap^{r}	This Study
Yp-YopJ^{YPTB}	KIM5 pCD1Ap *yopJL177F* (codon change of Leu177 to Phe177), Ap^{r}	This Study
Yp-YopJ^{KIME206K}	KIM5 pCD1Ap *yopJE206K* (codon change of Glu206 to Lys206), Ap^{r}	This Study
Y. pseudotuberculosis		
IP26	Serogroup O3, IP2666 pYV *yopJΔ1-867*	(114)

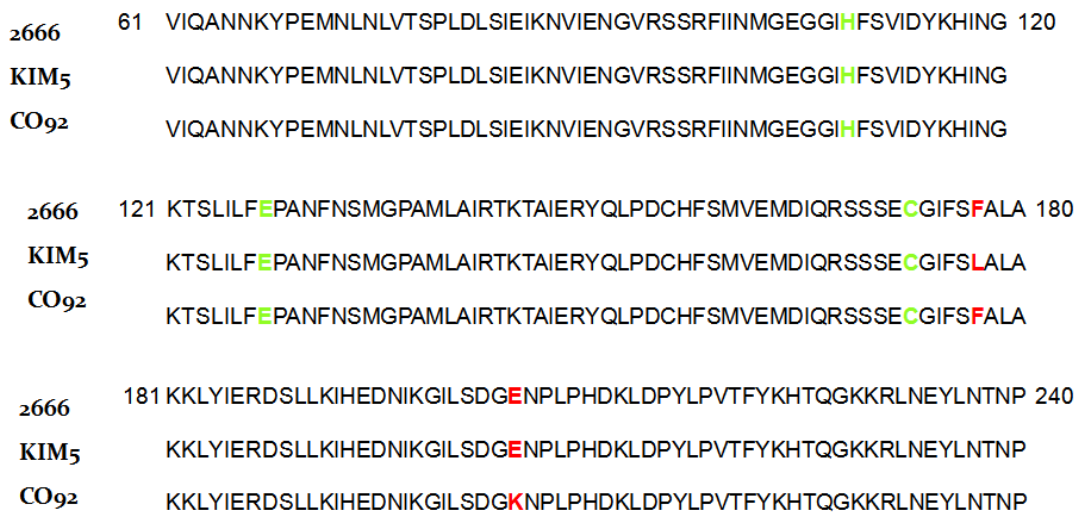

Figure 2.1. Alignment of YopJ from different *Yersinia* strains. Protein sequences are shown from amino acids 61-240 out of 288. Characters in green represent amino acid triads required for YopJ activity. Red letters display the amino acid differences.

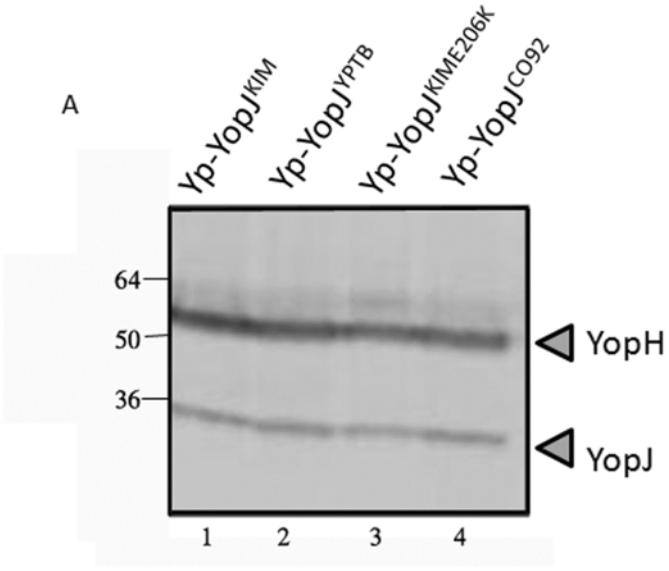
A
Yp-YopJ^KIM
Yp-YopJ^YPTB
Yp-YopJ^KIME206K
Yp-YopJ^CO92
64
50
36
YopH
YopJ
1
2
3
4

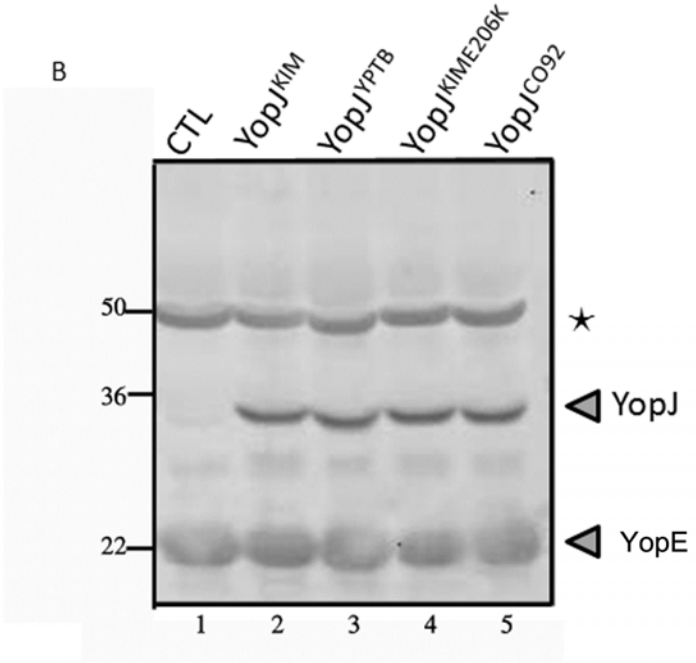
B
CTL
YopJ^KIM
YopJ^YPTB
YopJ^KIME206K
YopJ^CO92
50
36
22
★
YopJ
YopE
1
2
3
4
5

Figure 2.2. Different YopJ isoforms show equal expression and secretion profiles. (A) The indicated Yp-YopJ strains were grown at 37°C in TMH media containing 2.5mM Ca^{2+}, normalized by OD_{600} and lysed in 1× Laemmli buffer. Samples were analyzed by immunoblotting using monoclonal anti-YopJ and anti-YopH monoclonal antibodies. (B) *Y. pseudotuberculosis* IP26 (IP2666*ΔyopJ*) strains harboring pBAD plasmids expressing GSK-tagged $YopJ^{KIM}$ (lanes 1 and 2), $YopJ^{YPTB}$ (lane 3), $YopJ^{KIME206K}$ (lane 4), or $YopJ^{CO92}$ (lane 5), were induced to secrete Yops in low Ca^{2+} LB broth in the absence (lane 1, CTL) or presence (lanes 2-5) of arabinose. Bacterial broth supernatants were precipitated with TCA and dissolved in 1× Laemmli buffer. Samples were processed for SDS-PAGE and immunoblotting. Immunoblots were probed using anti-GSK and anti-YopE antibodies. Asterisk denotes non-specific signal.

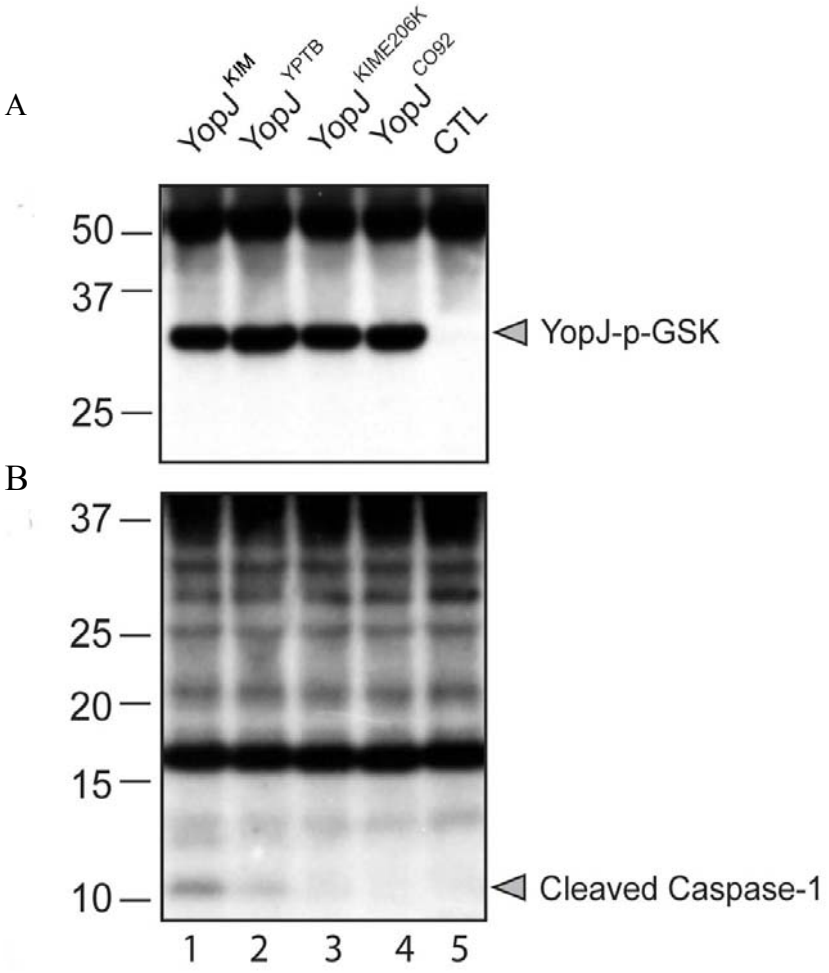

Figure 2.3. Translocation of different YopJ isoforms and caspase-1 activation in macrophages infected with *Y. pseudotuberculosis*. *Y. pseudotuberculosis* IP26 (IP2666Δ*yopJ)* carrying no pBAD plasmid as a control (CTL; lane 5) or pBAD vectors encoding the indicated YopJ-GSK isoforms (lanes 1-4), were grown under T3SS-inducing conditions in the presence of 0.2% of arabinose. Bacteria were added to BMDMs at an MOI of 20 and were allowed to infect for 2 hr. Arabinose (0.2%) was maintained in cell culture medium. Detergent lysates of infected macrophages were separated by SDS-PAGE and immunoblotting was performed with anti-phospho-GSK-3β antibody (A) and anti-caspase-1 antibody (B). Positions of molecular weight standards (kDa) are shown on the left and positions of YopJ- phospho-GSK and cleaved caspase-1 are shown on the right.

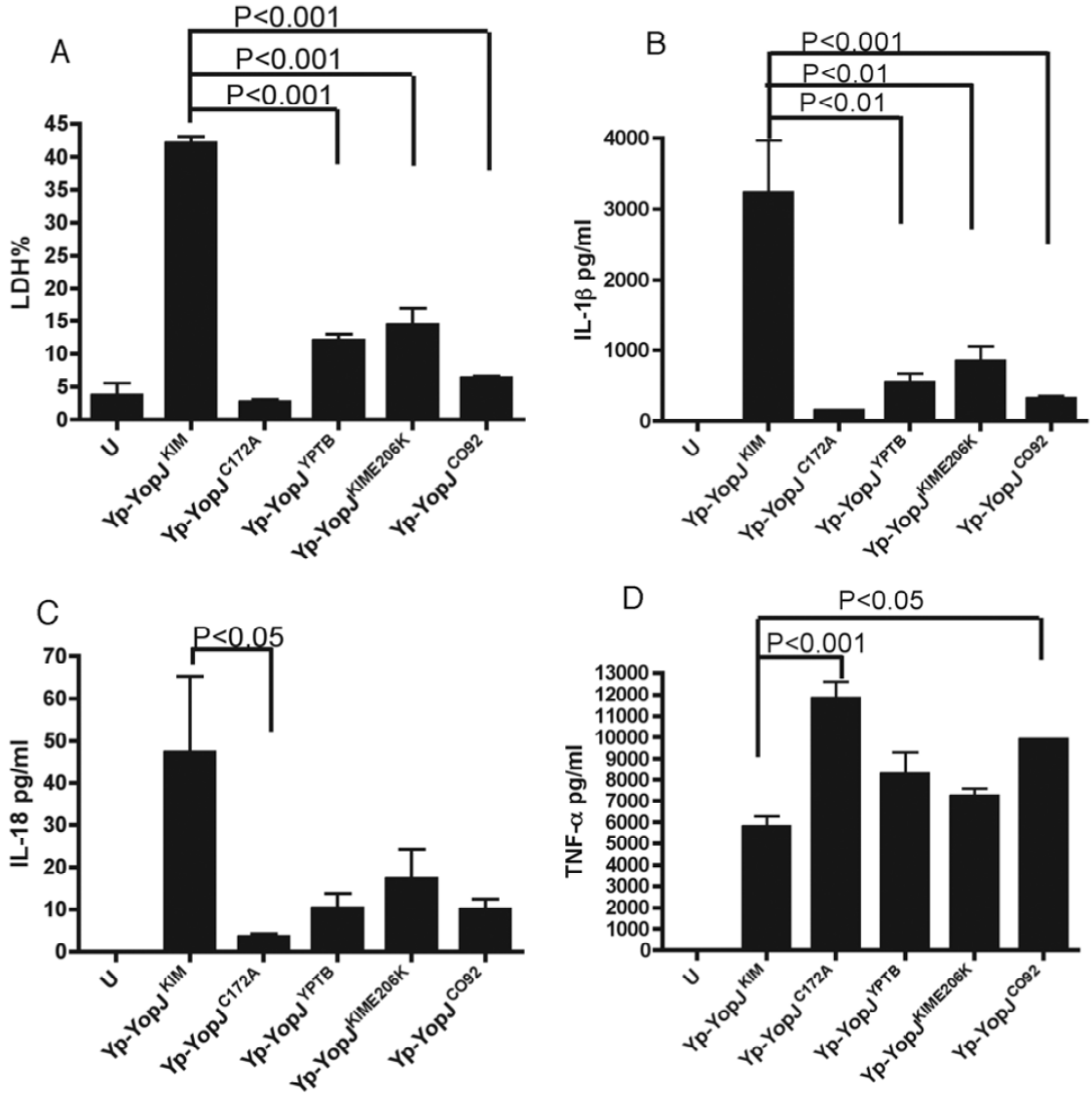

Figure 2.4. Cytokine secretion and cell death in macrophages infected with *Y. pestis* strains expressing different YopJ isoforms. BMDMs were left uninfected (U), or infected with the indicated Yp-YopJ strains at an MOI of 10. Supernatants collected after 24 hr of infection were used to measure cell death by LDH release (A) and secretion of IL-1β (B), IL-18 (C) and TNF-α (D) by ELISA. Results shown are the average of three independent experiments. Error bars represent standard deviation. Bracketing indicates P values (ANOVA) between different conditions.

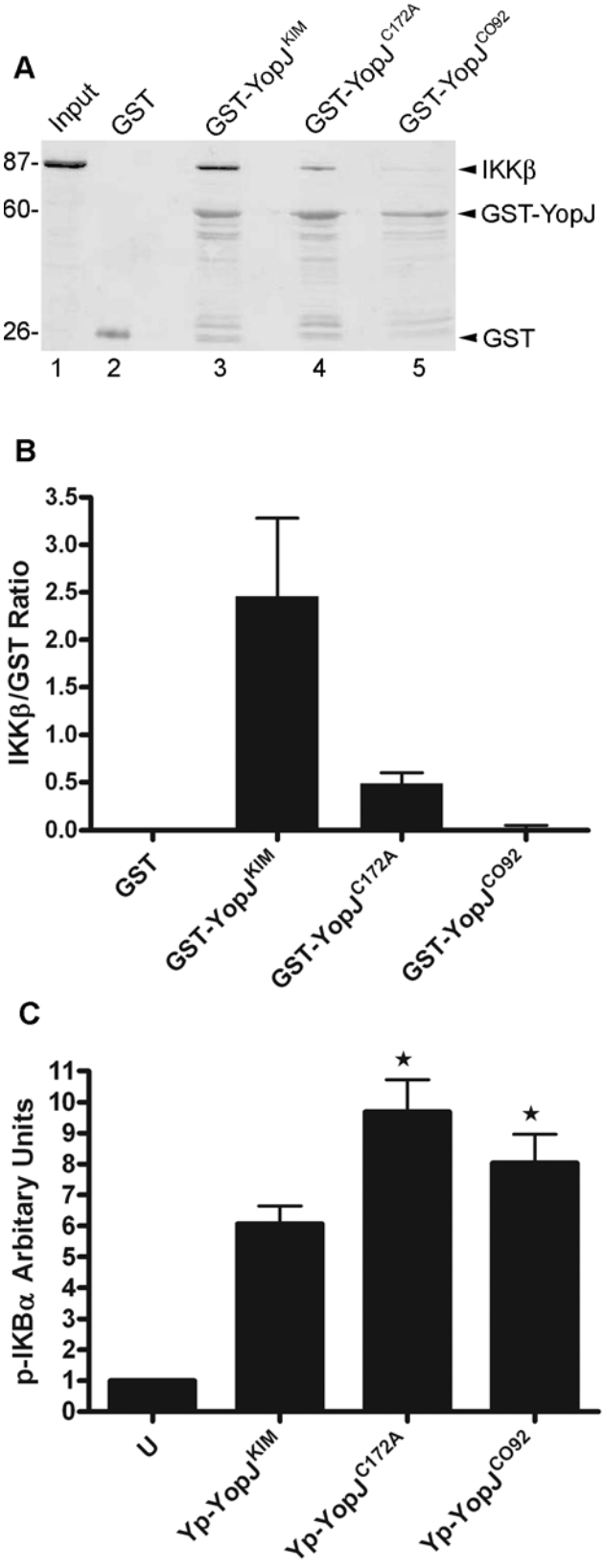
A
Input
GST
GST-YopJ KIM
GST-YopJ C172A
GST-YopJ CO92
87-
60-
26-
IKKβ
GST-YopJ
GST
1
2
3
4
5
B
IKKβ/GST Ratio
3.5
3.0
2.5
2.0
1.5
1.0
0.5
0.0
GST
GST-YopJ KIM
GST-YopJ C172A
GST-YopJ CO92
C
p-IKBα Arbitary Units
11
10
9
8
7
6
5
4
3
2
1
0
U
Yp-YopJ KIM
Yp-YopJ C172A
Yp-YopJ CO92

Figure 2.5. Measurement of IKKβ binding to different YopJ isoforms and phospho-IκBα levels in macrophages infected with different *Y. pestis* strains. (A) Binding of IKKβ to different YopJ isoforms as determined using a GST pull down procedure and lysates of transfected HEK293T cells. Purified proteins corresponding to GST (lane 2) or the indicated GST-YopJ fusion proteins (lanes 3-5) were immobilized on beads and incubated in cell lysates containing overexpressed IKKβ. After washing, proteins bound to the beads were detected and the signals quantified by immunoblotting using antibodies to IKKβ or GST and an Odyssey imaging system. Lane 1 contains a sample of the input transfected cell lysate (TranLys). Positions of molecular weight standards (kDa) are shown on the left and positions of IKKβ**,** GST, and GST-YopJ proteins are shown on the right. (B) Ratios of the signals for IKKβ and GST obtained by immunoblotting are presented in bar graph format, with values representing averages of two independent experiments. (C) BMDMs were left uninfected (U) or infected with Yp-YopJ^{KIM} or YopJ^{CO92} at an MOI of 50. At 1 hr post infection lysates of the infected macrophages were prepared and subjected to ELISA to determine levels of phospho-IκBα. Results show OD450 values averaged from three independent experiments and error bars represent standard deviations.

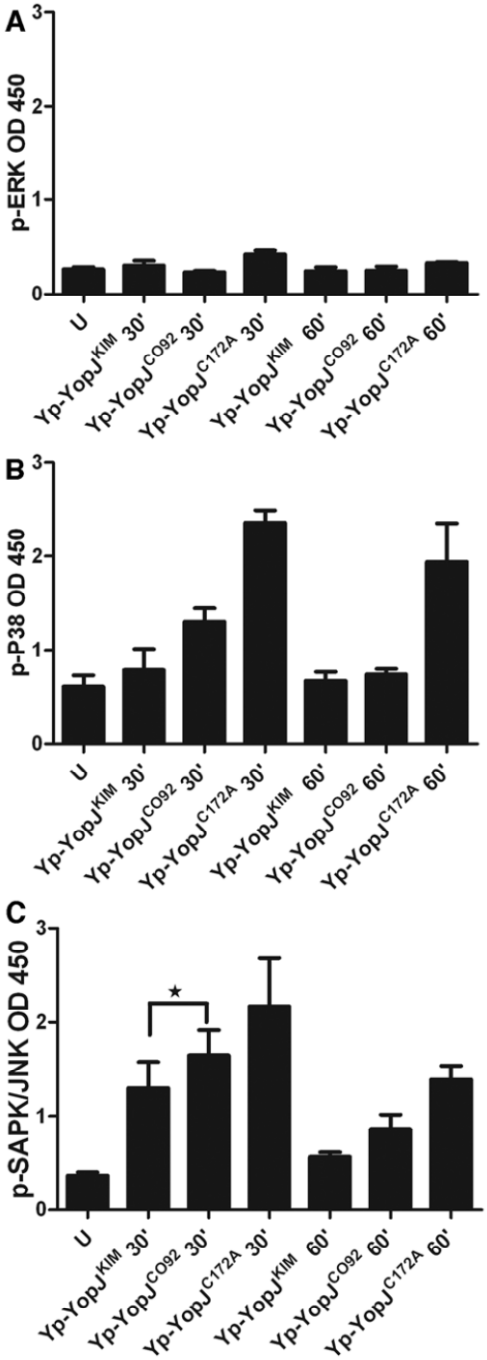

Figure 2.6. Measurement of phospho-MAPK levels in macrophages infected with *Y. pestis* strains expressing different YopJ isoforms. BMDMs were left uninfected (U), or infected with the indicated Yp-YopJ strains at an MOI of 20 At 30 or 60 min post infection lysates of the infected macrophages were prepared and subjected to ELISA to determine levels of phospho-ERK (A), -p38 (B) or –SAPK/JNK (C). Results show OD450 values averaged from three independent experiments and error bars represent standard deviations. P value <0.05 (t test) is indicated by bracket.

Chapter 3: The important role of IKKβ in the negative regulation of caspase-1 activation

3.1 Summary

Caspase-1 activation in *Y. pestis* KIM5-infected macrophages could be linked to enhanced targeting of IKKβ by YopJ^{KIM} as described in Chapter 2. Our aim in the studies described in this chapter was to confirm an important role for IKKβ in the negative regulation of caspase-1 activation. We infected IKKβ-deficient (*Ikkβ*$^{\Delta}$) or wild type (*Ikkβ*$^{F/F}$) macrophages with *Y. pestis* expressing different YopJ isoforms and compared caspase-1 activation levels. Stronger caspase-1 activation and elevated IL-1β were observed in *Ikkβ*$^{\Delta}$ macrophages as compared to the wild type macrophages. Treatment of macrophages with a small molecule IKKβ inhibitor followed by LPS priming was performed to further examine the role of this kinase in regulating caspase-1 activation. A significant increase in IL-1β release was seen in inhibitor-treated macrophages. These results establish that IKKβ plays an important role as a negative regulator of caspase-1 activation in macrophages in response to infection with a live Gram-negative pathogen or exposure to LPS.

3.2 Introduction

Recent studies indicate that YopJ has acetyltransferase activity, acetylating Ser and Thr residues that are critical for the activation of the MKKs and IKKβ (133, 138). A potential explanation for the ability of YopJ to cause caspase-1 activation came from the work of Greten *et al*. who showed that susceptibility to LPS-induced toxicity was increased in mice in which both *Ikkβ* genes were deleted by Cre-mediated recombination (*Ikkβ*$^{\Delta}$ mice) (72). In addition, following

LPS challenge a higher serum level of IL-1β was detected in $Ikk\beta^{\Delta}$ mice as compared to $Ikk\beta^{F/F}$ mice, suggesting caspase-1 activation increased in the absence of IKKβ (74). In vitro study determined that although IL-1β mRNA was dramatically decreased in $Ikk\beta^{\Delta}$ macrophages, mature IL-1β increased profoundly following LPS stimulation, which is consistent with up-regulated caspase-1 activity in the $Ikk\beta^{\Delta}$ cells (74). Similar results were obtained when a small molecule IKKβ inhibitor was used to treat $Ikk\beta^{F/F}$ macrophages, confirming the existence of negative regulation of capase-1 by the IKKβ-NF-κB pathway (74). Based on these data, we hypothesized that $YopJ^{KIM}$ indirectly actives caspase-1 through inhibition of IKKβ. Although IKKα was also acetylated by YopJ when YopJ and IKKα were co-expressed in a cell line (131), when a macrophage-like cell line was infected with *Yersinia,* ectopic expression of IKKα by transfection did not decrease cell death, while ectopic expression of IKKβ and p65 by transfection rescued cell survival (169). These results indicate that YopJ has a preference for targeting IKKβ as compared to IKKα. So in my study, I only considered the canonical IKKβ pathway by using $Ikk\beta^{\Delta}$ macrophages or an IKKβ inhibitor to demonstrate our idea.

3.3 Experimental Methods

Yersinia **strains and growth conditions.** The *Y. pestis* strain KIM5 (Yp-$YopJ^{KIM}$) and KIM5 expressing a catalytically inactivated YopJ (Yp-$YopJ^{C172A}$) were used in this study (Table 2.1, Chapter 2). Bacterial cultures were grown as described in Chapter 2.

Bone marrow macrophage isolation and culture conditions. Bone marrow derived macrophages (BMDM) were isolated from the femurs of 6- to 8-week-old C57BL/6J female mice (Jackson Laboratories), $Ikk\beta^{f/f}$ or $Ikk\beta^{f/f}$*;MLysCre* mice (32, 151) and cultured as previously described in Chapter 2.

Macrophage infections for LDH release, cytokine ELISA and FLICA. Macrophages were seeded and infected as mentioned before. Staining with 6-carboxyfluorescein–YVAD–fluoromethylketone (FAM-YVAD-FMK; fluorescent inhibitor of apoptosis (FLICA)) (Immunochemistry Technologies) to detect active caspase-1 in infected macrophages was performed using fluorescence and phase microscopy as described (114) with the exception that the procedure was performed 9 hr post-infection. Quantification of percent caspase-1 positive BMDMs was performed by scoring macrophages for positive signal in three different randomly selected fields (~50-100 cells per field) on a coverslip.

Cytokine ELISA. Assays were performed as described in Chapter 2.

LPS and IKKβ inhibitor treatment. Macrophages were seeded as mentioned in Chapter 2. Macrophages were exposed to the IKKβ inhibitor [5-(p-Fluorophenyl)-2-ureido] thiophene-3-carboxamide (TPCA-1, Sigma, 10uM in DMSO) for 1 hr in BMM-low. Media containing the inhibitor was removed and was replaced with fresh media containing 100ng/ml of LPS (from *E. coli*, Sigma) for the remaining time.

Quantitative RT-PCR (qRT-PCR). Infections of BMDMs were carried out with $1x10^6$ BMDMs infected at an MOI of 50. At 4 hr post infection, RNA extraction, reverse transcription and real-time quantitative PCR were done as described before (225). The sequences of primer pairs used were: for il-1b 5'- TACAAGGAGAACCAAGCAACGAC -3' and 5'-GCCCATACTTTAGGAAGACACGG -3'; for il-18 5'-GCGTCAACTTCAAGGAAATGATG -3' and 5'- TCACAGAGAGGGTCACAGCCAGTCC -3'. The primers used for *Ikkb* were 5'-GTGGAGCCTGGGAAATGAAAG -3' and 5'- TAAGAGCCGATGCGATGTCAC -3'. The primer pairs used for GAPDH and tnf were as described previously (225).

Statistical analysis. Experimental data analyzed for significance (GraphPad Prism 4.0) were performed three independent times. Probability (P) values for multiple comparisons of cytokine were calculated by one-way ANOVA and Tukey's multiple comparisons post-test. P values for two group comparisons of cytokine and FLICA were calculated by two-tailed paired student t test. P values were considered significant if less than 0.05.

3.4 Results

Partial genetic ablation of IKKβ increases caspase-1 activation in *Y. pestis*-infected macrophages

Greten *et al*. have shown that treatment of IKKβ-deficient macrophages with LPS causes activation of caspase-1 and secretion of IL-1β (74). If IKKβ activity is important to suppress activation of the inflammasome in macrophages infected with a live Gram-negative pathogen, then increased caspase-1 activation and IL-1β secretion should be observed in IKKβ-deficient as compared to wild-type BMDMs infected with *Y. pestis*. The effect of genetic inactivation of *Ikkβ* on caspase-1 activation in *Y. pestis* infected macrophages was therefore investigated. IKKβ-deficient BMDMs were generated by conditional Cre-lox-mediated deletion of a ''floxed'' *Ikkβ* gene (referred to as $Ikk\beta^{\Delta}$ BMDMs; Experimental Methods). The $Ikk\beta^{\Delta}$ BMDMs or wild-type control $Ikk\beta^{F/F}$ macrophages were left uninfected or infected with Yp-YopJ^{KIM}, Yp-YopJ^{CO92} or Yp-YopJ^{C172A} for 4 hr. Quantitative RT-PCR of *Ikkβ* message was used to estimate the efficiency of Cre-lox mediated deletion of the *Ikkβ* gene in the BMDMs. Results indicated that, 50% of the *Ikkβ* genes had been deleted in the population of $Ikk\beta^{\Delta}$ cells (Figure 3.1A). The impact of this partial deficiency in *Ikkβ* on the expression and secretion of cytokines in the *Y. pestis* infected macrophages was determined. As compared to the $Ikk\beta^{F/F}$ macrophages, the $Ikk\beta^{\Delta}$ BMDMs were

compromised for infection-induced expression of mRNA for the cytokines IL-18, TNF-α and IL-1β, as shown by qRT-PCR (Figure 3.1B–D). This result was expected since the NF-κB pathway positively regulates expression the il-18, tnf and il-1b genes. Accordingly, the *Ikkβ*$^{\Delta}$ BMDMs secreted lower levels of TNF-α as compared to *Ikkβ*$^{F/F}$ macrophages after a 24 hr infection (Figure 3.2A). In addition, during infection with Yp-YopJ^{CO92} or Yp-YopJ^{C172A}, higher amounts of IL-1β were secreted from *Ikkβ*$^{\Delta}$ BMDMs as compared to *Ikkβ*$^{F/F}$ macrophages (Figure 3.2B), consistent with the idea that the NF-κB pathway negatively regulates processing and secretion of IL-1β via control of caspase-1 activation (74). Unexpectedly, the amount of IL-1β secreted following infection with Yp-YopJ^{KIM} appeared to be lower in *Ikkβ*$^{\Delta}$ BMDMs as compared to *Ikkβ*$^{F/F}$ macrophages, although the observed difference was not statistically significant (Figure 3.2B). The interpretation of this latter result was complicated because of the fact that there was only partial deficiency of *Ikkβ* in the *Ikkβ*$^{\Delta}$ BMDMs, but one possible explanation was that synthesis of pro-IL-1β was reduced due to the extremely low level il-1b message in the *Ikkβ*$^{\Delta}$ BMDMs infected with Yp-YopJ^{KIM} (Figure 3.1D).

Activation of caspase-1 was measured by immunoblotting to detect the cleaved enzyme in lysates prepared 2 hr after infection of *Ikkβ*$^{\Delta}$ or *Ikkβ*$^{F/F}$ BMDMs with Yp-YopJ^{KIM}, Yp-YopJ^{CO92} or Yp-YopJ^{C172A}. Caspase-1 activation in uninfected BMDMs or in macrophages treated with LPS and ATP was determined in parallel for comparison. Increased caspase-1 cleavage occurred in *Ikkβ*$^{\Delta}$ macrophages infected with Yp-YopJ^{KIM} or Yp-YopJ^{CO92} as compared to *Ikkβ*$^{F/F}$ BMDMs infected with the same strains (Figure 3.3A, compare lanes 7 and 8 with 2 and 3). Cleaved caspase-1 was below the limit of detection in *Ikkβ*$^{\Delta}$ macrophages infected with Yp-YopJ^{C172A} (Figure 3.3A, lane 9). Activation of caspase-1 was also measured by a microscopic assay utilizing FAM-YVAD-FMK, a fluorescent probe for active caspase-1, in *Ikkβ*$^{\Delta}$ or *Ikkβ*$^{F/F}$

BMDMs infected for 9 hr. The results showed overall higher levels of caspase-1 positive cells in *Ikkβ*$^{\Delta}$ as compared to *Ikkβ*$^{F/F}$ macrophages (Figure 3.3B and C). Taken together, these results show that loss of IKKβ activity can increase caspase-1 activation in macrophages infected with *Y. pestis*, and are consistent with the idea that IKKβ is an important target of YopJ for activation of the inflammasome.

IKKβ inhibitor TPCA-1 induced IL-1β release followed by LPS priming in macrophages. I further proved the negative effect of the NF-κB pathway on caspase-1 activation by using an IKKβ inhibitor, TPCA-1. TPCA-1 is an ATP competitor, which reversibly blocks IKKβ activity by inhibition of phosphorylation in a highly selective property (146). Macrophages were treated with TPCA-1 for 1 hr, the inhibitor was then removed and replaced with medium supplemented with LPS to initiate activation of LPS-TLR4 pathway. IL-1β release was undetectable in TPCA-1 (Figure 3.4) or LPS (data not shown) treatment alone conditions. The inhibitor followed by LPS condition, however, led to a notable increase in IL-1β release after 24 hr (Figure 3.4). This result provided evidence that YopJ mimics an IKKβ pharmacological inhibitor to active caspase-1 by inhibition of the NF-κB pathway.

3.5 Discussion

Although the knowledge of mechanisms of activation of inflammasomes and caspase-1 has been greatly enriched in recent years, the negative modulation of this system is still poorly characterized. Greten's study showed the evidence that the NF-κB pathway may be able to negatively regulate caspase-1 activation in an unknown mechanism (74). In that study, the NF-κB pathway was disabled through genetic deletion of *Ikkβ* gene, and the resulting mice or isolated cells when exposed to LPS exhibited strong IL-1β production *in vivo* and *in vitro*,

respectively (74). In addition, wild type macrophages incubated with an ATP-competitive IKKβ inhibitor also underwent intensive caspase-1 activation following LPS stimulation (74).

YopJ exclusively targets and acetylates IKKβ, but not IKKα, to inhibit the NF-κB pathway (169). We proposed that inhibition of IKKβ is important for YopJ-induced caspase-1 activation in *Yersinia* infected macrophages. As $YopJ^{KIM}$ is a better binding partner for IKKβ as compared to other YopJ isoforms, the increased caspase-1 activation in KIM5-infected macrophages may be a result of increased inactivation of IKKβ under this condition. To verify our hypothesis, infection of $Ikk\beta^{\Delta}$ BMDMs was carried out. If caspase-1 activation happens in this way, we would expect to see up-regulated caspase-1 activation in *Y. pestis* infected macrophages.

Increased IL-1β secretion and active caspase-1 were detected in $Ikk\beta^{\Delta}$ BMDMs infected with Yp-$YopJ^{CO92}$ or Yp-$YopJ^{C172A}$ as compared to the $Ikk\beta^{F/F}$ cells, supporting our hypothesis. A slight decrease of IL-1β secretion was seen in $Ikk\beta^{\Delta}$ cells as compared to the $Ikk\beta^{F/F}$ macrophages following Yp-$YopJ^{KIM}$ infection. The interpretation of this latter result was complicated because of the fact that there was only partial deficiency in *Ikkβ* in the $Ikk\beta^{\Delta}$ BMDMs. The discrepancy in the level of IL-1β secretion could be explained as a result of pro-IL-1β transcription and processing. Unlike il-18 gene, the il-1b gene is not transcribed in unstimulated cells and it is dominantly controlled by NF-κB pathway (8, 142). In Yp-$YopJ^{KIM}$ infected $Ikk\beta^{\Delta}$ cells, *il-1b* mRNA is barely detectable (Figure 3.1D). As a consequence, less pro-IL-1β could be synthesized and processed, despite stronger activation of the caspase-1 processing machinery.

Finally, a reversible IKKβ inhibitor, TPCA-1, was applied to macrophages to extend our idea (Figure 3.4). We selected TPCA-1 to perform this assay, because this inhibitor is very

selective for IKKβ over IKKα and MAPKs (101). The TPCA-1 and LPS treatment successfully induced IL-1β secretion, supporting the results seen in *Ikkβ*$^{\Delta}$ macrophages. Other NF-κB inhibitors including IκBα degradation inhibitor, or IKKγ binding peptides (101), could be tested in this same model to see if caspase-1 activation is a general effect or a random outcome for blockage of the IKKβ-NF-κB pathway.

Acknowledgement

I thank Ms. Tomomi Suda for breeding and maintenance of the *Ikkβ*$^{f/f}$*;MLysCre* mouse strain. I would also thank Igor Brodsky to perform caspase-1 immunoblotting and Yue Zhang for running qRT-PCR detecting tnf, il-18 and il-1b transcription levels.

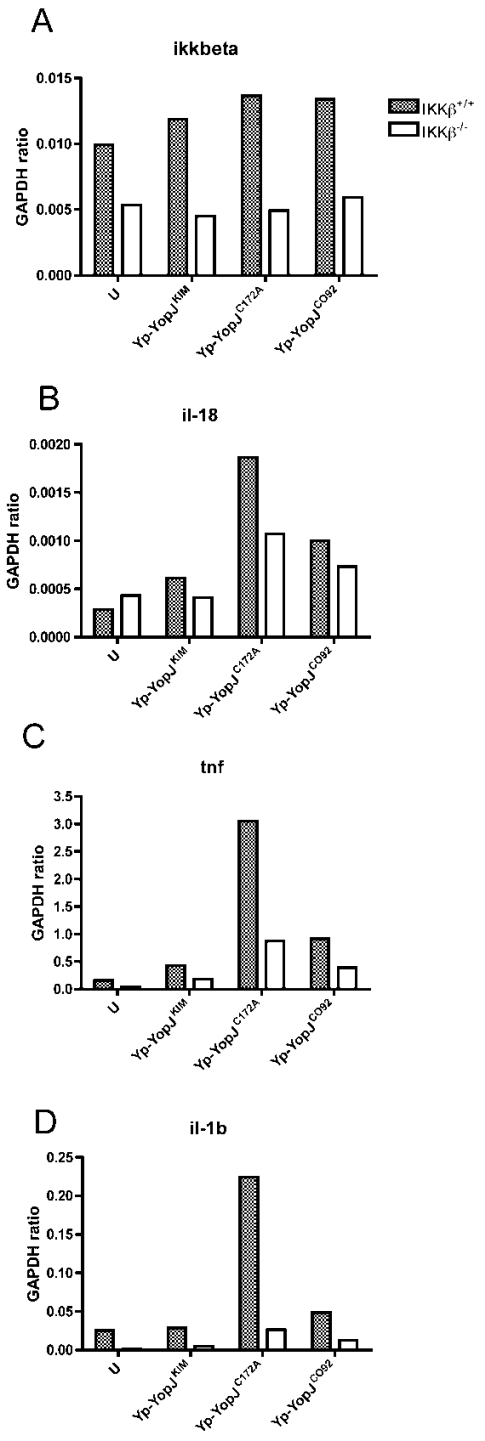

Figure 3.1. Measurement of *Ikkβ* and cytokine message levels by quantitative real time PCR. *Ikkβ*$^{F/F}$ or *Ikkβ*$^{\Delta}$ macrophages were infected with the indicated Yp-YopJ strains at an MOI of 50. At 4 hr post infection, mRNA was extracted and analyzed by qRT-PCR to quantify levels of *Ikkb* (A), *il-18* (B), *tnf* (C) or *il-1b* (D). Results are from one experiment.

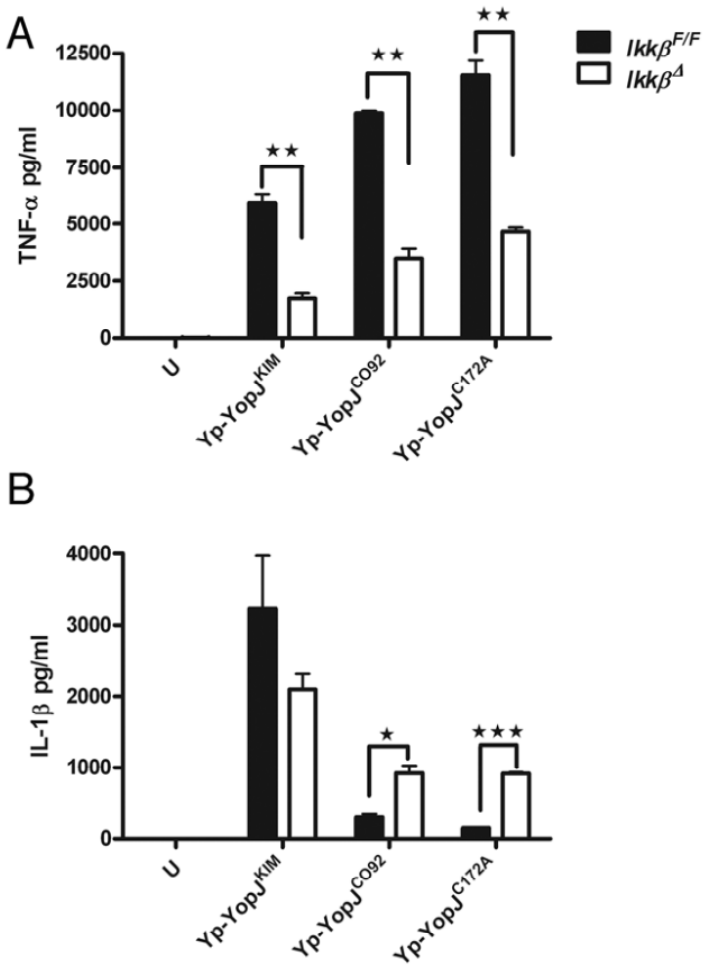

Figure 3.2. IL-1β and TNF-α secretion in *Ikkβ*$^{F/F}$ or *Ikkβ*^{Δ} macrophages infected with *Y. pestis* strains expressing different YopJ isoforms. *Ikkβ*$^{F/F}$ or *Ikkβ*^{Δ} macrophages were left uninfected (U) or infected with the indicated Yp-YopJ strains at an MOI of 10. Twenty-four hr post infection, cell supernatants were collected. Secreted TNF-α (A) IL-1β (B) were measured by ELISA. Results were averaged from three independent experiments, and error bars represent standard deviation. P values (t test) are indicated for comparison between two cell types in each condition (★, P<0.5; ★★, P<0.1; ★★★, P<0.001).

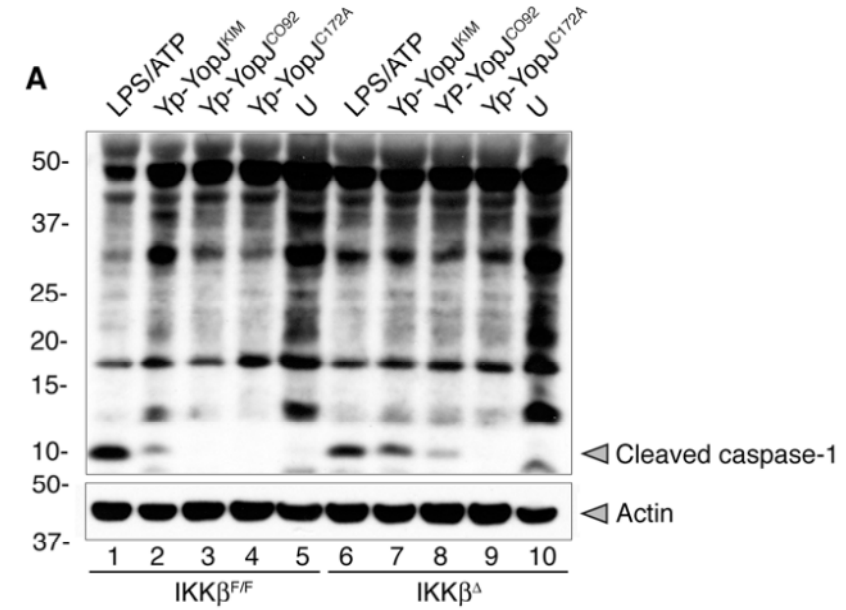
A
LPS/ATP
Yp-YopJKIM
Yp-YopJCO92
Yp-YopJC172A
U
LPS/ATP
Yp-YopJKIM
YP-YopJCO92
Yp-YopJC172A
U
50-
37-
25-
20-
15-
10-
50-
37-
Cleaved caspase-1
Actin
1 2 3 4 5 6 7 8 9 10
IKKβF/F
IKKβΔ

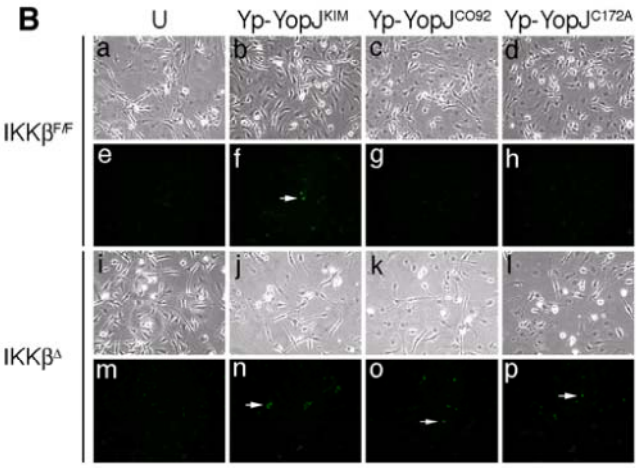
B
U
Yp-YopJKIM
Yp-YopJCO92
Yp-YopJC172A
IKKβF/F
IKKβΔ
a
b
c
d
e
f
g
h
i
j
k
l
m
n
o
p

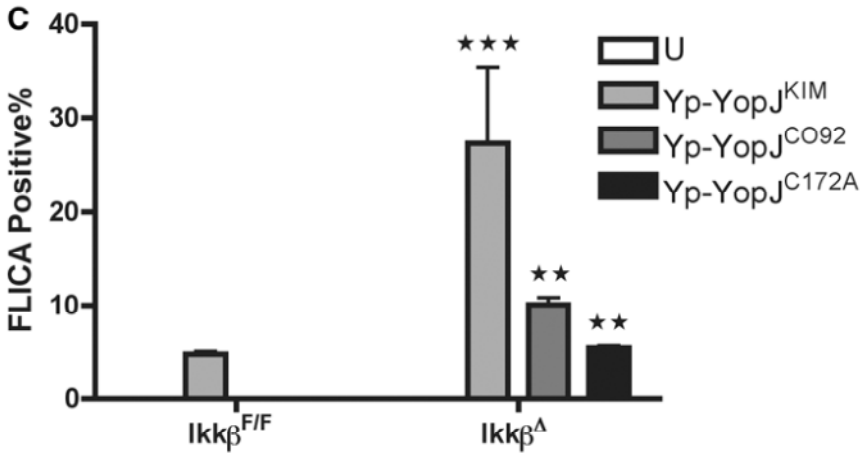
C
FLICA Positive%
40
30
20
10
0
★★★
★★
★★
U
Yp-YopJKIM
Yp-YopJCO92
Yp-YopJC172A
IkkβF/F
IkkβΔ

Figure 3.3. Caspase-1 activation in *Ikkβ*$^{F/F}$ or *Ikkβ*^{Δ} macrophages infected with *Y. pestis* strains expressing different YopJ isoforms. *Ikkβ*$^{F/F}$ or *Ikkβ*^{Δ} BMDMs were left uninfected (U) or infected with the indicated Yp-YopJ strains at an MOI of 20, or treated with LPS for 3 hr and then exposed to ATP (LPS/ATP). (A) Caspase-1 cleavage was determined at 1 hr post ATP treatment or 2 hr post infection. In (A) samples of detergent lysates were separated by SDS-PAGE and immunoblotted with anti-caspase-1 antibody (upper panel) or anti-actin antibody (lower panel). Positions of molecular weight standards (kDa) are shown on the left and positions of cleaved caspase-1 and actin are shown on the right. In (B) uninfected or infected macrophages on coverslips were incubated with FLICA reagent (FAM-YVAD-FMK) at 9 hr post infection to stain for active caspase-1 (green fluorescence). The samples were fixed, mounted on slides, and light microscopy was used to detect phase (a-d, i-l) or fluorescence (e-h, m-p) signals. Representative images of uninfected or infected cells were captured by digital photomicroscopy. White arrows point to FLICA positive cells. In (C), average percentages (error bars show standard deviation) of FLICA positive cells counted from three random fields per coverslip in three independent experiments is shown. N.D., none detected. P values (t test) are indicated for comparison between two cell types in each condition (★★, $P<0.01$; ★★★, $P<0.001$).

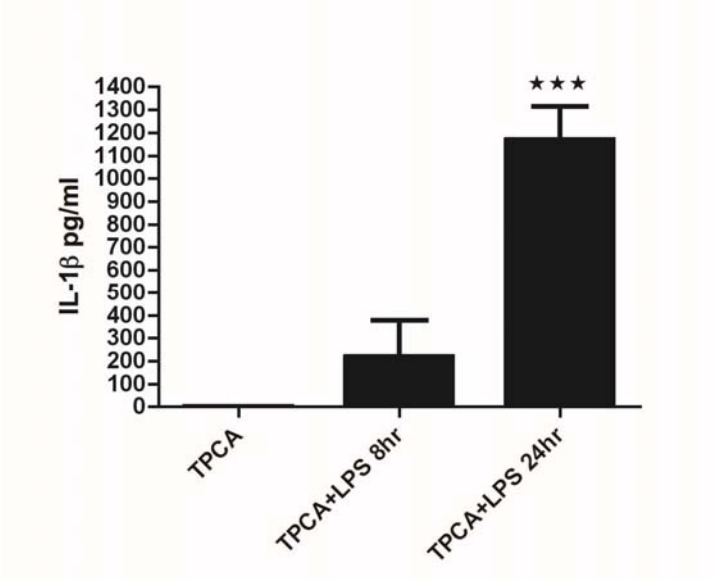

Figure 3.4. IL-1β production and cell death in IKKβ inhibitor TPCA-1 treated macrophages. Macrophages were treated with 10uM of TPCA-1 for 1 hr with or without following 100ng/ml of LPS for remaining time. Culture media were collected for IL-1β production. Results were averaged from three independent experiments, and error bars represent standard deviation. P values (one way ANOVA) are indicated (★★★, $P<0.001$).

Chapter 4. YopJ^{KIM}-induced caspase-1 activation in *Yersinia*-infected macrophages is independent of apoptosis, but is associated with necrosis

4.1 Summary

As *Y. pestis* KIM5-infected macrophages release high levels of proinflammatory cytokines such as IL-18 and IL-1β (114), macrophage may not die from apoptosis as studied before (43, 222). The NLRP3 inflammasome and K^+ efflux were shown to be important for secretion of IL-18 and IL-1β in KIM5-infected macrophages. In this chapter, our aim is to characterize the features of KIM5-induced macrophage cytotoxicity and uncover the underlying relationship between cell death and caspase-1 activation. Apoptotic markers including caspase-3/-7 activities, and PARP cleavage were evaluated. A caspase-8 inhibitor was used and BaxBak double knockout (DKO) cells were tested to study the importance of the canonical apoptotic pathways. Results showed that canonical apoptotic pathways are dispensable for KIM5-induced macrophage death. KIM5-infected macrophages stained positively for annexin V and propidium iodide (PI) and released HMGB1, suggesting a necrosis-like death was occurring. Staining for active caspase-1 and PI showed that macrophages having active caspase-1 are the same population as those undergoing necrotic death. To detect if blockage of necrosis could reduce IL-1β production, the RIP1 inhibitor necrostatin-1 was applied during KIM5 infection. However, neither cell death nor IL-1β production was affected by necrostatin-1. Inhibitors of ROS or cathepsin B were used to

investigate the signals activating the NLRP3 inflammasome in KIM5-infected macrophages, and results suggest a role for leakage of cathepsin B from lysosomes during necrosis.

4.2 Introduction

Yersinia-induced macrophage death dependent on YopJ is generally regarded as apoptosis, initiating from caspase-8 activation and amplified through mitochondria and finally activating downstream caspase-3, -7 and -9 (43). Apoptosis is known to be a type of cell death that does not release inflammatory contents (65). It seems that *Y. pestis* KIM5-infected macrophages are unlikely die through apoptosis, since high levels of proinflammatory cytokines IL-18 and IL-1β are released. Caspase-1 is able to elicit a type of cell death, termed pyroptosis, which is an important pathway in many cases of pathogen-triggered macrophage death (65). Interestingly, Lilo *et al*. showed that KIM5-infected macrophages die independent of caspase-1 (114). Recent studies identified that RIP1-mediated necrosis occurs downstream of TLR3/4 signaling in the presence of a caspase-8 inhibitor and the absence of NF-κB signaling in macrophages (98, 121). RIP1 activity has been found to be involved in *Y. enterocolitica*-induceddendritic cell death (74) which was evaluated as necrosis in an earlier study from the same group (77). In addition, necrosis-directed caspase-1 activation was reported through two different pathways (93, 111). The small necrotic molecule BIO7 triggered caspase-1 activation, and this process was determined not to occur through ATP by the us of $P2X_7$ deficient cells or ATP inhibitors (93, 111). In contrast, pressure-damaged tumor cells had activated NLRP3 due to mitochondrial ATP release from dead cells (93, 111). In this chapter, $YopJ^{KIM}$-induced macrophage death is examined by looking at the roles of different cytotoxic pathways and the RIP1 inhibitor treatment. Caspase-1/PI double staining were performed to test the relationship between necrosis and IL-1β production.

The NLRP3 inflammasome is known to be required for caspase-1 activation in response to a variety of danger stimuli, but the identity of the proximal signal(s) recognized by this sensor is not clear. Proposed pathways activating NLRP3 include ROS, lysosome rupture and plasma membrane channel formation (197). The NLRP3 inflammasome and K^+ efflux were shown to be important for secretion of IL-18 and IL-1β in KIM5-infected macrophages. YopJ has never been reported as a pore-forming toxin, so the channel model does not seem to apply to our context. Lysosome rupture results in cathepsin B release, and this pathway to inflammasome activation could be blocked by a cathepsin B inhibitor (197). ROS-mediated activation of caspase-1 occurs in response to many pathogen infections or in macrophages stimulated with LPS and ATP, and in this case, inflammasome activation can be blocked by ROS inhibitors (35, 197). To find out which pathway may be involved in $YopJ^{KIM}$-induced caspase-1 activation through the NLRP3 inflammasome, we determined IL-1β secretion levels in KIM5-infected macrophages in the presence of cathepsin B or ROS inhibitors.

4.3 Experimental Methods

Bacterial strains and growth conditions. The *Yersinia* strains and growth conditions were mentioned in Chapter 3.

Bone marrow macrophage isolation and culture conditions. BMDMs were isolated from bone marrow taken from femurs of 6- to 8-week old C57BL/6 female mice (Jackson Laboratories) as previously described (157). Frozen stocks of bone marrow cells from C57BL/6 mice deficient for Bax and Bak ($bax^{-/-}bak^{-/-}$) or heterozyous ($bax^{+/-}bak^{+/-}$) (117) (obtained from Tullia Lindsten, University of Pennsylvania and Craig Roy, Yale University) were propagated in DMEM GlutaMax supplemented with 20% fetal bovine serum, 30% L-cell-conditioned medium and 1% 0.1M sodium pyruvate (BMM-high) to obtain BMDM.

Macrophage infection. Twenty-four hours before infection, BMDMs were seeded in 24-well plate at a density of 1.5×10^5 cells/well in DMEM GlutaMax supplemented with 10% fetal bovine serum, 15% L-cell-conditioned medium and 1% 0.1M sodium pyruvate (BMM-low). Next day, macrophages were infected with *Yersinia* at a multiplicity of infection (MOI) of 10 as described (114). In some experiments, cells were treated with 10mM of N-acetyl cysteine (NAC, Sigma), or 10uM of diphenyleneiodonium chloride (DPI, Sigma) for 2 hr before infection. In other experiments the BMDMs were treated with 30uM of necrostatin-1 (Biomol), 25uM of CA-074 Me (Biomol), 40uM of IETD-CHO (Calbiochem) or 25uM of E64d (Biomol) for 1 hr before infection and during the remainder of the infection period. For the caspase-8 inhibitor positive control experiment, cells were pretreated with 5uM of MG-132 (Sigma) for 30min with or without 40uM of IETD-CHO and then incubated with 1ug/ml of LPS for 3 hours.

Microscopic assay to detect surface staining with annexin V and propidium iodide uptake. BMDMs were plated on glass coverslips in 24-well plates and infected as described above. At 4, 8 and 12 hr post infection, annexin V and PI were diluted in HBSS according to manufacturer's protocol (Roche) and added to the cells. After 15 minutes of staining, the reagents were removed and cells were washed with PBS. Cells were maintained in PBS and visualized by fluorescence microscopy using a Zeiss Axiovert S100 microscope equipped with a 40× objective. Images were captured using Spot camera (Diagnostic Instruments, Inc.) and processed by Adobe Photoshop 7.0. Quantification of percent caspase-1 positive BMDMs was performed by scoring macrophages for positive signal in three different randomly selected fields (~70–130 cells per field) on a coverslip.

Microscopic assay to detect propidium iodide uptake and active caspase-1. BMDMs were plated on glass coverslips in 24-well plates and infected as described above. Nine hours post-

infection, macrophages were stained with 6-carboxyfluorescein–YVAD– fluoromethylketone (FAM-YVAD-FMK; fluorescent inhibitor of apoptosis (FLICA) (Immunochemistry Technologies)) as described before (114) and 1ug/ml propidium iodide immediately before observation. Cells were maintained in PBS and visualized by phase and fluorescence microscopy. Images were captured and processed as mentioned above. Quantification of caspase-1 positive or PI positive cell percentages was performed by counting for positive cells in randomly selected fields (~100-300 cells/field) from three independent experiments.

Caspase-3/7 luminol assay. Caspase-3/7 activity was measured by Caspase-Glo 3/7 Assay Kit (Promega) according to manufacturer's instruction. BMDMs were seeded in a 96-well white-walled plate at a concentration of 10^4cells/well in 100ul medium. Infection was performed as described above. At each time point, a 100ul of detection buffer was added to a well and the plate was read using a luminescence reader (SpectrcMax M2, Molecular Devices).

Immunoblot analysis. For detection of HMGB1 and PARP by immunoblotting, macrophages were infected as above except that BMDMs were seeded in 6-well plates at a concentration of 10^6cells/well. Infected cells were maintained in 1ml of culture medium per well supplemented with 4.5ug/ml of gentamicin for 24 hr. For detection of HMGB1, harvested culture medium was centrifuged, the supernatant mixed with the same volume of 2×Laemmli buffer, and boiled samples were resolved SDS-PAGE (15% gels). BMDMs were lysed in 1×Laemmli buffer to obtain a sample of lysate for use as a positive control. Cell lysates for PARP immunoblotting were prepared by removing the media overlaying BMDM monolayers and adding 1×Laemmli buffer into the wells. Boiled lysate samples were resolved SDS-PAGE (8% gels). Uninfected BMDMs were treated with staurosporine (1uM, Biomol) 16 hours before lysis to provide a control for cleaved PARP. Proteins were transferred from gels to PVDF membranes and the

membranes were probed sequentially with rabbit anti-HMGB1 (Abcam) or anti-PARP (Santa Cruz) primary antibodies, and goat anti-rabbit HRP conjugated secondary antibody (Jackson). Signals on blots were detected with ECL reagents (Perkin Elmer Life Sciences, Inc.)

IL-1β ELISA. IL-1β was measured from supernatants by ELISA according to manufacturer's instructions (R&D).

LDH Release. Cell death was determined by CytoTox-96 nonradioactive cytotoxicity assay (Promega) from supernatants following manufacturer's instructions. The total LDH release was made by freezing and thaw untreated cells. The percentage of dead cells was calculated as followed: (sample LDH-background LDH)/ (total LDH-background LDH) × 100%.

Statistical analysis. Statistical analysis was performed with Prism 4.0 (Graphpad) software. The tests used are as indicated in the figure legends or main text. *P* values of less than 0.05 were considered significant.

4.4 Results

Caspase-3/7 activity is low in KIM5-infected macrophages. Activation of apoptotic caspases, such as caspase-3, -7 and -9, has been detected in macrophages undergoing YopP-dependent cell death in response to *Y. enterocolitica* infection (43). Caspase-3/7 activity assay was performed to examine apoptotic caspase activation at 4, 8, 12 and 24 hr post-infection in macrophages undergoing $YopJ^{KIM}$-induced cell death following infection with *Y. pestis*. BMDMs were infected at an MOI of 10 for 20 min. The tissue culture media was then supplemented with gentamicin for the remaining period of incubation to prevent growth of extracellular bacteria (114, 227). This "low MOI" infection procedure has previously been shown to cause cytotoxicity, activation of caspase-1, and high level secretion of IL-1β (114, 227). As controls, some macrophages were left uninfected or infected with a *Y. pestis* strain expressing catalytically

inactive YopJ^{C172A}. Caspase -3/7 activity in KIM5-infected macrophages was higher as compared to the controls at all time points, but the difference was not significant (Figure 4.1A). Lysates of macrophages infected as in Figure 4.1 were subjected to immunoblotting to detect cleavage of the caspase-3 substrate PARP. Lysates of control macrophages treated with staurosporin, a strong inducer of apoptosis, were analyzed in parallel. The 86 kDa cleaved PARP (c-PARP) fragment was not detected in lysates of KIM5-infected cells, but it was seen in staurosporin-treated cell lysates (Figure 4.1B). These results show that apoptotic caspases are not strongly activated in macrophages undergoing YopJ^{KIM}-induced cell death.

Apoptotic signaling through caspase-8 and mitochondria is dispensable for KIM5-induced macrophage death. It has been shown that YopP-induced apoptosis is initiated from caspase-8 in macrophages and dendritic cells infected with *Y. enterocolitica*, and can be blocked by caspase-8 or pan-caspase inhibitors (76, 170). A detailed study detected Bid truncation before cytochrome *c* release and apoptosome activation, which suggests that the death signal coming from caspase-8 may require mitochondria and is amplified through caspase -3,-7 and -9 cleavage (43). Bcl-2 family members Bax and Bak play a central role in controlling mitochondrial-dependent apoptosis (209). Bax and Bak when activated create a channel in the mitochondrial membrane, releasing cytochrome *c* to activate the apoptosome. In order to test if the YopJ^{KIM}-dependent death signal goes through mitochondria, we infected *bax*$^{-/-}$*bak*$^{-/-}$ macrophages with KIM5, using heterozygous *bax*$^{+/-}$*bak*$^{+/-}$ cells as the control. The *bax*$^{-/-}$*bak*$^{-/-}$ macrophages have been shown to be fully defective for mitochondrial-induced apoptosis (170). Cell death was measured by LDH release assay and secreted IL-1β was measured by ELISA at 24 hr post infection. No significant differences in YopJ^{KIM}-induced cell death or IL-1β release could be identified between *bax*$^{-/-}$*bak*$^{-/-}$ or *bax*$^{-/+}$*bak*$^{-/+}$ macrophages (Figure 4.2A and B).

To determine if caspase-8 is required for cell death in KIM5-infected macrophages, cells were exposed to the caspase-8 inhibitor IETD. IETD treatment did not significantly reduce macrophage death or IL-1β secretion after 8 or 24 hr of infection (Figure 4.3A and B). As a control, IETD treatment was shown to effectively block cell death in macrophages caused by treatment with LPS and the proteasome inhibitor MG-132 (Figure 4.3C). Thus, apoptotic signaling through caspase-8 and mitochondria is not required for $YopJ^{KIM}$-induced macrophage death.

KIM5-infected macrophages exhibit necrotic features. To characterize the morphology of KIM5-infected macrophages, we performed annexin V staining/ PI uptake assay at different times (4, 8 and 12 hr post infection) and analyzed the results by fluorescence microscopy. Macrophages infected with *Y. pestis* expressing $YopJ^{C172A}$ were analyzed in parallel as a control. As summarized in Figure 4.4, two populations of dead cells that were either annexin V single positive (apoptotic) or annexin V/ PI double positive (necrotic) were detected beginning at 8 hr post infection with KIM5. The number of annexin V single positive cells (~11% at 8 hr) declined slightly to 8% of total by 12 hr post infection. The double positive population (~13% at 8 hr) increased with time to reach 17% of total by 12 hr (Figure 4.4).

Release of HMGB1, a chromatin protein, can be used to differentiate apoptosis from necrosis (175). Immunoblotting was used to detect HMGB1 in culture supernatants of macrophages following 24 hr infection with KIM5 or KIM5 expressing $YopJ^{C172A}$. As shown in Figure 4.5, HMGB1 was released from macrophages infected with *Y. pestis* expressing $YopJ^{KIM}$ but not $YopJ^{C172A}$ (lanes 3 and 4, respectively). Together, these results suggest that a population of KIM5-infected macrophages undergo necrosis.

KIM5-infected necrotic macrophages contain active caspase-1. As both cell death and IL-1β release require YopJ^{KIM} and they display the same trends, caspase-1 activation and cell death appear to be related (114). It is possible that necrotic cell death triggers caspase-1 activation. To determine if necrotic cell death and caspase-1 activation could be correlated at the single cell level, infected macrophages were analyzed by microscopy after labeling for active caspase-1 and PI uptake. Representative images of macrophages infected with KIM5 or *Y. pestis* expressing YopJ^{C172A} for 9 hr are shown in Figure 4.6A, and a summary of the percentages of cells that were positive for one or both signals is shown in Figure 4.6B. The percentages of KIM5-infected macrophages that were caspase-1 positive, PI positive and double positive were not significantly different (Figure 4.6B), which suggests that membrane damage in necrotic cells is associated with caspase-1 activation.

RIP1 is not required for YopJ^{KIM}-induced cell death or IL-1β secretion. YopP-mediated dendritic cell death in response to *Y. enterocolitica* infection is reduced by treatment with geldanamycin, an Hsp90 inhibitor, which promotes Receptor Interaction Protein 1 (RIP1) degradation (76). Furthermore, YopP-induced dendritic cell death is partially independent of caspases and exhibits necrotic features (77), which are similar to our findings with YopJ^{KIM}. To test if RIP1 is involved in KIM5-induced macrophage death, we treated cells with the specific RIP1 inhibitor necrostatin-1, which blocks necrosis in many cell types (41). The treated macrophages were then infected with KIM5 or *Y. pestis* expressing YopJ^{C172A} for 8 or 24 hours. Necrostatin-1 did not significantly reduce cell death at either time point in KIM5-infected macrophages (Figure 4.7A). IL-1β release was significantly reduced at 8 hr, but not at 24 hr post infection with KIM5 (Figure 4.7B). From these results we conclude that RIP1 is not required for

YopJ^{KIM}-induced cell death or IL-1β secretion, however it may enhance IL-1β secretion at early infection times.

ROS are not required for cytotoxicity or IL-1β secretion in macrophages infected with KIM5. NLRP3 is important for IL-1β secretion in KIM5-infected macrophages (227). NLRP3 senses several structurally unrelated PAMPs and DAMPs that share the common property of generating ROS (197). It has therefore been proposed that ROS is a major signal detected by NLRP3 (197). The NADPH oxidase inhibitor DPI and the radical scavenger NAC were used to examine the importance of ROS for cytotoxicity and IL-1β secretion in KIM5-infected macrophages. Pretreatment of macrophages with DPI or NAC did not reduce IL-1β release or cell death following KIM5 infection of macrophages for 8 or 24 hr (Figure 4.8A and 4.8B). As a control, LPS-stimulated macrophages were exposed to DPI or NAC and NLRP3-dependent pyroptosis was induced by ATP treatment. The amount of IL-1β released was significantly reduced by DPI and cytotoxicity was significantly reduced by DPI and NAC (Figure 4.8C and 4.8D). Therefore, ROS are not required for YopJ^{KIM}-induced cell death or IL-1β secretion.

Inhibitors of cathepsin B reduce caspase-1 activation in macrophages infected with KIM5. Lysosomal rupture leads to release of lysosome-localized protease cathepsin B into the cytoplasm which directly or indirectly activates NLRP3/caspase-1 (90). We examined the lysosome rupture pathway using the cathepsin inhibitor E64d and specific cathepsin B inhibitor CA-074 Me. Treatment of macrophages with either of these two inhibitors during a 24 hr KIM5 infection resulted in a significant decrease in secretion of IL-1β (Figure 4.9A) but had no effect on cytotoxicity (Figure 4.9B). Microscopic imaging of KIM5-infected macrophages after straining them with a fluorescent substrate for caspase-1 and PI showed that E64d and CA-074

Me blocked caspase-1 activation (Figure 4.9C). These results suggest that cathepsin B activity is required for YopJ^{KIM}-mediated activation of caspase-1.

4.5 Discussion

YopJ inhibits NF-κB and MAPK pathways that activate transcription of cell survival genes, promoting macrophage cell death in response to apoptotic signaling from TLR4 (223). In addition, inhibition of the NF-κB pathway by YopJ (227) or IKKβ genetic deficiency (74) triggers TLR4-dependent activation of caspase-1. The conditions used for infection of macrophages with *Yersinia* affect the outcome of YopJ-mediated caspase-1 activation. Incubation of macrophages with *Y. pseudotuberculosis* under conditions of high MOI (20) and extended contact with extracellular bacteria (1 hr) results in rapid activation of caspase-1 but IL-1β release is undetectable and caspase-1 activation does not depend on NLRP3 nor ASC (22). Infection of macrophages with *Y. pestis* KIM5 under low MOI (10) and short contact time (20 min) results in delayed caspase-1 activation, high level of IL-1β release and cytotoxicity in a YopJ dependent manner (114). In addition, NLRP3 and ASC are important for IL-1β release from macrophages infected with KIM5 under the low MOI procedure (227). As an outcome of YopJ blocking the NF-κB pathway, less pro-IL-1β would be synthesized in macrophages, but processing of even a small pool of pro-IL-1β by active caspase-1 activation can lead to detectable released IL-1β. In the low MOI infection conditions used here, it is likely that low amounts of YopJ are injected into macrophages, resulting in a delay in caspase-1 activation and cell death in macrophages. This infection condition may allow macrophages sufficient time to synthesize pro-IL-1β before cell death occurs.

To investigate the mechanism of YopJ^{KIM}-induced caspase-1 activation and its connection to cell death in macrophages, we first investigated the importance of apoptosis. The

low caspase-3/7 activity (Figure 4.1) and the dispensable role for caspase-8 (Figure 4.3) in cell death are consistent with the idea that apoptosis is not strongly activated in KIM5-infected macrophages. It is important to point out that caspase-8 activation has never been directly demonstrated in *Yersinia*-infected macrophages; the evidence for caspase-8 activation comes from Bid cleavage assays. Caspase-8 cleavage has been detected in *Yersinia* infected dendritic cells and in macrophages treated with LPS and MG-132 to activate apoptosis (43, 78, 171). Caspase-8 has been reported to process pro-IL-1β after stimulation of TLR3/TLR4 signaling in macrophages (122), but in our studies a caspase-8 inhibitor did not decrease IL-1β release in KIM5-infected macrophages (Figure 4.3). Participation of mitochondrial-induced apoptosis in death of macrophages infected with *Y. enterocolitica* has been implicated by the observed release of cytochrome *c* (43). However, YopP-induced cell death in dendritic cells was not inhibited by overexpression of Bcl-2 (77). In our studies the use of Bax/Bak DKO BMDMs would mimic Bcl-2 over-expression by preventing pore formation on the mitochondrial membrane, however loss of Bax and Bak did not decrease cell death or IL-1β secretion in KIM5-infected infected macrophages (Figure 4.2).

Necrosis releases inflammatory cell contents, which is consistent with proinflammatory cytokine production in KIM5-infected macrophages (114). Annexin V/ PI staining was performed to observe macrophage plasma membrane integrity over time. Annexin V single positive cells representing the early apoptosis population occurred in parallel with annexin V/ PI double positive cells representing the late apoptosis or necrosis population (Figure 4.4). The presence of the two populations indicates that apoptosis and necrosis may coincide. However, cells with the double positive phenotype may not arise from necrosis, especially in cell culture when apoptotic cells are not engulfed by bystander phagocytes, but rather from “secondary

necrosis" (230). Thus, to be sure that KIM5-infected macrophages are dying of necrosis, accumulation of more evidence is needed.

HMGB1 release is a very distinctive marker of necrosis (175). The observed release of HMGB1 from KIM5-infected macrophages (Figure 4.5) strongly suggests that these cells are dying of necrosis. Although HMGB1 can be passively secreted by activated dendritic cells and macrophages (17), infection of macrophages with *Y. pestis* expressing YopJ^{C172A}, which would activate macrophages through LPS-TLR4 signaling, did not result in HMGB1 release (Figure 4.5). To determine if released HMGB1 could be important for cell death and activation of caspase-1, medium from KIM5-infected macrophages was transferred to naive uninfected macrophages (data not shown). Although HMGB1 has been shown to stimulate proinflammatory cytokine production, is the results of the media transfer experiment indicate that it is unlikely that HMGB1 interacts with TLR4 to promote IL-1β production and cell death in our system (4, 104, 178).

Since necrotic cells release inflammatory cytokines and KIM5-infected macrophages showed necrotic properties (Figure 4.4 and 4.5), we performed caspase-1 /PI staining to see if caspase-1 activation takes place in necrotic cells (Figure 4.6). The highly overlapped caspase-1/PI positive cell population supports the idea that these two events occur in same cells. However, it is difficult to discriminate if necrosis occurs earlier than caspase-1 activation. A previous LDH and IL-1β time course release assay detected LDH release 4 hr ahead of IL-1β secretion, suggesting that cell death may happen earlier than caspase-1 activation (114).

As macrophages infected with KIM5 seem to die by necrosis, and cell death initiated earlier than IL-1β release (114), we hypothesized that necrosis could activate inflammasomes and caspase-1. We tried to blocked necrosis through use of the RIP1 inhibitor necrostatin-1.

RIP1 has been identified as an important mediator of non-apoptotic death in many cell types. When caspase-8 activity is inhibited, preventing cleavage of RIP1, RIP1 positively activates a necrotic (necroptosis) pathway (115). Cell death triggered with FasL or TNF-α through caspase-8 activation, combined with pan-caspase or caspase-8 inhibitor treatment, is RIP1 dependent and could be prevented by specific RIP1 inhibitor necrostatin-1 (40, 89, 226). In macrophages after TLR4 stimulation, when the cellular NF-κB survival signaling pathway and caspase-8 activation are inhibited, RIP1 causes necrosis (64, 76, 121). RIP1 has also been implicated in death of dendritic cells infected with *Y. enterocolitica* O:8 strain WA-314, and the same group obtained evidence that dendritic cells could die by necrosis in the same infection conditions (76, 77). However, in our infection model, the RIP1 specific inhibitor necrostatin-1 did not reduce cell death (Figure 4.7). Treatment with necrostatin-1 did inhibit IL-1β release at 8 hours post infection (Figure 4.7), which may due to lack of interaction between RIP1 and the NF-κB pathway (64). RIP3 has also been implicated in necrosis, and although it is not clear if RIP3 and RIP1 can form a heterodimer, RIP3 alone could induce necrosis (39, 198, 221). It would be interesting to test RIP3 knockout BMDMs in the future to determine the role of this kinase in $YopJ^{KIM}$-induced cell death and caspase-1 activation.

Two recent studies discovered that necrosis could activate the caspase-1 (93, 111). In the study of Iyer *et al*., mitochondrial ATP release from necrotic cells activated caspase-1 in LPS primed macrophages through $P2X_7$ receptor (93). This pathway does not occur in our model, since we have previous shown that $P2X_7$ receptor is not required for secretion of IL-1β in KIM5-infected macrophages (227).

We previously showed that NLRP3 and ASC were important for secretion of IL-1β from KIM5-infected macrophages, although these inflammasome components were dispensable for

cell death (227). Consistent with an important role for NLRP3 and ASC in caspase-1 activation was the observation that exogenous K^+ inhibited secretion of IL-1β from KIM5-infected macrophages. Specifically, extracellular K^+, but not Na^+, down regulated IL-1β release in KIM5-infected macrophages, suggesting that NLRP3 activation requires a low concentration of intracellular K^+. Low intracellular K^+ levels could result from intracellular K^+ passing through ATP-sensitive K^+ channels (such as $P2X_7$), or by its release from dying cells (19). As mentioned above $P2X_7$ receptor is not required for IL-1β release in KIM5-infected macrophages, suggesting that pore formation in necrotic macrophages may allow K^+ efflux.

As NLRP3 can recognize ROS generation, or lysosome rupture leading to caspase-1 activation, we tested each of these processes for their importance in IL-1β secretion in KIM5-infected macrophages. With respect to the ROS generation model, most pathogens that activate caspase-1 through NLRP3 induce ROS generation and in many cases, K^+ efflux occurs simultaneously (197). However, two ROS inhibitors, DPI and NAC, had no significant effect on IL-1β release or cell death in KIM5-infected macrophages (Figure 4.8). These inhibitors did reduce pyroptosis of macrophages following LPS/ATP treatment (Figure 4.8C and 4.8D), conditions that are known to produce high levels of ROS (35).

The lysosome rupture model was tested by the use of cathepsin B inhibitors (Figure 4.9). Both inhibitors reduced IL-1β secretion and caspase-1 activation in KIM5-infected macrophages. Halle et al. showed reduced secretion of IL-1β in cathepsin B knockout macrophages as well as in cathepsin B inhibitor-treated wild type cells (83). However, off target effects of the inhibitors on caspase-1 activation in KIM5-infected macrophages cannot be ruled out.

A model of macrophage death and caspase-1 activation triggered by YopJ is proposed (Figure 4.10). *Yersinia* LPS activates a TLR4 signaling pathway, leading to downstream

activation of the canonical NF-κB pathway and a necrosis pathway, which is normally inhibited by NF-κB-driven survival genes. The NF-κB pathway may also upregulate unknown factors that negatively regulate inflammasome components NRLP3 and caspase-1. In the presence of YopJ, the NF-κB pathway is blocked by IKKβ acetylation, so the cell fate is biased to necrosis. Meanwhile, in the absence of negative regulation of caspase-1 activation from the NF-κB pathway, cytoplasmic K^+ efflux and cathepsin B released from lysosomes destroyed as a result of necrosis, may synergically facilitate NLRP3 and caspase-1 activation.

Acknowledgement

I thank Tullia Lindsten, University of Pennsylvania and Craig Roy, Yale University for providing bone marrow cells from *bax*$^{-/-}$*bak*$^{-/-}$ or *bax*$^{+/-}$ *bak*$^{+/-}$ mice. I wish to acknowledge Wei-Xing Zong and Yong-Jun Fan for kindly provide caspase-8 inhibitor and ROS scavenger NAC.

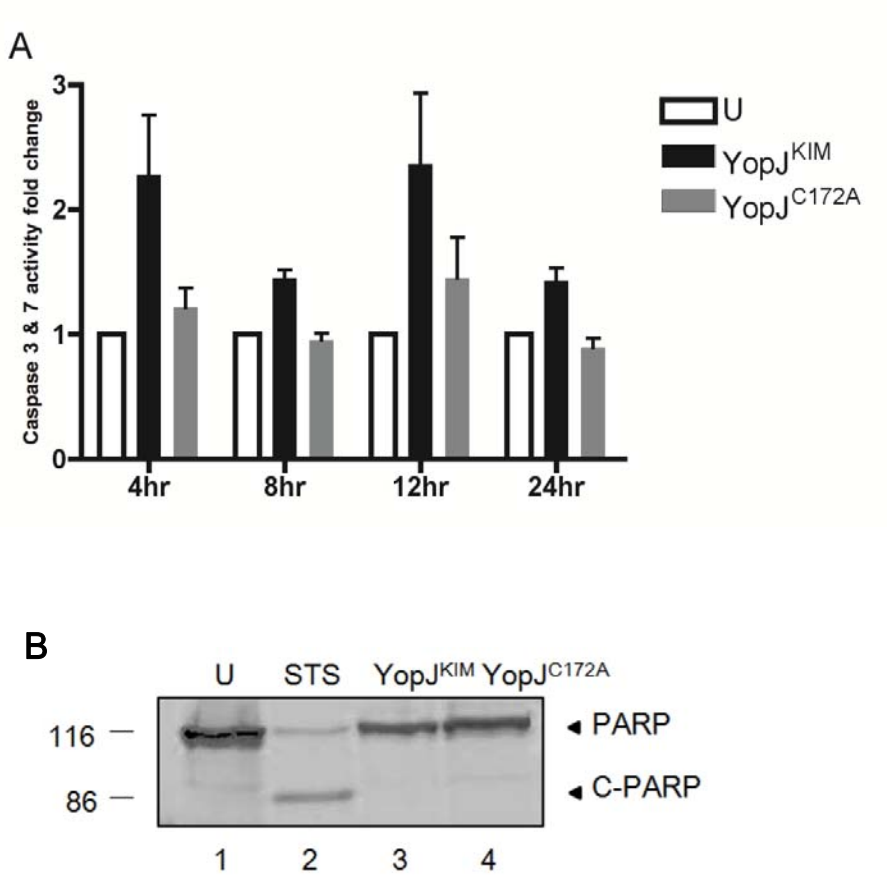

Figure 4.1. Caspase-3/-7 activity is low in KIM5-infected macrophages. (A) BMDMs were left uninfected (U) or infected with *Y. pestis* strains expressing YopJ^{KIM} or YopJ^{C172A} in 96-white walled tissue culture plates. Caspase-3/7 activity was measured 4, 8, 12 or 24 hr post-infection with fluorometer. The results from three independent experiments were averaged and are shown as fold change compared to uninfected cells. Error bars represent standard deviations. Differences in caspase-3/7 activities between uninfected and infected cells were not significant as determined by two way ANOVA (B) BMDMs were left uninfected (U) or infected with *Y. pestis* strains expressing YopJ^{KIM} or YopJ^{C172A} or treated with 1uM of staurosporine (STS) for 16 hr. Macrophage lysates were collected and analyzed by PARP immunoblotting. Sizes of molecular weight standards (kDa) are shown on the left. Positions of full length PARP and cleaved PARP (c-PARP) are showed on right.

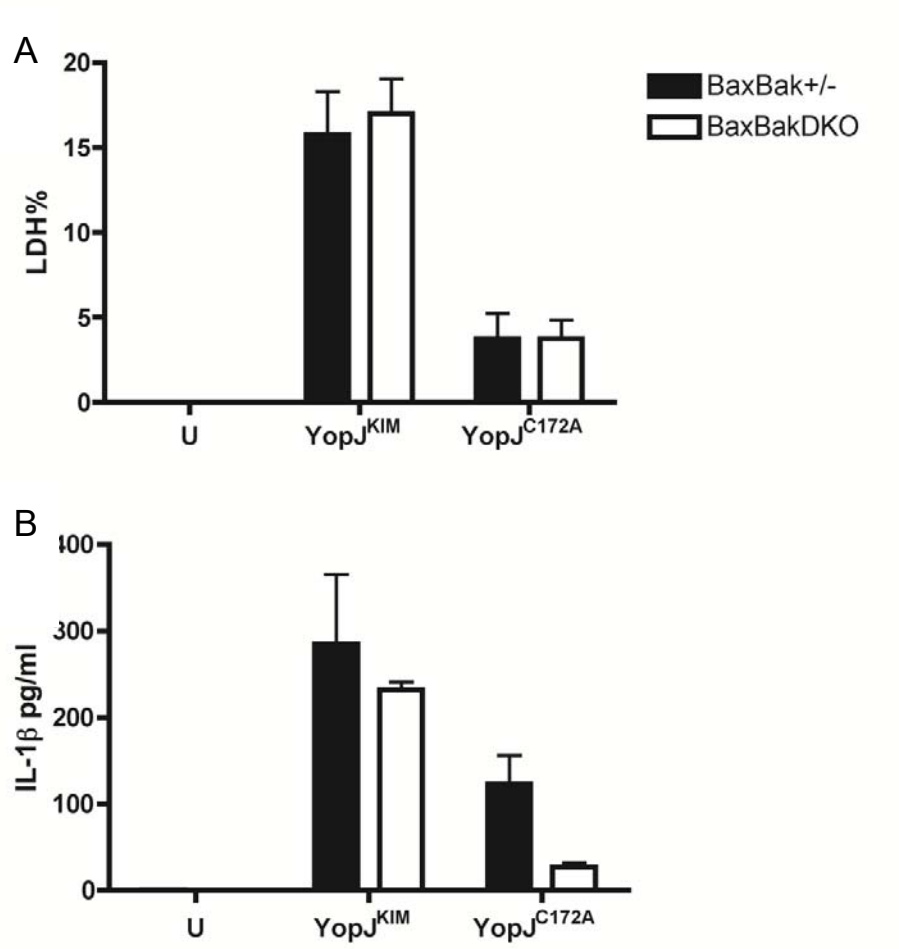

Figure 4.2. Mitochondrial-induced apoptosis is not required for KIM5-induced macrophage death and IL-1β secretion. BMDMs from *Bax Bak* heterozygous (BaxBak+/-) or *Bax Bak* double knockout (BaxBakDKO) C57BL/6 mice were left uninfected (U) or infected with *Y. pestis* strains expressing $YopJ^{KIM}$ or $YopJ^{C172A}$ for 24 hr. LDH (A) or IL-1β (B) released into supernatants were measured by CytoTox96 assay or ELISA, respectively. Results shown are the averages from three independent experiments. Error bars represent standard deviations. Differences average values between BaxBak+/- or BaxBakDKO conditions were not significant as determined by two way ANOVA.

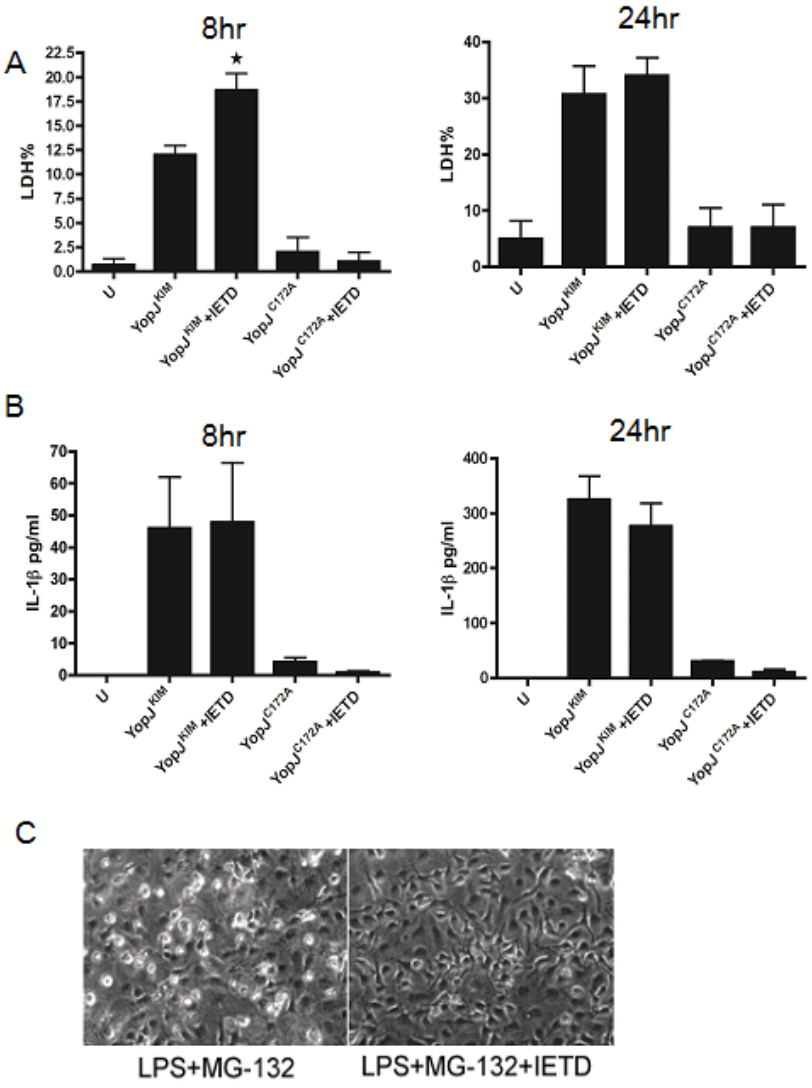
A
8hr
24hr
LDH%
B
IL-1β pg/ml
U
YopJ KIM
YopJ KIM +IETD
YopJ C172A
YopJ C172A +IETD
C
LPS+MG-132
LPS+MG-132+IETD

Figure 4.3. Caspase-8 activity is dispensable for KIM5-triggered macrophage death and IL-1β secretion. BMDMs were treated with 40uM caspase-8 inhibitor Z-IETD or vehicle 1 hr prior to infection. The BMDMs were then infected with *Y. pestis* strains expressing $YopJ^{KIM}$ or $YopJ^{C172A}$ or left uninfected (U). Infected cells were maintained in the presence of Z-IETD or the vehicle for the remainder of the experiment. At 8 hr or 24 hr post-infection, supernatants were collected and LDH release (A) and IL-1β (B) were measured. Results shown are averages from three independent experiments. Error bars represent standard deviations. ★, $P<0.05$ as determined by one way ANOVA compared to the $YopJ^{KIM}$ no inhibitor condition. (C) BMDMs were treated with 5uM of MG-132 in the presence or absence of 40uM Z-IETD for 30 min, followed by 1ug/ml of LPS for 3 hr. Representative phase images of the treated BMDMs were captured by digital photomicroscopy.

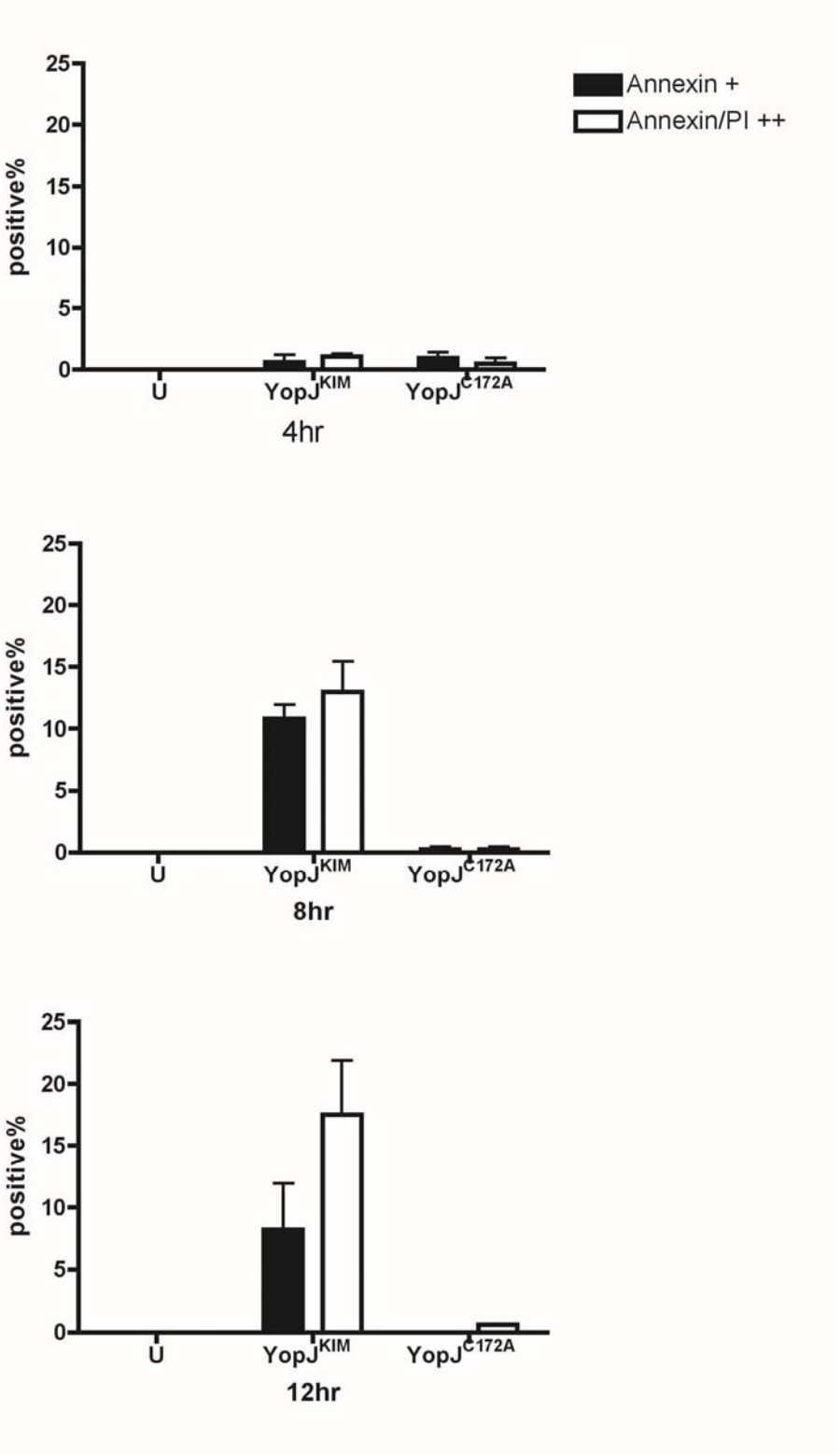
Annexin +
Annexin/PI ++
positive%
25
20
15
10
5
0
U
YopJKIM
YopJC172A
4hr
8hr
12hr

Figure 4.4. KIM5-infected macrophages have necrotic morphology as shown by annexin V staining and PI uptake assay. BMDMs were seeded on glass coverslips in a 24-well plate and infected with *Y. pestis* strains expressing $YopJ^{KIM}$ or $YopJ^{C172A}$ or left uninfected (U). Annexin V staining and PI uptake assay was performed at 4 hr, 8 hr or 12 hr post-infection. Representative images were captured by digital photomicroscopy. Average percentages of annexin V positive or annexin V/ PI double positive cells as counted from three random fields in three independent experiments are shown. Error bars represent standard deviations. Difference in values of single or double positive cells were not significant as determined by one way ANOVA.

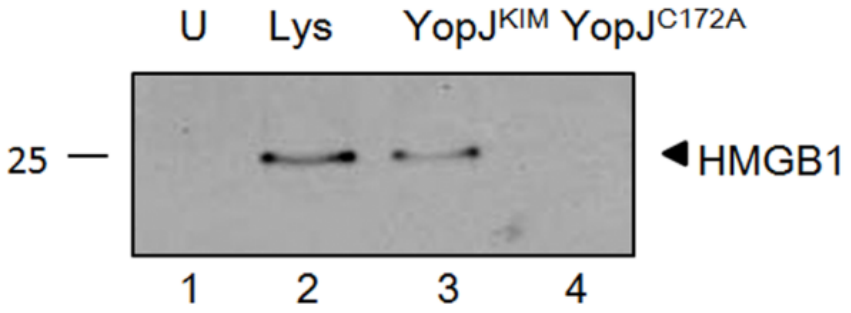

Figure 4.5. HMGB1 is released from KIM5-infected macrophages. BMDMs were infected with *Y. pestis* strains expressing YopJ^{KIM} or YopJ^{C172A} or left uninfected (U). Medium from infected macrophages was collected at 24 hr post infection and immunoblotted for HMGB1. Total cell lysate (Lys) was used as a positive control. Position of molecular weight standard (kDa) is shown on the left.

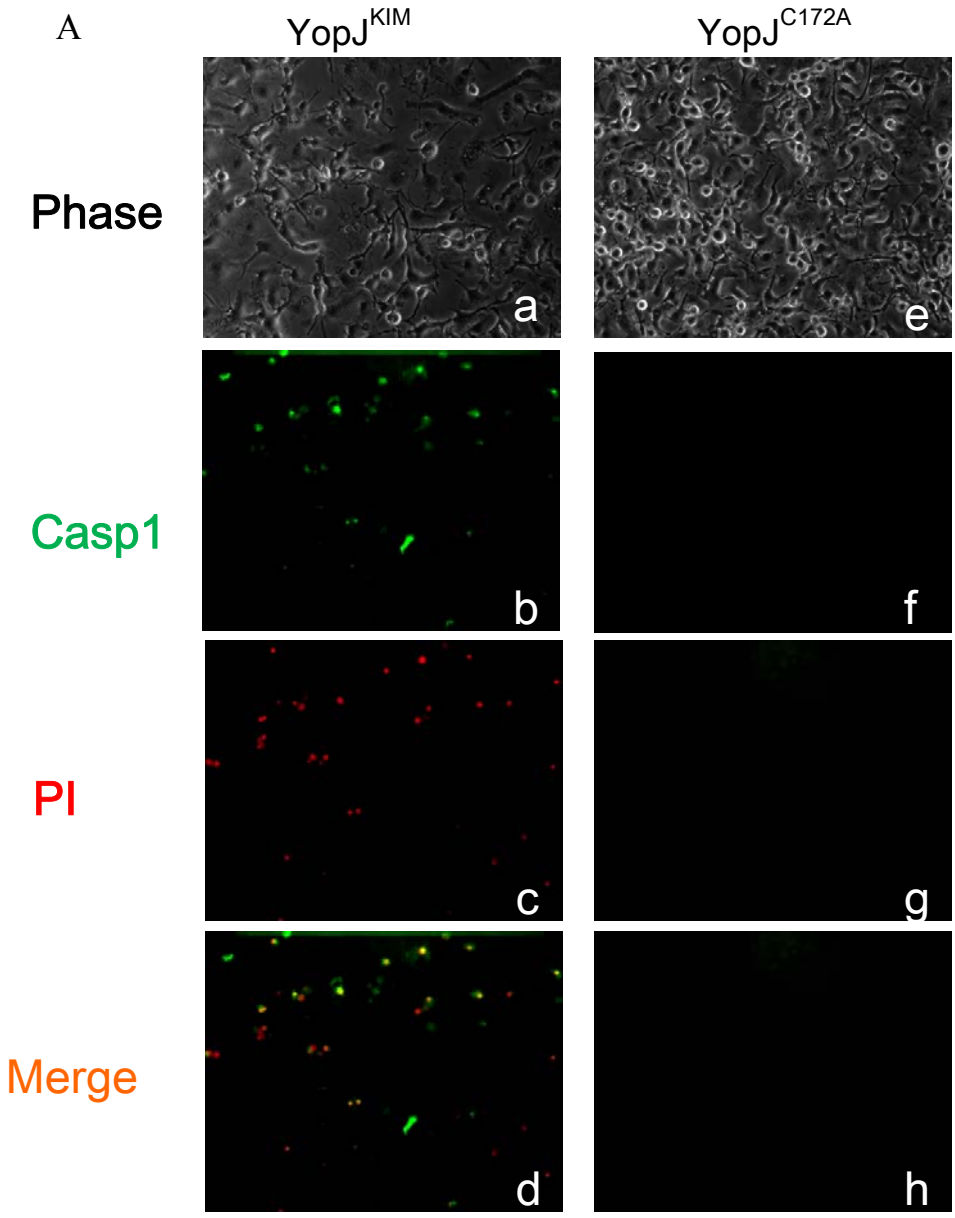
A
YopJ^KIM
YopJ^C172A
Phase
Casp1
PI
Merge
a
b
c
d
e
f
g
h

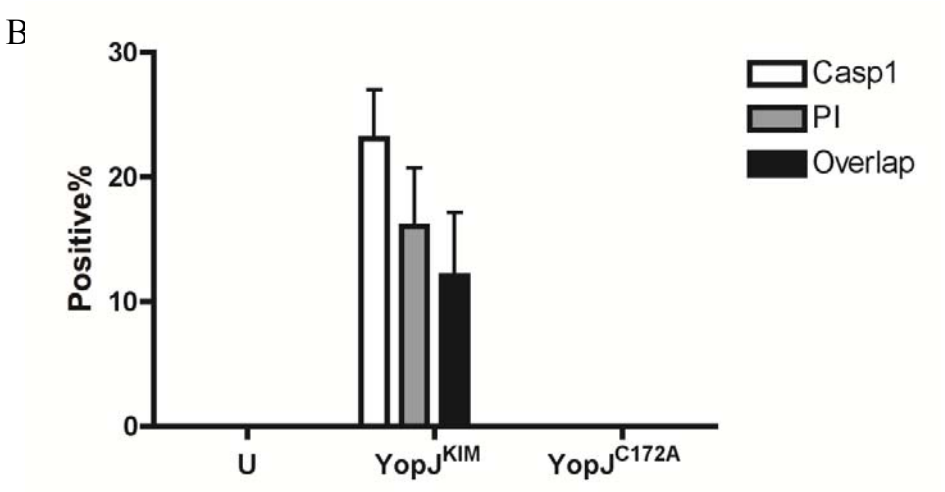

Figure 4.6. KIM5-infected necrotic macrophages contain active caspase-1. BMDMs were seeded on glass coverslips in a 24-well plate and infected with *Y. pestis* strains expressing $YopJ^{KIM}$ or $YopJ^{C172A}$. FAM-YVAD-FMK was added at 9hr post infection to stain for active caspase-1 and PI uptake assay was performed immediately before microscopic analysis. (A) Representative images of phase, active caspase-1 (green) and PI uptake (red) signals captured by digital photomicroscopy are shown in a-c and e-g, respectively. Panels d and h show merged images of green and red signals. (B) Average percentages of BMDMs positive for active caspase-1, PI or both signals was calculated (~100-300 cells per field) from three random fields in three independent experiments.

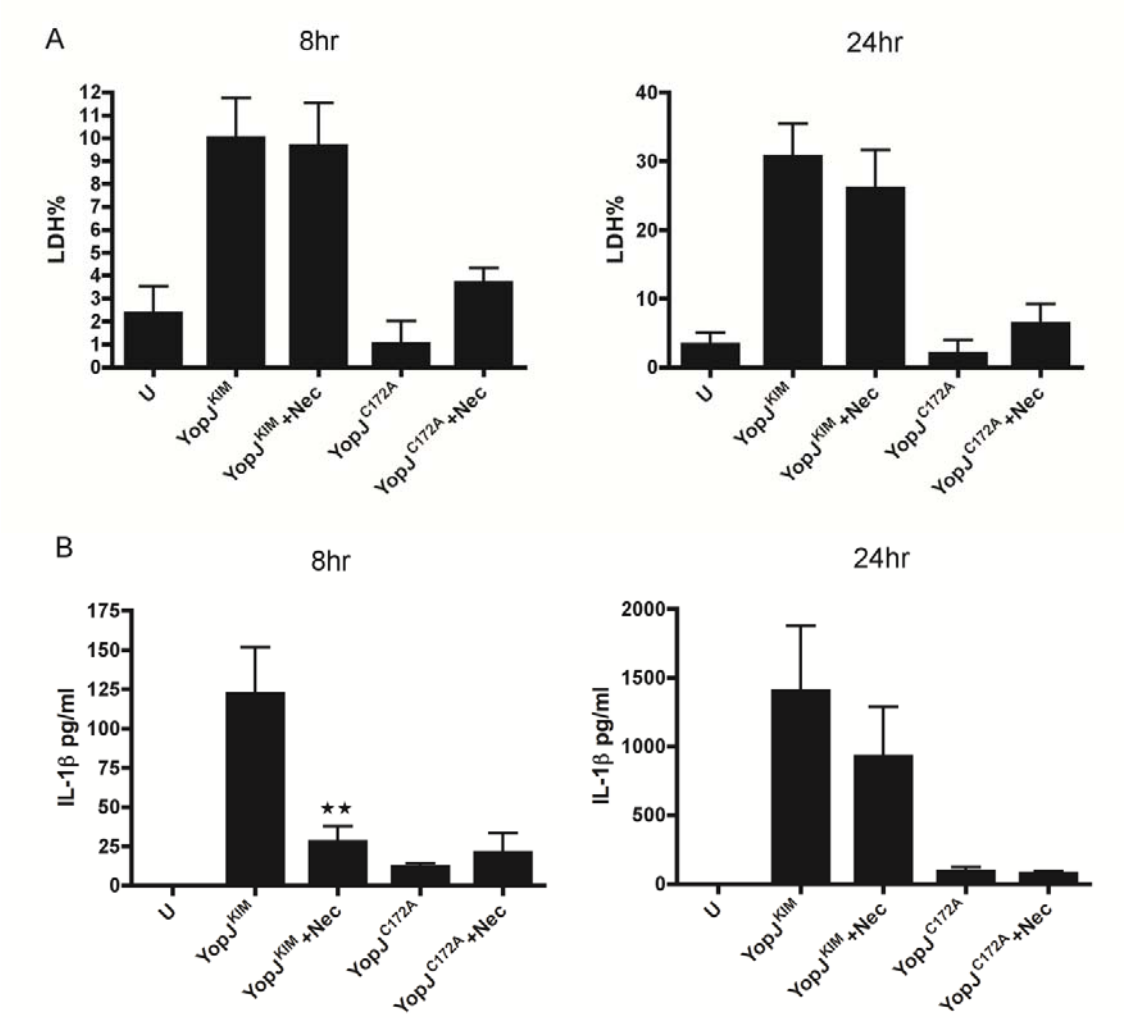

Figure 4.7. RIP1 is not required for YopJ^{KIM}-induced cell death or IL-1β secretion. BMDMs were treated with 30uM RIP1 inhibitor necrostatin-1 or vehicle 1 hr prior to and during infection. BMDMs were infected with *Y. pestis* strains expressing YopJ^{KIM} or YopJ^{C172A} or left uninfected (U). Supernatants were collected and LDH release (A) and secreted IL-1β (B) were measured at 8 hr or 24 hr post-infection from three independent experiments. Results shown are averages and error bars represent standard deviations (★★, P<0.01 as determined by one way ANOVA as compared to YopJ^{KIM} no inhibitor).

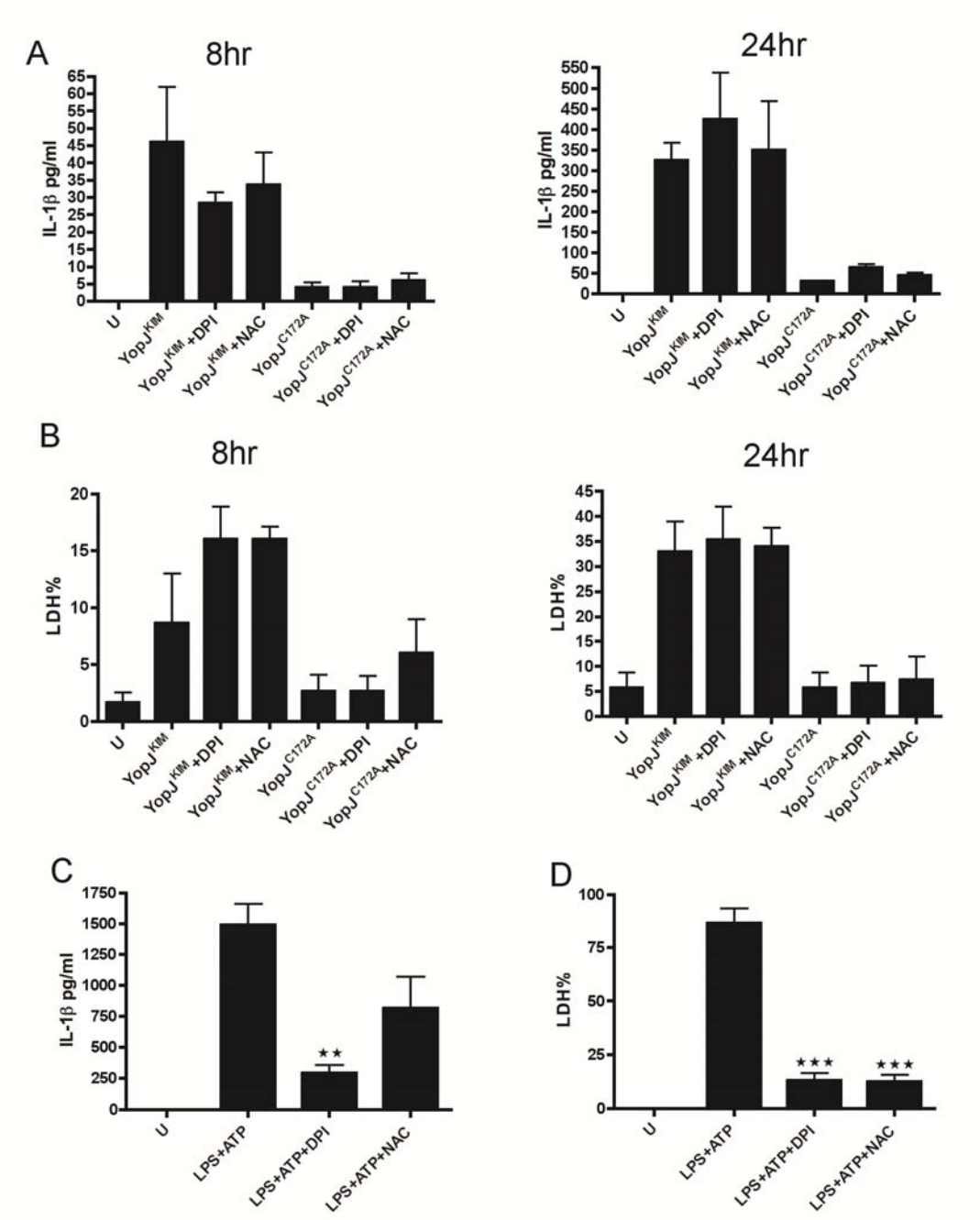
A
8hr
IL-1β pg/ml
65
60
55
50
45
40
35
30
25
20
15
10
5
0
U
YopJ KIM
YopJ KIM +DPI
YopJ KIM +NAC
YopJ C172A
YopJ C172A +DPI
YopJ C172A +NAC
24hr
IL-1β pg/ml
550
500
450
400
350
300
250
200
150
100
50
0
B
8hr
LDH%
20
15
10
5
0
24hr
LDH%
45
40
35
30
25
20
15
10
5
0
C
IL-1β pg/ml
1750
1500
1250
1000
750
500
250
0
★★
U
LPS+ATP
LPS+ATP+DPI
LPS+ATP+NAC
D
LDH%
100
75
50
25
0
★★★
★★★

Figure 4.8. ROS are not required for cytotoxicity or IL-1β secretion in macrophages infected with KIM5. BMDMs were treated with 10uM of DPI or 10mM of NAC or left untreated for 2 hours. (A and B) BMDMs were infected with *Y. pestis* strains expressing $YopJ^{KIM}$ or $YopJ^{C172A}$ or left uninfected (U). Supernatants were collected at 8 hr and 24 hr post-infection and analyzed by IL-1β ELISA (A) or LDH release assay (B). (C and D) BMDMs treated or not with DPI or NAC as above were exposed to 50ng/ml of LPS for 3hr.The treated BMDMs were then exposed to 5mM ATP for 1 hr to activate pyroptosis. Supernatants were tested by IL-1β ELISA (C) or LDH release assay (D). Results shown are the averages from three independent experiments. Error bars represent standard deviations (★★, $P<0.01$;★★★, $P<0.001$, determined by one way ANOVA as compared to LPS+ATP no inhibitor) .

A B

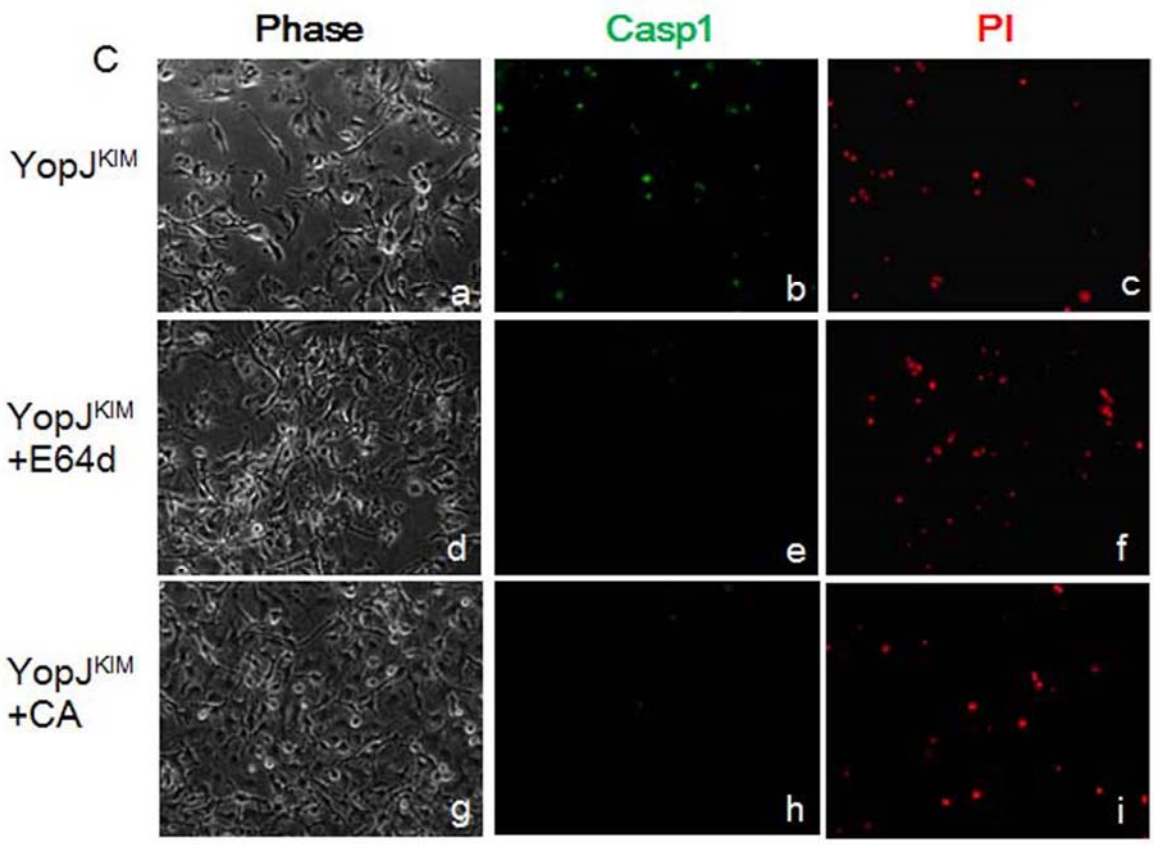

Figure 4.9. Inhibitors of cathepsin B reduce caspase-1 activation in macrophages infected with KIM5. BMDMs were left untreated or treated with 25uM of E64d or CA-074 Me (CA) for 1 hr. Following infection with *Y. pestis* strains expressing $YopJ^{KIM}$ in the absence or presence of the inhibitors, supernatants were collected (A, B) or microscopic assay was performed (C). IL-1β ELISA (A) and LDH release assay (B) was done on supernatants collected 24 hr post-infection. Results shown are the averages from three independent experiments. Error bars represent standard deviations. (★★, $P<0.01$ as determined by one way ANOVA as compared to KIM) (C) Infected BMDMs on coverslips were incubated with FAM-YVAD-FAM 9hr post-infection stained for active caspase-1 (green) for 1 hr and PI uptake (red) immediately before observation. Representative images of phase, green and red signals were captured by digital photomicroscopy.

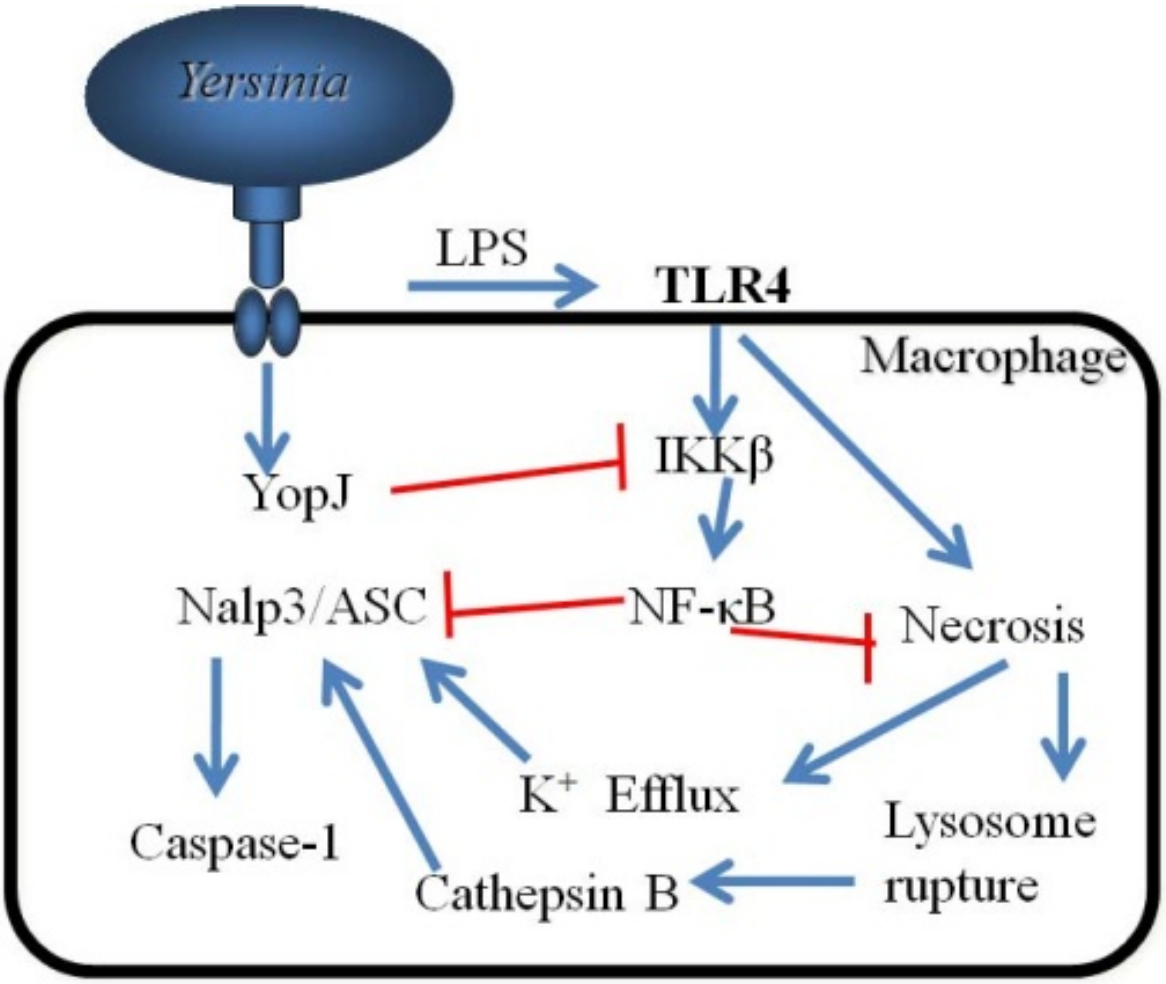

Figure 4.10 Model of caspase-1 activation and cell death in *Yersinia*-infected macrophages triggered by YopJ. NF-κB blocks necrosis downstream of TLR4 and LPS interaction. Unknown negative regulators of the inflammasome components NRLP3 and caspase-1 are also transcribed through NF-κB pathway. When YopJ is translocated into macrophages by *Yersinia* infection, the NF-κB pathway is inhibited by IKKβ acetylation. Necrosis and inflammasome/ caspase-1 activations are de-repressed. Meanwhile, K^+ efflux and lysosomal cathepsin B release resulting from necrosis may synergically activate NLRP3 and caspase-1.

Chapter 5. The role of caspase-1 in *in vivo Yersinia* infection

5.1 Summary

Caspase-1 plays a protective role in many microbial infections (124, 164, 173). As I showed in previous chapters, *Y. pestis* KIM5 infection triggers YopJ-dependent caspase-1 activation and IL-1β secretion in macrophages. Therefore, YopJ-mediated caspase-1 activation may also affect survival of *Yersinia*-infected mice. Two recent *in vivo* studies demonstrated that *Y. pseudotuberculosis* and *Y. pestis* strains ectopically expressing highly cytotoxic YopP are attenuated compared to the YopJ-expressing strain background (21, 220). Zauberman *et al.* showed that the YopP expressing *Y. pestis* strain could work as a vaccine to protect mice from concurrent lethal infection with a virulent *Y. pestis* strain (220). This rapid and efficient protection is unlikely to be mediated by an adaptive immune response, but rather an innate immune response (220). My previous results indicated a positive correlation between YopJ cytotoxicity and caspase-1 activation, therefore, we hypothesized that the attenuation of highly cytotoxic YopP-expressing *Yersinia* strains may come from activation of caspase-1. Thus, I expected to see a decreased survival rate in *Casp1*$^{-/-}$ mice as compared to wild type mice following challenge with a YopP-expressing strain. In this chapter, I constructed *Y. pseudotuberculosis* strains encoding YopP or YopJ^{YPTB} isoforms, and verified that the YopP-expressing strain caused high-level secretion of IL-1β following macrophage infection. Caspase-1 knockout and wild type mice were orogastrically infected with the YopP- or YopJ^{YPTB}-expressing *Y. pseudotuberculosis* strains, and survival was recorded.

5.2 Introduction

A protective effect of caspase-1 has been determined by infection of caspase-1 knockout mice with a variety of bacterial pathogens. An increased survival rate and lower bacterial burden in organs were detected in wild type as compared to caspase-1-deficient mice, indicating a caspase-1-based protective immune responses (124, 164, 173). The contribution of caspase-1 against infection cannot be explained only by IL-18 and IL-1β production. Pyroptosis is also beneficial for the host against pathogen infection (130). For example, neutrophils may phagocytose and eradicate bacteria released from pyroptotic macrophages (130). *Yersinia* strains expressing the hypercytotoxic YopP isoform are more attenuated in mouse models as compared to strains expressing less cytotoxic YopJ, which was suggested by the authors to result from killing of infected macrophages which protect bacteria from neutrophils (21, 220). According to my results, *Yersinia* strains expressing the highly cytotoxic $YopJ^{KIM}$ isoform cause strong caspase-1 activation in infected macrophages. Thus, I hypothesized that *Yersinia* strains expressing the hypercytotoxic YopP isoform would also be able to induce even stronger caspase-1 activation and IL-1β release in macrophages. To determine if the increased survival rate of mice infected by YopP-encoding *Yersinia* strains requires caspase-1, isogenic $Casp1^{+/+}$ and $Casp1^{-/-}$ mice were utilized.

5.3 Experimental Methods

Bacterial strains and growth conditions. The pACYC184 plasmids encoding *Y. enterocolitica* 8081 YopP or *Y. pseudotuberculosis* IP2666 YopJ (termed as $YopJ^{YPTB}$) were a kind gift of Dr. Igor Brodsky (21). Condon changes were introduced into the plasmid encoding $YopJ^{YPTB}$ to yield $YopJ^{KIM}$ (F177L) or into the plasmid encoding YopP to yield $YopP^{C172A}$ (C172A) using Quikchange (Invitrogen). *Y. pseudotuberculosis* strain IP2666*ΔyopJ* (termed as IP26, Table 2.1)

(114) was transformed with pACYC184 or pACYC184 plasmids encoding the different YopP or YopJ isoforms. Plasmid transformation of IP26 was achieved by electroporation, followed by selection on Luria Broth (LB) plates containing chloramphenicol (30ug/ml) (114). Cultures of *Y. pseudotuberculosis* for macrophage infection were prepared as described in Chapter 2.

Bone marrow macrophage isolation and culture conditions. BMDMs were isolated from the femurs of 6- to 8-week-old C57BL/6J female mice (Jackson Laboratories) and cultured as previously described in Chapter 2.

Mouse infection assay. The mouse infection protocol was approved by the Stony Brook University IACUC. Caspase-1-deficient (*Casp1*$^{-/-}$) mice on the C57BL/6 background (218) were obtained from Richard Flavell and Craig Roy, Yale University. The *Casp1*$^{-/-}$ mice upon receipt had been backcrossed to C57BL/6 mice for 7 generations. The *Casp1*$^{-/-}$ mice were backcrossed to C57BL/6J mice (Jackson Laboratories) for an additional three generations. Deletion of both *Casp1* genes in offspring was verified by PCR. The offspring were mated to generate colonies of *Casp1*$^{-/-}$ or *Casp1*$^{+/+}$ mice that were used for infection at 8-10 weeks of age. *Y. pseudotuberculosis* cultures were grown overnight with shaking in LB at 26°C. Bacteria were harvested by centrifugation and resuspended in PBS. Male and female mice were fasted for 14-16 hr prior to infection. Infection was achieved orogastrically with $1x10^9$ colony forming units of bacteria in 0.2 ml of HBSS using a 20 gauge feeding needle. Mice were monitored three times a day for 21 days. Mice displaying severe signs of disease and deemed unable to survive were euthanized by CO_2 asphyxiation.

IL-1β ELISA. IL-1β was measured from supernatants of infected macrophages by ELISA according to manufacturer's instructions (R&D).

LDH Release. Cell death of infected macrophages was determined by CytoTox-96 nonradioactive cytotoxicity assay (Promega) from supernatants following manufacturer's instructions. The total LDH release was made by freezing and thaw untreated cells. The percentage of dead cells was calculated as followed: (sample LDH-background LDH)/ (total LDH-background LDH) × 100%.

Statistical analysis. Statistical analysis was performed with Prism 4.0 (Graphpad) software. The statistic for survival curve was calculated by LogRank assay. *P* values of less than 0.05 were considered significant.

5.4 Results

Enhanced YopP-mediated macrophage cell death is associated with elevated levels of IL-1β release. Higher levels of cell death are observed when dendritic cells are infected with *Y. pseudotuberculosis* ectopically expressing YopP as compared to the native isoform $YopJ^{YPTB}$ (21). Two amino acid polymorphisms in the N-terminal region of YopP specify increased secretion, translocation and cytotoxic activity as compared to $YopJ^{YPTB}$ (21). Macrophages were infected with *Y. pseudotuberculosis* ectopically expressing YopP to determine if the enhanced cell death caused by this isoform is correlated with higher caspase-1 activation and IL-1β secretion. Macrophages were also infected with *Y. pseudotuberculosis* expressing catalytically inactive YopP ($YopP^{C172A}$), the native isoform $YopJ^{YPTB}$, or $YopJ^{KIM}$. The different isoforms were expressed from a low copy plasmid (pACYC184) in a *Y. pseudotuberculosis ΔyopJ* mutant (IP26). Higher cytotoxicity and IL-1β release was detected in macrophages infected with *Y. pseudotuberculosis* expressing YopP as compared to the other isoforms or the control strain with the empty vector (Figure 5.1A and B). In ranking the different isoforms YopP had the highest cytotoxicity, $YopJ^{YPTB}$ the lowest killing effect, and $YopJ^{KIM}$ was intermediate. IL-1β release

followed the same order YopP> YopJ^{KIM} > YopJ^{YPTB}, which further supports the idea that cell death and caspase-1 activation are mechanistically linked.

Caspase-1 is not required for innate host protection against *Yersinia* endowed with enhanced cytotoxicity. *Y. pseudotuberculosis* or *Y. pestis* strains ectopically expressing YopP are attenuated in orogastric (21) or bubonic (220) models of mouse infection, respectively. The basis for attenuation of *Yersinia* strains endowed with enhanced cytotoxicity is not known, but it appears to result from an increased innate immune response and does not require CD8 T cell activation (21, 220). To determine if activation of caspase-1 is important for the increased innate immune response to *Yersinia* endowed with enhanced cytotoxicity, *Casp1*$^{+/+}$ or *Casp1*$^{-/-}$ C57BL/6 mice were orogastrically infected with *Y. pseudotuberculosis* ectopically expressing YopP. Control mice were infected with *Y. pseudotuberculosis* ectopically expressing YopJ^{YPTB}. Mouse survival was recorded over 21 days. As shown previously (21) more *Casp1*$^{+/+}$ mice infected with YopP-expressing strain survived as compared to mice infected with YopJ^{YPTB}-expressing bacteria (Figure 5.2A). However, *Casp1*$^{-/-}$ mice also showed enhanced survival following challenge with the YopP-expressing *Y. pseudotuberculosis*, indicating that caspase-1 is dispensable for the increased innate immune response to *Yersinia* with enhanced cytotoxicity. When the results were grouped according to the infecting strain while ignoring mouse genotype, the survival of mice infected with *Y. pseudotuberculosis* expressing YopP was significantly higher than the mice infected with bacteria expressing YopJ^{YPTB} (Figure 5.2B, $P<0.01$).

5.5 Discussion

Brodsky *et al.* reported that *Y. pseudotuberculosis* ectopically expressing YopP was more attenuated than the same strain expressing YopJ^{YPTB} in a mouse oral infection model (21). The author suggested that the hypercytotoxic strain eliminated infected macrophages that served as a

niche for *Yersinia* survival *in vivo* (21). Another study showed that a *Y. pestis* strain ectopically expressing YopP was attenuated in a mouse bubonic infection model (220). In addition, mice infected with the hypercytotoxic attenuated strain were protected against concurrent challenge with fully virulent *Y. pestis* (220). We hypothesized that the highly cytotoxic YopP could stimulate efficient caspase-1 activation *in vivo* leading to protection based on caspase-1 activation. In an *in vitro* macrophage infection, *Y. pseudotuberculosis* expressing YopP, the same strain used in Brodsky's study (21) triggered higher levels of IL-1β secretion and cytotoxicity than $YopJ^{KIM}$ (Figure 5.1A and B). This result confirmed the idea that there is a direct correlation between the cytotoxic potential of different YopJ/P isoforms and the level of IL-1β secretion in macrophage infection. So, YopP may elicit robust caspase-1 activation *in vivo*. However, resistance to the YopP-expressing strain did not show a difference between $Casp1^{+/+}$ and $Casp1^{-/-}$ mice (Figure 5.2A). When we pooled the results from caspase-1 deficient mice and wild type mice together, survival of mice infected with the YopP-expressing strain was significantly higher as compared to mice infected with the $YopJ^{YPTB}$-expressing strain. Thus, we obtained the same results as shown in Brodsky's study (21) (Figure 5.2B), proving that our *in vivo* assay was conducted correctly. It seems that caspase-1 does not protect mice from oral infection with *Yersinia* strains with enhanced cytotoxicity and the underlying mechanism for the attenuation of YopP-expressing strain is still unclear. It needs to be emphasized that YopJ/P-dependent caspase-1 activation has not been detected in mice. It is possible that caspase-1 is not activated or activated to similar levels in mice challenged with either strain. Zauberman *et al*. showed that increased protection against infection with YopP-expressing *Y. pestis* was obtained in subcutaneous challenge, but the attenuated strain was highly virulent in the intranasal or intravenous infection, revealing that infection route can affect the survive rate intensively (220).

In addition, caspase-1-based protection may be too subtle to show a significant difference in survival. So organ burden assay and IL-1β serum level need to be tested instead of survival curve.

Acknowledgement

I would like to thank Craig Roy and Richard Flavell for *Casp1*$^{-/-}$ mice. I wish to acknowledge Sarit Lilo, Maya Ivanov and Patricio Mena for maintenance and assistance with *Casp1*$^{-/-}$ mouse colonies, and mouse infection experiments. I thank Igor Brodsky for the gift of pACYC-YopP/J plasmids.

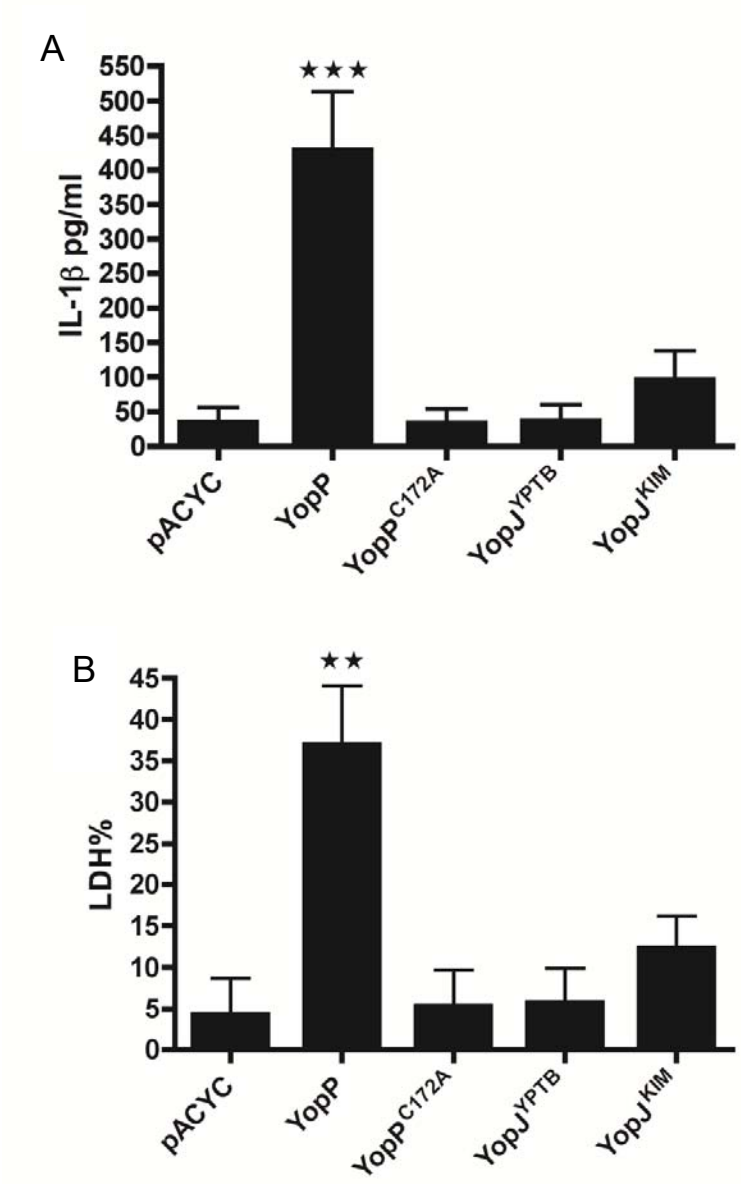

Figure 5.1. Enhanced YopP-mediated macrophage cell death is associated with elevated levels of IL-1β release. *Y. pseudotuberculosis* IP26 (*ΔyopJ*) carrying the empty pACYC184 plasmid (pACYC) or pACYC184 encoding the indicated YopP or YopJ isoforms was used to infect BMDMs. Twenty four hours post-infection, medium was collected for IL-1β ELISA (A) and LDH release assay (B). Results shown are the averages from three independent experiments. Error bars represent standard deviations (★★, $P<0.01$; ★★★, $P<0.001$ as determined by one way ANOVA as compared to pACYC condition).

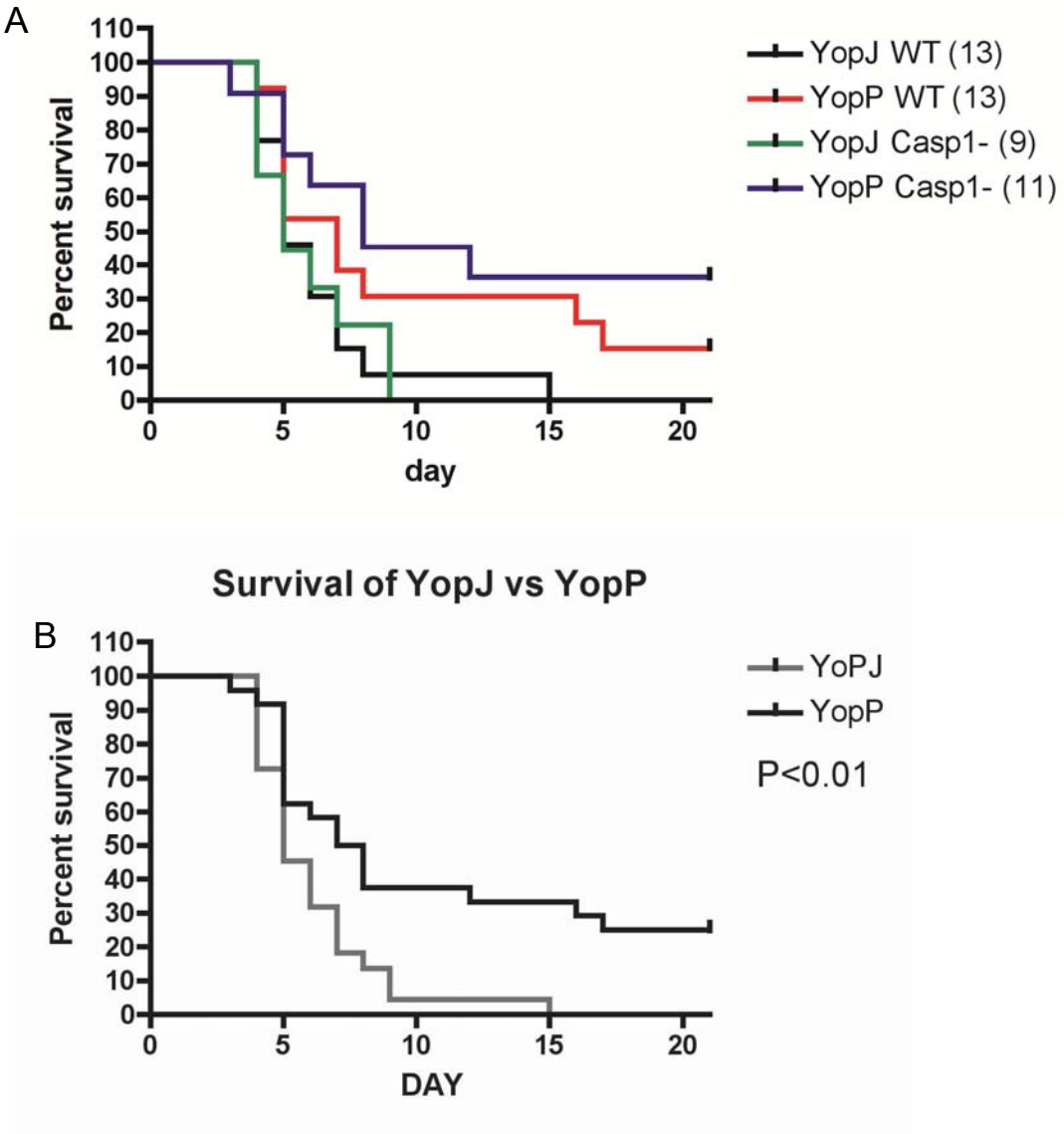

Figure 5.2. Caspase-1 is not required for innate host protection against *Yersinia* endowed with enhanced cytotoxicity. Six to eight-week old *Casp1*$^{+/+}$ (wild type, WT) or *Casp1*$^{-/-}$ C57BL/6J mice were infected orogastrically with 1x10^{9} CFU of *Y. pseudotuberculosis* IP26 carrying pACYC184 encoding YopP or YopJ^{YPTB}. Results shown are pooled from two independent experiments. Mouse survival was monitored for 21 days. (A) Comparison in caspase-1 or wild type mice with YopP or YopJ^{YPTB}. Total numbers of mice infected are shown in parenthesis. (B) Comparing between YopP and YopJ^{YPTB}. Significant differences in survival curves were determined by LogRank test (P<0.01 comparing infecting strain groups).

Chapter 6. Conclusion Remarks and Future Directions

My studies in this dissertation focused on the mechanism of caspase-1 activation and cell death in *in vitro* macrophage infection with *Yersinia* and determined the role of caspase-1 in host protection using an *in vivo* mouse model.

Lilo *et al.* showed that $YopJ^{KIM}$ is required to trigger enhanced caspase-1 activation, IL-1β secretion and cytotoxicity in *Y. pestis*-infected macrophages (114). When $YopJ^{KIM}$ was expressed in a *Y. pseudotuberculosis* strain, it conferred on the strain a significantly increased ability to induce cell death and IL-1β secretion (114). In Chapter 2, I identified two amino acid changes at residues 177 and 206 that are necessary for the increased activity of $YopJ^{KIM}$ as compared to other YopJ isoforms. The amino acid changes allow $YopJ^{KIM}$ to inhibit the NF-κB pathway more efficiently as compared to other YopJ isoforms, in part by up-regulated binding to IKKβ. In Chapter 3, I obtained evidence that inhibition of IKKβ by $YopJ^{KIM}$ is important for caspase-1 activation in *Yersinia*-infected macrophages, which extended the finding from Greten *et al*. showing that the NF-κB pathway negatively controls caspase-1 activation (74). When I infected IKKβ deficient ($Ikk\beta^{\Delta}$) macrophages with *Y. pestis* strains expressing different YopJ isoforms, or treated macrophages with a small molecule IKKβ inhibitor, I found that caspase-1 activation was amplified as compared to that seen in the wild type macrophages or to the no-inhibitor condition. Measurement of *Ikkβ* mRNA levels and IKKβ protein amounts by Western blot provided evidence that $Ikk\beta^{\Delta}$ macrophages contain 50% less IKKβ than $Ikk\beta^{F/F}$ macrophages (data not shown), but we do not know if some "$Ikk\beta^{\Delta}$" cells have a complete deletion of both

alleles while others have no deletions, or the whole population is has half of the alleles deleted. So in this case, it is hard to determine if caspase-1 hyperactivation really happens in the *Ikkβ*$^{\Delta}$ macrophages. In the future, a reporter gene for *Ikkβ* expression could let us know if caspase-1 is profoundly activated exclusively in the knockdown cells by examining the reporter and caspase-1 fluorescent staining. Since very little is known about signaling pathway(s) controlling inflammasome/caspase-1 activation, it would be very valuable to uncover the NF-κB-regulated factor(s) interacting negatively with inflammasomes/caspase-1. This chapter focused primarily on understanding the negative regulation caspase-1 by IKKβ and the NF-κB pathway, since YopJ targets this line of signaling. However, it is likely that the TLR4 signaling pathway contributes positive signals for activation of caspase-1 in *Yersinia*-infected macrophages or in macrophages treated with IKKβ inhibitors, and it would be interesting to know more about this mechanism. It would also be interesting to test a variety of IKKβ inhibitors in this assay, especially inhibitors of different classes (e.g. IKKγ binding peptides and Hsp90 inhibitors (101) to see if the same results would be obtained.

In Chapter 4, I aimed to determine the macrophage death pathway triggered by *Y. pestis* KIM5 infection and molecular patterns that could be recognized by the NLRP3 inflammasome. Our previous results showed that macrophage death is independent of caspase-1 and NLRP3 (114, 227). This is unusual, because all known pathogen-induced macrophage death mechanisms that are associated with caspase-1 activation are caspase-1 or inflammasome-dependent (37). A very important question we need to answer in the future is if the IL-1β production is an autocrine effect, i.e. that only bacteria-containing macrophages produce IL-1β, or a paracrine effect in which bacteria-containing macrophages secrete some factor triggering neighbor uninfected macrophages to produce IL-1β. A *Y. pestis* strain expressing GFP has been constructed, so

staining for active caspase-1 could help determine if GFP positive bacteria co-localize with the caspase-1 positive cells, Alternatively, after the infection, GFP positive cells could be sorted by FACS and IL-1β ELISA used to measure cytokine secretion. As to the classification of cell death, although the evidence supports necrosis occurring in macrophages infected with *Y. pestis* KIM5, we cannot distinguish between primary necrosis and secondary necrosis. Under our *in vitro* infection conditions, without removal of nascent apoptotic cells by phagocytes, apoptosis can proceed to secondary necrosis in the end (183). In our *in vitro* infection model, weak apoptosis is observed and may cause necrosis at a later stage. A time-lapse microscopy experiment would supply powerful evidence of such a kinetic morphology change. According to LDH release and IL-1β secretion time course studies, as well as caspase-1/PI double staining, and cathepsin B inhibitor results, we hypothesized that K^+ efflux and cathepsin B released from necrotic macrophages activate NLRP3/caspase-1. However, as YopJ can block IKKβ activity to elicit both caspase-1 activation and cell death (Chapter 2 and 3), we could not rule out the possibility that caspase-1 and cell death may not be correlated to each other, but only correlated to inhibition of IKKβ. So in the future, if a new inhibitor could be made available to specifically abrogate necrotic death, it would be very meaningful to check if caspase-1 activation occurs in *Y. pestis*-infected macrophages when necrosis is blocked. The cathepsin B inhibitor study examined the possibility that lysosomal cathepsin B activates NRLP3 during infection. However, in KIM5-infected macrophages, lysosome acidification was not detectable, indicating that lysosomes may not undergo destruction (159). In the future, cathepsin B release and lysosome rupture have to be evaluated by cathepsin B staining or lysotracker. Additionally, KIM5 infection should be conducted in cathepsin B deficient macrophages.

We performed an *in vivo* assay to test if caspase-1 is important for the enhanced protective innate immune response that mice exhibit against *Yersinia* strains with the hypercytotoxic phenotype. Importantly, I showed that a *Y. pseudotuberculosis* strain ectopically expressing YopP did cause enhanced cytotoxicity and caspase-1 activation in infected macrophages in vitro. However, when this hypercytotoxic strain was used in orogastric infection, *Casp1*$^{+/+}$ and *Casp1*$^{-/-}$ mice were equally resistant to challenge. In addition, the *Casp1*$^{+/+}$ and *Casp1*$^{-/-}$ mice were equally sensitive to challenge with the strain expressing YopJ, with a native cytotoxic phenotype. Thus, our data show that caspase-1 has no major protective effect for survival of mice infected by this route with *Y. pseudotuberculosis* strains exhibiting normal or hypercytotoxic phenotypes. Destruction of cells containing intracellular bacteria may be the underlying mechanism of host resistance to *Yersinia* strains expressing highly cytotoxic YopP (19, 216). Other infection routes with *Y. pestis* should be examined, since Zauberman *et al*. found that a YopP-expressing hypercytotoxic strain was only attenuated in subcutaneous mouse infection, not in pneumonic and septicemic models (220). Our data do not rule out the possibility that caspase-1 is important for the enhanced innate immune response of mice against YopP-expressing *Y. pestis.* Additionally, since a subtle protective role for caspase-1 may not be revealed in a survival test, organ burden assays or measurements of serum IL-1β levels may show that caspase-1 does significantly impact the immune response to *Yersinia* infection. Besides the short-term effect, T cell responses have been demonstrated to be important for protection of mice from secondary *Yersinia* infection (7, 12, 149). Transferring murine T cells raised in mice immunized with *Y. pestis* to naïve mice significantly decreased mortality of *Y. pestis* lethal challenge (149). Depletion of $CD8^+$ T reduced resistance to virulent *Y. pseudotuberculosis* in mice vaccinated with attenuated*Y. pseudotuberculosis* (12). Bergman *et al.*

demonstrated that during *in vitro Yersinia* infection, $CD8^+$ T cells are required for directing activated macrophages to phagocytose bacteria-associated antigen presenting cells.This result suggests that $CD8^+$ T cells may kill bacteria attached to antigen present cells indirectly by facilitating bystander phagocytes to remove apoptotic antigen presenting cells and their attached bacteria (12). Because IL-18 is processed by caspase-1, and promotes T cell activation (131, 195, 215, 216), it would be interesting to know if caspase-1 is involved in T cell priming during immunization with attenuated *Yersinia* strains. This could be tested by measuring T cell activation in *Yersinia*-immunized *Casp1*$^{-/-}$ mice.

References

1. **Akhter, A., M. A. Gavrilin, L. Frantz, S. Washington, C. Ditty, D. Limoli, C. Day, A. Sarkar, C. Newland, J. Butchar, C. B. Marsh, M. D. Wewers, S. Tridandapani, T. D. Kanneganti, and A. O. Amer.** 2009. Caspase-7 activation by the Nlrc4/Ipaf inflammasome restricts Legionella pneumophila infection. PLoS Pathog **5:**e1000361.
2. **Aksentijevich, I., M. Nowak, M. Mallah, J. J. Chae, W. T. Watford, S. R. Hofmann, L. Stein, R. Russo, D. Goldsmith, P. Dent, H. F. Rosenberg, F. Austin, E. F. Remmers, J. E. Balow, Jr., S. Rosenzweig, H. Komarow, N. G. Shoham, G. Wood, J. Jones, N. Mangra, H. Carrero, B. S. Adams, T. L. Moore, K. Schikler, H. Hoffman, D. J. Lovell, R. Lipnick, K. Barron, J. J. O'Shea, D. L. Kastner, and R. Goldbach-Mansky.** 2002. De novo CIAS1 mutations, cytokine activation, and evidence for genetic heterogeneity in patients with neonatal-onset multisystem inflammatory disease (NOMID): a new member of the expanding family of pyrin-associated autoinflammatory diseases. Arthritis Rheum **46:**3340-3348.
3. **Amer, A., L. Franchi, T. D. Kanneganti, M. Body-Malapel, N. Ozoren, G. Brady, S. Meshinchi, R. Jagirdar, A. Gewirtz, S. Akira, and G. Nunez.** 2006. Regulation of Legionella phagosome maturation and infection through flagellin and host Ipaf. J Biol Chem **281:**35217-35223.
4. **Andersson, U., H. Wang, K. Palmblad, A. C. Aveberger, O. Bloom, H. Erlandsson-Harris, A. Janson, R. Kokkola, M. Zhang, H. Yang, and K. J. Tracey.** 2000. High mobility group 1 protein (HMG-1) stimulates proinflammatory cytokine synthesis in human monocytes. J Exp Med **192:**565-570.
5. **Andor, A., K. Trulzsch, M. Essler, A. Roggenkamp, A. Wiedemann, J. Heesemann, and M. Aepfelbacher.** 2001. YopE of Yersinia, a GAP for Rho GTPases, selectively modulates Rac-dependent actin structures in endothelial cells. Cell Microbiol **3:**301-310.
6. **Andrei, C., C. Dazzi, L. Lotti, M. R. Torrisi, G. Chimini, and A. Rubartelli.** 1999. The secretory route of the leaderless protein interleukin 1beta involves exocytosis of endolysosome-related vesicles. Mol Biol Cell **10:**1463-1475.
7. **Autenrieth, I. B., A. Tingle, A. Reske-Kunz, and J. Heesemann.** 1992. T lymphocytes mediate protection against Yersinia enterocolitica in mice: characterization of murine T-cell clones specific for Y. enterocolitica. Infect Immun **60:**1140-1149.
8. **Basak, C., S. K. Pathak, A. Bhattacharyya, D. Mandal, S. Pathak, and M. Kundu.** 2005. NF-kappaB- and C/EBPbeta-driven interleukin-1beta gene expression and PAK1-mediated caspase-1 activation play essential roles in interleukin-1beta release from Helicobacter pylori lipopolysaccharide-stimulated macrophages. J Biol Chem **280:**4279-4288.
9. **Bauernfeind, F. G., G. Horvath, A. Stutz, E. S. Alnemri, K. MacDonald, D. Speert, T. Fernandes-Alnemri, J. Wu, B. G. Monks, K. A. Fitzgerald, V. Hornung, and E. Latz.** 2009. Cutting edge: NF-kappaB activating pattern recognition and cytokine receptors license NLRP3 inflammasome activation by regulating NLRP3 expression. J Immunol **183:**787-791.
10. **Bedoya, F., L. L. Sandler, and J. A. Harton.** 2007. Pyrin-only protein 2 modulates NF-kappaB and disrupts ASC:CLR interactions. J Immunol **178:**3837-3845.

11. **Benchoua, A., J. Braudeau, A. Reis, C. Couriaud, and B. Onteniente.** 2004. Activation of proinflammatory caspases by cathepsin B in focal cerebral ischemia. J Cereb Blood Flow Metab **24:**1272-1279.
12. **Bergman, M. A., W. P. Loomis, J. Mecsas, M. N. Starnbach, and R. R. Isberg.** 2009. CD8(+) T cells restrict Yersinia pseudotuberculosis infection: bypass of anti-phagocytosis by targeting antigen-presenting cells. PLoS Pathog **5:**e1000573.
13. **Bergsbaken, T., and B. T. Cookson.** 2007. Macrophage activation redirects yersinia-infected host cell death from apoptosis to caspase-1-dependent pyroptosis. PLoS Pathog **3:**e161.
14. **Bergsbaken, T., S. L. Fink, and B. T. Cookson.** 2009. Pyroptosis: host cell death and inflammation. Nat Rev Microbiol **7:**99-109.
15. **Billiau, A.** 2006. Anti-inflammatory properties of Type I interferons. Antiviral Res **71:**108-116.
16. **Black, D. S., and J. B. Bliska.** 2000. The RhoGAP activity of the Yersinia pseudotuberculosis cytotoxin YopE is required for antiphagocytic function and virulence. Mol Microbiol **37:**515-527.
17. **Bonaldi, T., F. Talamo, P. Scaffidi, D. Ferrera, A. Porto, A. Bachi, A. Rubartelli, A. Agresti, and M. E. Bianchi.** 2003. Monocytic cells hyperacetylate chromatin protein HMGB1 to redirect it towards secretion. EMBO J **22:**5551-5560.
18. **Boone, E., T. Vanden Berghe, G. Van Loo, G. De Wilde, N. De Wael, D. Vercammen, W. Fiers, G. Haegeman, and P. Vandenabeele.** 2000. Structure/Function analysis of p55 tumor necrosis factor receptor and fas-associated death domain. Effect on necrosis in L929sA cells. J Biol Chem **275:**37596-37603.
19. **Bortner, C. D., and J. A. Cidlowski.** 2002. Apoptotic volume decrease and the incredible shrinking cell. Cell Death Differ **9:**1307-1310.
20. **Brennan, M. A., and B. T. Cookson.** 2000. Salmonella induces macrophage death by caspase-1-dependent necrosis. Mol Microbiol **38:**31-40.
21. **Brodsky, I. E., and R. Medzhitov.** 2008. Reduced secretion of YopJ by Yersinia limits in vivo cell death but enhances bacterial virulence. PLoS Pathog **4:**e1000067.
22. **Brodsky, I. E., N. W. Palm, S. Sadanand, M. B. Ryndak, F. S. Sutterwala, R. A. Flavell, J. B. Bliska, and R. Medzhitov.** 2010. A Yersinia effector protein promotes virulence by preventing inflammasome recognition of the type III secretion system. Cell Host Microbe **7:**376-387.
23. **Bruey, J. M., N. Bruey-Sedano, F. Luciano, D. Zhai, R. Balpai, C. Xu, C. L. Kress, B. Bailly-Maitre, X. Li, A. Osterman, S. Matsuzawa, A. V. Terskikh, B. Faustin, and J. C. Reed.** 2007. Bcl-2 and Bcl-XL regulate proinflammatory caspase-1 activation by interaction with NALP1. Cell **129:**45-56.
24. **Bryan, N. B., A. Dorfleutner, S. J. Kramer, C. Yun, Y. Rojanasakul, and C. Stehlik.** 2010. Differential splicing of the apoptosis-associated speck like protein containing a caspase recruitment domain (ASC) regulates inflammasomes. J Inflamm (Lond) **7:**23.
25. **Burnstock, G.** 2006. Pathophysiology and therapeutic potential of purinergic signaling. Pharmacol Rev **58:**58-86.
26. **Cai, X., C. Stoicov, H. Li, J. Carlson, M. Whary, J. G. Fox, and J. Houghton.** 2005. Overcoming Fas-mediated apoptosis accelerates Helicobacter-induced gastric cancer in mice. Cancer Res **65:**10912-10920.

27. **Cameron, L. A., R. A. Taha, A. Tsicopoulos, M. Kurimoto, R. Olivenstein, B. Wallaert, E. M. Minshall, and Q. A. Hamid.** 1999. Airway epithelium expresses interleukin-18. Eur Respir J **14:**553-559.
28. **Cassel, S. L., S. C. Eisenbarth, S. S. Iyer, J. J. Sadler, O. R. Colegio, L. A. Tephly, A. B. Carter, P. B. Rothman, R. A. Flavell, and F. S. Sutterwala.** 2008. The Nalp3 inflammasome is essential for the development of silicosis. Proc Natl Acad Sci U S A **105:**9035-9040.
29. **Cervantes, J., T. Nagata, M. Uchijima, K. Shibata, and Y. Koide.** 2008. Intracytosolic Listeria monocytogenes induces cell death through caspase-1 activation in murine macrophages. Cell Microbiol **10:**41-52.
30. **Chan, F. K., J. Shisler, J. G. Bixby, M. Felices, L. Zheng, M. Appel, J. Orenstein, B. Moss, and M. J. Lenardo.** 2003. A role for tumor necrosis factor receptor-2 and receptor-interacting protein in programmed necrosis and antiviral responses. J Biol Chem **278:**51613-51621.
31. **Choi, K. S., J. T. Park, and J. S. Dumler.** 2005. Anaplasma phagocytophilum delay of neutrophil apoptosis through the p38 mitogen-activated protein kinase signal pathway. Infect Immun **73:**8209-8218.
32. **Clausen, B. E., C. Burkhardt, W. Reith, R. Renkawitz, and I. Forster.** 1999. Conditional gene targeting in macrophages and granulocytes using LysMcre mice. Transgenic Res **8:**265-277.
33. **Comi, G., M. Filippi, F. Barkhof, L. Durelli, G. Edan, O. Fernandez, H. Hartung, P. Seeldrayers, P. S. Sorensen, M. Rovaris, V. Martinelli, and O. R. Hommes.** 2001. Effect of early interferon treatment on conversion to definite multiple sclerosis: a randomised study. Lancet **357:**1576-1582.
34. **Craven, R. R., X. Gao, I. C. Allen, D. Gris, J. Bubeck Wardenburg, E. McElvania-Tekippe, J. P. Ting, and J. A. Duncan.** 2009. Staphylococcus aureus alpha-hemolysin activates the NLRP3-inflammasome in human and mouse monocytic cells. PLoS ONE **4:**e7446.
35. **Cruz, C. M., A. Rinna, H. J. Forman, A. L. Ventura, P. M. Persechini, and D. M. Ojcius.** 2007. ATP activates a reactive oxygen species-dependent oxidative stress response and secretion of proinflammatory cytokines in macrophages. J Biol Chem **282:**2871-2879.
36. **Cui, J., L. Zhu, X. Xia, H. Y. Wang, X. Legras, J. Hong, J. Ji, P. Shen, S. Zheng, Z. J. Chen, and R. F. Wang.** 2010. NLRC5 negatively regulates the NF-kappaB and type I interferon signaling pathways. Cell **141:**483-496.
37. **Davis, B. K., H. Wen, and J. P. Ting.** 2011. The inflammasome NLRs in immunity, inflammation, and associated diseases. Annu Rev Immunol **29:**707-735.
38. **Decker, T., M. Muller, and S. Stockinger.** 2005. The yin and yang of type I interferon activity in bacterial infection. Nat Rev Immunol **5:**675-687.
39. **Declercq, W., T. Vanden Berghe, and P. Vandenabeele.** 2009. RIP kinases at the crossroads of cell death and survival. Cell **138:**229-232.
40. **Degterev, A., J. Hitomi, M. Germscheid, I. L. Ch'en, O. Korkina, X. Teng, D. Abbott, G. D. Cuny, C. Yuan, G. Wagner, S. M. Hedrick, S. A. Gerber, A. Lugovskoy, and J. Yuan.** 2008. Identification of RIP1 kinase as a specific cellular target of necrostatins. Nat Chem Biol **4:**313-321.

41. **Degterev, A., Z. Huang, M. Boyce, Y. Li, P. Jagtap, N. Mizushima, G. D. Cuny, T. J. Mitchison, M. A. Moskowitz, and J. Yuan.** 2005. Chemical inhibitor of nonapoptotic cell death with therapeutic potential for ischemic brain injury. Nat Chem Biol **1:**112-119.
42. **Delaleu, N., and M. Bickel.** 2004. Interleukin-1 beta and interleukin-18: regulation and activity in local inflammation. Periodontol 2000 **35:**42-52.
43. **Denecker, G., W. Declercq, C. A. Geuijen, A. Boland, R. Benabdillah, M. van Gurp, M. P. Sory, P. Vandenabeele, and G. R. Cornelis.** 2001. Yersinia enterocolitica YopP-induced apoptosis of macrophages involves the apoptotic signaling cascade upstream of bid. J Biol Chem **276:**19706-19714.
44. **Denecker, G., S. Totemeyer, L. J. Mota, P. Troisfontaines, I. Lambermont, C. Youta, I. Stainier, M. Ackermann, and G. R. Cornelis.** 2002. Effect of low- and high-virulence Yersinia enterocolitica strains on the inflammatory response of human umbilical vein endothelial cells. Infect Immun **70:**3510-3520.
45. **Devin, A., A. Cook, Y. Lin, Y. Rodriguez, M. Kelliher, and Z. Liu.** 2000. The distinct roles of TRAF2 and RIP in IKK activation by TNF-R1: TRAF2 recruits IKK to TNF-R1 while RIP mediates IKK activation. Immunity **12:**419-429.
46. **Devin, A., Y. Lin, and Z. G. Liu.** 2003. The role of the death-domain kinase RIP in tumour-necrosis-factor-induced activation of mitogen-activated protein kinases. EMBO Rep **4:**623-627.
47. **Dinarello, C. A.** 1988. Biology of interleukin 1. FASEB J **2:**108-115.
48. **Dinarello, C. A.** 1998. Interleukin-1 beta, interleukin-18, and the interleukin-1 beta converting enzyme. Ann N Y Acad Sci **856:**1-11.
49. **Dinarello, C. A.** 2011. Interleukin-1 in the pathogenesis and treatment of inflammatory diseases. Blood **117:**3720-3732.
50. **Dinarello, C. A.** 2000. Proinflammatory cytokines. Chest **118:**503-508.
51. **Dinarello, C. A., and B. J. Pomerantz.** 2001. Proinflammatory cytokines in heart disease. Blood Purif **19:**314-321.
52. **Divangahi, M., M. Chen, H. Gan, D. Desjardins, T. T. Hickman, D. M. Lee, S. Fortune, S. M. Behar, and H. G. Remold.** 2009. Mycobacterium tuberculosis evades macrophage defenses by inhibiting plasma membrane repair. Nat Immunol **10:**899-906.
53. **Dockrell, D. H.** 2001. Apoptotic cell death in the pathogenesis of infectious diseases. J Infect **42:**227-234.
54. **Dostert, C., V. Petrilli, R. Van Bruggen, C. Steele, B. T. Mossman, and J. Tschopp.** 2008. Innate immune activation through Nalp3 inflammasome sensing of asbestos and silica. Science **320:**674-677.
55. **Duprez, L., E. Wirawan, T. Vanden Berghe, and P. Vandenabeele.** 2009. Major cell death pathways at a glance. Microbes Infect **11:**1050-1062.
56. **Fadok, V. A., D. L. Bratton, L. Guthrie, and P. M. Henson.** 2001. Differential effects of apoptotic versus lysed cells on macrophage production of cytokines: role of proteases. J Immunol **166:**6847-6854.
57. **Faherty, C. S., and A. T. Maurelli.** 2008. Staying alive: bacterial inhibition of apoptosis during infection. Trends Microbiol **16:**173-180.
58. **Fairbairn, I. P.** 2004. Macrophage apoptosis in host immunity to mycobacterial infections. Biochem Soc Trans **32:**496-498.
59. **Fantuzzi, G., A. J. Puren, M. W. Harding, D. J. Livingston, and C. A. Dinarello.** 1998. Interleukin-18 regulation of interferon gamma production and cell proliferation as

shown in interleukin-1beta-converting enzyme (caspase-1)-deficient mice. Blood **91:**2118-2125.

60. **Faustin, B., L. Lartigue, J. M. Bruey, F. Luciano, E. Sergienko, B. Bailly-Maitre, N. Volkmann, D. Hanein, I. Rouiller, and J. C. Reed.** 2007. Reconstituted NALP1 inflammasome reveals two-step mechanism of caspase-1 activation. Mol Cell **25:**713-724.
61. **Feldmann, J., A. M. Prieur, P. Quartier, P. Berquin, S. Certain, E. Cortis, D. Teillac-Hamel, A. Fischer, and G. de Saint Basile.** 2002. Chronic infantile neurological cutaneous and articular syndrome is caused by mutations in CIAS1, a gene highly expressed in polymorphonuclear cells and chondrocytes. Am J Hum Genet **71:**198-203.
62. **Feldmann, M., F. M. Brennan, and R. N. Maini.** 1996. Role of cytokines in rheumatoid arthritis. Annu Rev Immunol **14:**397-440.
63. **Festjens, N., S. Cornelis, M. Lamkanfi, and P. Vandenabeele.** 2006. Caspase-containing complexes in the regulation of cell death and inflammation. Biol Chem **387:**1005-1016.
64. **Festjens, N., T. Vanden Berghe, S. Cornelis, and P. Vandenabeele.** 2007. RIP1, a kinase on the crossroads of a cell's decision to live or die. Cell Death Differ **14:**400-410.
65. **Fink, S. L., and B. T. Cookson.** 2005. Apoptosis, pyroptosis, and necrosis: mechanistic description of dead and dying eukaryotic cells. Infect Immun **73:**1907-1916.
66. **Fink, S. L., and B. T. Cookson.** 2006. Caspase-1-dependent pore formation during pyroptosis leads to osmotic lysis of infected host macrophages. Cell Microbiol **8:**1812-1825.
67. **Franchi, L., A. Amer, M. Body-Malapel, T. D. Kanneganti, N. Ozoren, R. Jagirdar, N. Inohara, P. Vandenabeele, J. Bertin, A. Coyle, E. P. Grant, and G. Nunez.** 2006. Cytosolic flagellin requires Ipaf for activation of caspase-1 and interleukin 1beta in salmonella-infected macrophages. Nat Immunol **7:**576-582.
68. **Garcia, J. T., F. Ferracci, M. W. Jackson, S. S. Joseph, I. Pattis, L. R. Plano, W. Fischer, and G. V. Plano.** 2006. Measurement of effector protein injection by type III and type IV secretion systems by using a 13-residue phosphorylatable glycogen synthase kinase tag. Infect Immun **74:**5645-5657.
69. **Ge, Y., and Y. Rikihisa.** 2006. Anaplasma phagocytophilum delays spontaneous human neutrophil apoptosis by modulation of multiple apoptotic pathways. Cell Microbiol **8:**1406-1416.
70. **Gogos, C. A., E. Drosou, H. P. Bassaris, and A. Skoutelis.** 2000. Pro- versus anti-inflammatory cytokine profile in patients with severe sepsis: a marker for prognosis and future therapeutic options. J Infect Dis **181:**176-180.
71. **Gonzalez-Benitez, J. F., M. A. Juarez-Verdayes, S. Rodriguez-Martinez, M. E. Cancino-Diaz, F. Garcia-Vazquez, and J. C. Cancino-Diaz.** 2008. The NALP3/Cryopyrin-inflammasome complex is expressed in LPS-induced ocular inflammation. Mediators Inflamm **2008:**614345.
72. **Gracie, J. A., R. J. Forsey, W. L. Chan, A. Gilmour, B. P. Leung, M. R. Greer, K. Kennedy, R. Carter, X. Q. Wei, D. Xu, M. Field, A. Foulis, F. Y. Liew, and I. B. McInnes.** 1999. A proinflammatory role for IL-18 in rheumatoid arthritis. J Clin Invest **104:**1393-1401.
73. **Green, D. R., and H. M. Beere.** 2000. Apoptosis. Gone but not forgotten. Nature **405:**28-29.

74. **Greten, F. R., M. C. Arkan, J. Bollrath, L. C. Hsu, J. Goode, C. Miething, S. I. Goktuna, M. Neuenhahn, J. Fierer, S. Paxian, N. Van Rooijen, Y. Xu, T. O'Cain, B. B. Jaffee, D. H. Busch, J. Duyster, R. M. Schmid, L. Eckmann, and M. Karin.** 2007. NF-kappaB is a negative regulator of IL-1beta secretion as revealed by genetic and pharmacological inhibition of IKKbeta. Cell **130:**918-931.
75. **Griffin, W. S., L. C. Stanley, C. Ling, L. White, V. MacLeod, L. J. Perrot, C. L. White, 3rd, and C. Araoz.** 1989. Brain interleukin 1 and S-100 immunoreactivity are elevated in Down syndrome and Alzheimer disease. Proc Natl Acad Sci U S A **86:**7611-7615.
76. **Grobner, S., I. Adkins, S. Schulz, K. Richter, S. Borgmann, S. Wesselborg, K. Ruckdeschel, O. Micheau, and I. B. Autenrieth.** 2007. Catalytically active Yersinia outer protein P induces cleavage of RIP and caspase-8 at the level of the DISC independently of death receptors in dendritic cells. Apoptosis **12:**1813-1825.
77. **Grobner, S., S. E. Autenrieth, I. Soldanova, D. S. Gunst, M. Schaller, E. Bohn, S. Muller, M. Leverkus, S. Wesselborg, I. B. Autenrieth, and S. Borgmann.** 2006. Yersinia YopP-induced apoptotic cell death in murine dendritic cells is partially independent from action of caspases and exhibits necrosis-like features. Apoptosis **11:**1959-1968.
78. **Grobner, S., S. Schulz, I. Soldanova, D. S. Gunst, M. Waibel, S. Wesselborg, S. Borgmann, and I. B. Autenrieth.** 2007. Absence of Toll-like receptor 4 signaling results in delayed Yersinia enterocolitica YopP-induced cell death of dendritic cells. Infect Immun **75:**512-517.
79. **Gu, Y., K. Kuida, H. Tsutsui, G. Ku, K. Hsiao, M. A. Fleming, N. Hayashi, K. Higashino, H. Okamura, K. Nakanishi, M. Kurimoto, T. Tanimoto, R. A. Flavell, V. Sato, M. W. Harding, D. J. Livingston, and M. S. Su.** 1997. Activation of interferon-gamma inducing factor mediated by interleukin-1beta converting enzyme. Science **275:**206-209.
80. **Guarda, G., M. Braun, F. Staehli, A. Tardivel, C. Mattmann, I. Forster, M. Farlik, T. Decker, R. A. Du Pasquier, P. Romero, and J. Tschopp.** 2011. Type I interferon inhibits interleukin-1 production and inflammasome activation. Immunity **34:**213-223.
81. **Guinet, F., P. Ave, L. Jones, M. Huerre, and E. Carniel.** 2008. Defective innate cell response and lymph node infiltration specify Yersinia pestis infection. PLoS ONE **3:**e1688.
82. **Gurcel, L., L. Abrami, S. Girardin, J. Tschopp, and F. G. van der Goot.** 2006. Caspase-1 activation of lipid metabolic pathways in response to bacterial pore-forming toxins promotes cell survival. Cell **126:**1135-1145.
83. **Halle, A., V. Hornung, G. C. Petzold, C. R. Stewart, B. G. Monks, T. Reinheckel, K. A. Fitzgerald, E. Latz, K. J. Moore, and D. T. Golenbock.** 2008. The NALP3 inflammasome is involved in the innate immune response to amyloid-beta. Nat Immunol **9:**857-865.
84. **Hao, Y. H., Y. Wang, D. Burdette, S. Mukherjee, G. Keitany, E. Goldsmith, and K. Orth.** 2008. Structural requirements for Yersinia YopJ inhibition of MAP kinase pathways. PLoS ONE **3:**e1375.
85. **Harder, J., L. Franchi, R. Munoz-Planillo, J. H. Park, T. Reimer, and G. Nunez.** 2009. Activation of the Nlrp3 inflammasome by Streptococcus pyogenes requires

streptolysin O and NF-kappa B activation but proceeds independently of TLR signaling and P2X7 receptor. J Immunol **183:**5823-5829.

86. **Hilbi, H., J. E. Moss, D. Hersh, Y. Chen, J. Arondel, S. Banerjee, R. A. Flavell, J. Yuan, P. J. Sansonetti, and A. Zychlinsky.** 1998. Shigella-induced apoptosis is dependent on caspase-1 which binds to IpaB. J Biol Chem **273:**32895-32900.
87. **Hoffman, H. M., J. L. Mueller, D. H. Broide, A. A. Wanderer, and R. D. Kolodner.** 2001. Mutation of a new gene encoding a putative pyrin-like protein causes familial cold autoinflammatory syndrome and Muckle-Wells syndrome. Nat Genet **29:**301-305.
88. **Hofstra, C. L., I. Van Ark, G. Hofman, M. Kool, F. P. Nijkamp, and A. J. Van Oosterhout.** 1998. Prevention of Th2-like cell responses by coadministration of IL-12 and IL-18 is associated with inhibition of antigen-induced airway hyperresponsiveness, eosinophilia, and serum IgE levels. J Immunol **161:**5054-5060.
89. **Holler, N., R. Zaru, O. Micheau, M. Thome, A. Attinger, S. Valitutti, J. L. Bodmer, P. Schneider, B. Seed, and J. Tschopp.** 2000. Fas triggers an alternative, caspase-8-independent cell death pathway using the kinase RIP as effector molecule. Nat Immunol **1:**489-495.
90. **Hornung, V., F. Bauernfeind, A. Halle, E. O. Samstad, H. Kono, K. L. Rock, K. A. Fitzgerald, and E. Latz.** 2008. Silica crystals and aluminum salts activate the NALP3 inflammasome through phagosomal destabilization. Nat Immunol **9:**847-856.
91. **Howard, A. D., M. J. Kostura, N. Thornberry, G. J. Ding, G. Limjuco, J. Weidner, J. P. Salley, K. A. Hogquist, D. D. Chaplin, R. A. Mumford, and et al.** 1991. IL-1-converting enzyme requires aspartic acid residues for processing of the IL-1 beta precursor at two distinct sites and does not cleave 31-kDa IL-1 alpha. J Immunol **147:**2964-2969.
92. **Inglesby, T. V., D. T. Dennis, D. A. Henderson, J. G. Bartlett, M. S. Ascher, E. Eitzen, A. D. Fine, A. M. Friedlander, J. Hauer, J. F. Koerner, M. Layton, J. McDade, M. T. Osterholm, T. O'Toole, G. Parker, T. M. Perl, P. K. Russell, M. Schoch-Spana, and K. Tonat.** 2000. Plague as a biological weapon: medical and public health management. Working Group on Civilian Biodefense. JAMA **283:**2281-2290.
93. **Iyer, S. S., W. P. Pulskens, J. J. Sadler, L. M. Butter, G. J. Teske, T. K. Ulland, S. C. Eisenbarth, S. Florquin, R. A. Flavell, J. C. Leemans, and F. S. Sutterwala.** 2009. Necrotic cells trigger a sterile inflammatory response through the Nlrp3 inflammasome. Proc Natl Acad Sci U S A **106:**20388-20393.
94. **Jesenberger, V., K. J. Procyk, J. Yuan, S. Reipert, and M. Baccarini.** 2000. Salmonella-induced caspase-2 activation in macrophages: a novel mechanism in pathogen-mediated apoptosis. J Exp Med **192:**1035-1046.
95. **Jonas, D., I. Walev, T. Berger, M. Liebetrau, M. Palmer, and S. Bhakdi.** 1994. Novel path to apoptosis: small transmembrane pores created by staphylococcal alpha-toxin in T lymphocytes evoke internucleosomal DNA degradation. Infect Immun **62:**1304-1312.
96. **Jones, N. L., A. S. Day, H. Jennings, P. T. Shannon, E. Galindo-Mata, and P. M. Sherman.** 2002. Enhanced disease severity in Helicobacter pylori-infected mice deficient in Fas signaling. Infect Immun **70:**2591-2597.
97. **Jones, R. M., H. Wu, C. Wentworth, L. Luo, L. Collier-Hyams, and A. S. Neish.** 2008. Salmonella AvrA Coordinates Suppression of Host Immune and Apoptotic Defenses via JNK Pathway Blockade. Cell Host Microbe **3:**233-244.

98. **Kalai, M., G. Van Loo, T. Vanden Berghe, A. Meeus, W. Burm, X. Saelens, and P. Vandenabeele.** 2002. Tipping the balance between necrosis and apoptosis in human and murine cells treated with interferon and dsRNA. Cell Death Differ **9:**981-994.
99. **Kanaly, S. T., M. Nashleanas, B. Hondowicz, and P. Scott.** 1999. TNF receptor p55 is required for elimination of inflammatory cells following control of intracellular pathogens. J Immunol **163:**3883-3889.
100. **Kariko, K., H. Ni, J. Capodici, M. Lamphier, and D. Weissman.** 2004. mRNA is an endogenous ligand for Toll-like receptor 3. J Biol Chem **279:**12542-12550.
101. **Karin, M., Y. Yamamoto, and Q. M. Wang.** 2004. The IKK NF-kappa B system: a treasure trove for drug development. Nat Rev Drug Discov **3:**17-26.
102. **Keane, J., H. G. Remold, and H. Kornfeld.** 2000. Virulent Mycobacterium tuberculosis strains evade apoptosis of infected alveolar macrophages. J Immunol **164:**2016-2020.
103. **Keller, M., A. Ruegg, S. Werner, and H. D. Beer.** 2008. Active caspase-1 is a regulator of unconventional protein secretion. Cell **132:**818-831.
104. **Klune, J. R., R. Dhupar, J. Cardinal, T. R. Billiar, and A. Tsung.** 2008. HMGB1: endogenous danger signaling. Mol Med **14:**476-484.
105. **Labbe, K., and M. Saleh.** 2008. Cell death in the host response to infection. Cell Death Differ **15:**1339-1349.
106. **Lamkanfi, M., T. D. Kanneganti, P. Van Damme, T. Vanden Berghe, I. Vanoverberghe, J. Vandekerckhove, P. Vandenabeele, K. Gevaert, and G. Nunez.** 2008. Targeted peptidecentric proteomics reveals caspase-7 as a substrate of the caspase-1 inflammasomes. Mol Cell Proteomics **7:**2350-2363.
107. **Lathem, W. W., S. D. Crosby, V. L. Miller, and W. E. Goldman.** 2005. Progression of primary pneumonic plague: a mouse model of infection, pathology, and bacterial transcriptional activity. Proc Natl Acad Sci U S A **102:**17786-17791.
108. **Lee, H. C., and J. L. Goodman.** 2006. Anaplasma phagocytophilum causes global induction of antiapoptosis in human neutrophils. Genomics **88:**496-503.
109. **Lemaitre, N., F. Sebbane, D. Long, and B. J. Hinnebusch.** 2006. Yersinia pestis YopJ suppresses tumor necrosis factor alpha induction and contributes to apoptosis of immune cells in the lymph node but is not required for virulence in a rat model of bubonic plague. Infect Immun **74:**5126-5131.
110. **Li, B., and R. Yang.** 2008. Interaction between Yersinia pestis and the host immune system. Infect Immun **76:**1804-1811.
111. **Li, H., A. Ambade, and F. Re.** 2009. Cutting edge: Necrosis activates the NLRP3 inflammasome. J Immunol **183:**1528-1532.
112. **Li, P., H. Allen, S. Banerjee, S. Franklin, L. Herzog, C. Johnston, J. McDowell, M. Paskind, L. Rodman, J. Salfeld, and et al.** 1995. Mice deficient in IL-1 beta-converting enzyme are defective in production of mature IL-1 beta and resistant to endotoxic shock. Cell **80:**401-411.
113. **Lich, J. D., K. L. Williams, C. B. Moore, J. C. Arthur, B. K. Davis, D. J. Taxman, and J. P. Ting.** 2007. Monarch-1 suppresses non-canonical NF-kappaB activation and p52-dependent chemokine expression in monocytes. J Immunol **178:**1256-1260.
114. **Lilo, S., Y. Zheng, and J. B. Bliska.** 2008. Caspase-1 activation in macrophages infected with Yersinia pestis KIM requires the type III secretion system effector YopJ. Infect Immun.

115. **Lin, Y., A. Devin, Y. Rodriguez, and Z. G. Liu.** 1999. Cleavage of the death domain kinase RIP by caspase-8 prompts TNF-induced apoptosis. Genes Dev **13:**2514-2526.
116. **Lindner, I., J. Torruellas-Garcia, D. Kolonias, L. M. Carlson, K. A. Tolba, G. V. Plano, and K. P. Lee.** 2007. Modulation of dendritic cell differentiation and function by YopJ of Yersinia pestis. Eur J Immunol **37:**2450-2462.
117. **Lindsten, T., A. J. Ross, A. King, W. X. Zong, J. C. Rathmell, H. A. Shiels, E. Ulrich, K. G. Waymire, P. Mahar, K. Frauwirth, Y. Chen, M. Wei, V. M. Eng, D. M. Adelman, M. C. Simon, A. Ma, J. A. Golden, G. Evan, S. J. Korsmeyer, G. R. MacGregor, and C. B. Thompson.** 2000. The combined functions of proapoptotic Bcl-2 family members bak and bax are essential for normal development of multiple tissues. Mol Cell **6:**1389-1399.
118. **Lockman, H. A., and R. Curtiss, 3rd.** 1990. Salmonella typhimurium mutants lacking flagella or motility remain virulent in BALB/c mice. Infect Immun **58:**137-143.
119. **Lotze, M. T., and K. J. Tracey.** 2005. High-mobility group box 1 protein (HMGB1): nuclear weapon in the immune arsenal. Nat Rev Immunol **5:**331-342.
120. **Lukaszewski, R. A., D. J. Kenny, R. Taylor, D. G. Rees, M. G. Hartley, and P. C. Oyston.** 2005. Pathogenesis of Yersinia pestis infection in BALB/c mice: effects on host macrophages and neutrophils. Infect Immun **73:**7142-7150.
121. **Ma, Y., V. Temkin, H. Liu, and R. M. Pope.** 2005. NF-kappaB protects macrophages from lipopolysaccharide-induced cell death: the role of caspase 8 and receptor-interacting protein. J Biol Chem **280:**41827-41834.
122. **Maelfait, J., E. Vercammen, S. Janssens, P. Schotte, M. Haegman, S. Magez, and R. Beyaert.** 2008. Stimulation of Toll-like receptor 3 and 4 induces interleukin-1beta maturation by caspase-8. J Exp Med **205:**1967-1973.
123. **March, C. J., B. Mosley, A. Larsen, D. P. Cerretti, G. Braedt, V. Price, S. Gillis, C. S. Henney, S. R. Kronheim, K. Grabstein, and et al.** 1985. Cloning, sequence and expression of two distinct human interleukin-1 complementary DNAs. Nature **315:**641-647.
124. **Mariathasan, S., D. S. Weiss, V. M. Dixit, and D. M. Monack.** 2005. Innate immunity against Francisella tularensis is dependent on the ASC/caspase-1 axis. J Exp Med **202:**1043-1049.
125. **Mariathasan, S., D. S. Weiss, K. Newton, J. McBride, K. O'Rourke, M. Roose-Girma, W. P. Lee, Y. Weinrauch, D. M. Monack, and V. M. Dixit.** 2006. Cryopyrin activates the inflammasome in response to toxins and ATP. Nature **440:**228-232.
126. **Marketon, M. M., R. W. DePaolo, K. L. DeBord, B. Jabri, and O. Schneewind.** 2005. Plague bacteria target immune cells during infection. Science **309:**1739-1741.
127. **Martinon, F., K. Burns, and J. Tschopp.** 2002. The inflammasome: a molecular platform triggering activation of inflammatory caspases and processing of proIL-beta. Mol Cell **10:**417-426.
128. **Master, S. S., S. K. Rampini, A. S. Davis, C. Keller, S. Ehlers, B. Springer, G. S. Timmins, P. Sander, and V. Deretic.** 2008. Mycobacterium tuberculosis prevents inflammasome activation. Cell Host Microbe **3:**224-232.
129. **Mejia, E., J. B. Bliska, and G. I. Viboud.** 2008. Yersinia controls type III effector delivery into host cells by modulating Rho activity. PLoS Pathog **4:**e3.

130. **Miao, E. A., I. A. Leaf, P. M. Treuting, D. P. Mao, M. Dors, A. Sarkar, S. E. Warren, M. D. Wewers, and A. Aderem.** 2010. Caspase-1-induced pyroptosis is an innate immune effector mechanism against intracellular bacteria. Nat Immunol **11:**1136-1142.
131. **Micallef, M. J., T. Ohtsuki, K. Kohno, F. Tanabe, S. Ushio, M. Namba, T. Tanimoto, K. Torigoe, M. Fujii, M. Ikeda, S. Fukuda, and M. Kurimoto.** 1996. Interferon-gamma-inducing factor enhances T helper 1 cytokine production by stimulated human T cells: synergism with interleukin-12 for interferon-gamma production. Eur J Immunol **26:**1647-1651.
132. **Miggin, S. M., E. Palsson-McDermott, A. Dunne, C. Jefferies, E. Pinteaux, K. Banahan, C. Murphy, P. Moynagh, M. Yamamoto, S. Akira, N. Rothwell, D. Golenbock, K. A. Fitzgerald, and L. A. O'Neill.** 2007. NF-kappaB activation by the Toll-IL-1 receptor domain protein MyD88 adapter-like is regulated by caspase-1. Proc Natl Acad Sci U S A **104:**3372-3377.
133. **Mittal, R., S. Y. Peak-Chew, and H. T. McMahon.** 2006. Acetylation of MEK2 and I kappa B kinase (IKK) activation loop residues by YopJ inhibits signaling. Proc Natl Acad Sci U S A **103:**18574-18579.
134. **Molofsky, A. B., B. G. Byrne, N. N. Whitfield, C. A. Madigan, E. T. Fuse, K. Tateda, and M. S. Swanson.** 2006. Cytosolic recognition of flagellin by mouse macrophages restricts Legionella pneumophila infection. J Exp Med **203:**1093-1104.
135. **Monack, D. M., J. Mecsas, D. Bouley, and S. Falkow.** 1998. Yersinia-induced apoptosis in vivo aids in the establishment of a systemic infection of mice. J Exp Med **188:**2127-2137.
136. **Monteleone, G., F. Trapasso, T. Parrello, L. Biancone, A. Stella, R. Iuliano, F. Luzza, A. Fusco, and F. Pallone.** 1999. Bioactive IL-18 expression is up-regulated in Crohn's disease. J Immunol **163:**143-147.
137. **Mukherjee, S., Y. H. Hao, and K. Orth.** 2007. A newly discovered post-translational modification--the acetylation of serine and threonine residues. Trends Biochem Sci **32:**210-216.
138. **Mukherjee, S., G. Keitany, Y. Li, Y. Wang, H. L. Ball, E. J. Goldsmith, and K. Orth.** 2006. Yersinia YopJ acetylates and inhibits kinase activation by blocking phosphorylation. Science **312:**1211-1214.
139. **Nakajima, R., Y. Nakajima, and K. Ikeda.** 1993. Minimum alveolar concentration of sevoflurane in elderly patients. Br J Anaesth **70:**273-275.
140. **Netea, M. G., A. Simon, F. van de Veerdonk, B. J. Kullberg, J. W. Van der Meer, and L. A. Joosten.** 2010. IL-1beta processing in host defense: beyond the inflammasomes. PLoS Pathog **6:**e1000661.
141. **Newman, Z. L., S. H. Leppla, and M. Moayeri.** 2009. CA-074Me protection against anthrax lethal toxin. Infect Immun **77:**4327-4336.
142. **Niyonsaba, F., H. Ushio, I. Nagaoka, K. Okumura, and H. Ogawa.** 2005. The human beta-defensins (-1, -2, -3, -4) and cathelicidin LL-37 induce IL-18 secretion through p38 and ERK MAPK activation in primary human keratinocytes. J Immunol **175:**1776-1784.
143. **Okamura, H., H. Tsutsi, T. Komatsu, M. Yutsudo, A. Hakura, T. Tanimoto, K. Torigoe, T. Okura, Y. Nukada, K. Hattori, and et al.** 1995. Cloning of a new cytokine that induces IFN-gamma production by T cells. Nature **378:**88-91.
144. **Orth, K.** 2002. Function of the Yersinia effector YopJ. Curr Opin Microbiol **5:**38-43.

145. **Orth, K., Z. Xu, M. B. Mudgett, Z. Q. Bao, L. E. Palmer, J. B. Bliska, W. F. Mangel, B. Staskawicz, and J. E. Dixon.** 2000. Disruption of signaling by Yersinia effector YopJ, a ubiquitin-like protein protease. Science **290:**1594-1597.
146. **Paland, N., K. Rajalingam, N. Machuy, A. Szczepek, W. Wehrl, and T. Rudel.** 2006. NF-kappaB and inhibitor of apoptosis proteins are required for apoptosis resistance of epithelial cells persistently infected with Chlamydophila pneumoniae. Cell Microbiol **8:**1643-1655.
147. **Palmer, L. E., S. Hobbie, J. E. Galan, and J. B. Bliska.** 1998. YopJ of Yersinia pseudotuberculosis is required for the inhibition of macrophage TNF-alpha production and downregulation of the MAP kinases p38 and JNK. Mol Microbiol **27:**953-965.
148. **Palmer, L. E., A. R. Pancetti, S. Greenberg, and J. B. Bliska.** 1999. YopJ of Yersinia spp. is sufficient to cause downregulation of multiple mitogen-activated protein kinases in eukaryotic cells. Infect Immun **67:**708-716.
149. **Parent, M. A., K. N. Berggren, L. W. Kummer, L. B. Wilhelm, F. M. Szaba, I. K. Mullarky, and S. T. Smiley.** 2005. Cell-mediated protection against pulmonary Yersinia pestis infection. Infect Immun **73:**7304-7310.
150. **Pelegrin, P., and A. Surprenant.** 2006. Pannexin-1 mediates large pore formation and interleukin-1beta release by the ATP-gated P2X7 receptor. EMBO J **25:**5071-5082.
151. **Penzo, M., R. Molteni, T. Suda, S. Samaniego, A. Raucci, D. M. Habiel, F. Miller, H. P. Jiang, J. Li, R. Pardi, R. Palumbo, E. Olivotto, R. R. Kew, M. E. Bianchi, and K. B. Marcu.** 2010. Inhibitor of NF-kappa B kinases alpha and beta are both essential for high mobility group box 1-mediated chemotaxis [corrected]. J Immunol **184:**4497-4509.
152. **Perry, R. D., and J. D. Fetherston.** 1997. Yersinia pestis--etiologic agent of plague. Clin Microbiol Rev **10:**35-66.
153. **Peter, M. E., and P. H. Krammer.** 2003. The CD95(APO-1/Fas) DISC and beyond. Cell Death Differ **10:**26-35.
154. **Petrilli, V., S. Papin, C. Dostert, A. Mayor, F. Martinon, and J. Tschopp.** 2007. Activation of the NALP3 inflammasome is triggered by low intracellular potassium concentration. Cell Death Differ **14:**1583-1589.
155. **Pirbhai, M., F. Dong, Y. Zhong, K. Z. Pan, and G. Zhong.** 2006. The secreted protease factor CPAF is responsible for degrading pro-apoptotic BH3-only proteins in Chlamydia trachomatis-infected cells. J Biol Chem **281:**31495-31501.
156. **Porcelli, S. A., and W. R. Jacobs, Jr.** 2008. Tuberculosis: unsealing the apoptotic envelope. Nat Immunol **9:**1101-1102.
157. **Pujol, C., and J. B. Bliska.** 2003. The ability to replicate in macrophages is conserved between Yersinia pestis and Yersinia pseudotuberculosis. Infect Immun **71:**5892-5899.
158. **Pujol, C., J. P. Grabenstein, R. D. Perry, and J. B. Bliska.** 2005. Replication of Yersinia pestis in interferon gamma-activated macrophages requires ripA, a gene encoded in the pigmentation locus. Proc Natl Acad Sci U S A **102:**12909-12914.
159. **Pujol, C., K. A. Klein, G. A. Romanov, L. E. Palmer, C. Cirota, Z. Zhao, and J. B. Bliska.** 2009. Yersinia pestis can reside in autophagosomes and avoid xenophagy in murine macrophages by preventing vacuole acidification. Infect Immun **77:**2251-2261.
160. **Puren, A. J., G. Fantuzzi, Y. Gu, M. S. Su, and C. A. Dinarello.** 1998. Interleukin-18 (IFNgamma-inducing factor) induces IL-8 and IL-1beta via TNFalpha production from non-CD14+ human blood mononuclear cells. J Clin Invest **101:**711-721.

161. **Qu, Y., L. Ramachandra, S. Mohr, L. Franchi, C. V. Harding, G. Nunez, and G. R. Dubyak.** 2009. P2X7 receptor-stimulated secretion of MHC class II-containing exosomes requires the ASC/NLRP3 inflammasome but is independent of caspase-1. J Immunol **182:**5052-5062.
162. **Rajalingam, K., M. Sharma, N. Paland, R. Hurwitz, O. Thieck, M. Oswald, N. Machuy, and T. Rudel.** 2006. IAP-IAP complexes required for apoptosis resistance of C. trachomatis-infected cells. PLoS Pathog **2:**e114.
163. **Rambaldi, A., M. Torcia, S. Bettoni, E. Vannier, T. Barbui, A. R. Shaw, C. A. Dinarello, and F. Cozzolino.** 1991. Modulation of cell proliferation and cytokine production in acute myeloblastic leukemia by interleukin-1 receptor antagonist and lack of its expression by leukemic cells. Blood **78:**3248-3253.
164. **Raupach, B., S. K. Peuschel, D. M. Monack, and A. Zychlinsky.** 2006. Caspase-1-mediated activation of interleukin-1beta (IL-1beta) and IL-18 contributes to innate immune defenses against Salmonella enterica serovar Typhimurium infection. Infect Immun **74:**4922-4926.
165. **Riedl, S. J., and G. S. Salvesen.** 2007. The apoptosome: signalling platform of cell death. Nat Rev Mol Cell Biol **8:**405-413.
166. **Rosenstiel, P., K. Huse, A. Till, J. Hampe, S. Hellmig, C. Sina, S. Billmann, O. von Kampen, G. H. Waetzig, M. Platzer, D. Seegert, and S. Schreiber.** 2006. A short isoform of NOD2/CARD15, NOD2-S, is an endogenous inhibitor of NOD2/receptor-interacting protein kinase 2-induced signaling pathways. Proc Natl Acad Sci U S A **103:**3280-3285.
167. **Rubartelli, A., F. Cozzolino, M. Talio, and R. Sitia.** 1990. A novel secretory pathway for interleukin-1 beta, a protein lacking a signal sequence. EMBO J **9:**1503-1510.
168. **Ruckdeschel, K., J. Machold, A. Roggenkamp, S. Schubert, J. Pierre, R. Zumbihl, J. P. Liautard, J. Heesemann, and B. Rouot.** 1997. Yersinia enterocolitica promotes deactivation of macrophage mitogen-activated protein kinases extracellular signal-regulated kinase-1/2, p38, and c-Jun NH2-terminal kinase. Correlation with its inhibitory effect on tumor necrosis factor-alpha production. J Biol Chem **272:**15920-15927.
169. **Ruckdeschel, K., O. Mannel, K. Richter, C. A. Jacobi, K. Trulzsch, B. Rouot, and J. Heesemann.** 2001. Yersinia outer protein P of Yersinia enterocolitica simultaneously blocks the nuclear factor-kappa B pathway and exploits lipopolysaccharide signaling to trigger apoptosis in macrophages. J Immunol **166:**1823-1831.
170. **Ruckdeschel, K., O. Mannel, and P. Schrottner.** 2002. Divergence of apoptosis-inducing and preventing signals in bacteria-faced macrophages through myeloid differentiation factor 88 and IL-1 receptor-associated kinase members. J Immunol **168:**4601-4611.
171. **Ruckdeschel, K., G. Pfaffinger, R. Haase, A. Sing, H. Weighardt, G. Hacker, B. Holzmann, and J. Heesemann.** 2004. Signaling of apoptosis through TLRs critically involves toll/IL-1 receptor domain-containing adapter inducing IFN-beta, but not MyD88, in bacteria-infected murine macrophages. J Immunol **173:**3320-3328.
172. **Ruckdeschel, K., K. Richter, O. Mannel, and J. Heesemann.** 2001. Arginine-143 of Yersinia enterocolitica YopP crucially determines isotype-related NF-kappaB suppression and apoptosis induction in macrophages. Infect Immun **69:**7652-7662.

173. **Sansonetti, P. J., A. Phalipon, J. Arondel, K. Thirumalai, S. Banerjee, S. Akira, K. Takeda, and A. Zychlinsky.** 2000. Caspase-1 activation of IL-1beta and IL-18 are essential for Shigella flexneri-induced inflammation. Immunity **12:**581-590.
174. **Sauter, B., M. L. Albert, L. Francisco, M. Larsson, S. Somersan, and N. Bhardwaj.** 2000. Consequences of cell death: exposure to necrotic tumor cells, but not primary tissue cells or apoptotic cells, induces the maturation of immunostimulatory dendritic cells. J Exp Med **191:**423-434.
175. **Scaffidi, P., T. Misteli, and M. E. Bianchi.** 2002. Release of chromatin protein HMGB1 by necrotic cells triggers inflammation. Nature **418:**191-195.
176. **Schotte, P., G. Denecker, A. Van Den Broeke, P. Vandenabeele, G. R. Cornelis, and R. Beyaert.** 2004. Targeting Rac1 by the Yersinia effector protein YopE inhibits caspase-1-mediated maturation and release of interleukin-1beta. J Biol Chem **279:**25134-25142.
177. **Sebbane, F., D. Gardner, D. Long, B. B. Gowen, and B. J. Hinnebusch.** 2005. Kinetics of disease progression and host response in a rat model of bubonic plague. Am J Pathol **166:**1427-1439.
178. **Sha, Y., J. Zmijewski, Z. Xu, and E. Abraham.** 2008. HMGB1 develops enhanced proinflammatory activity by binding to cytokines. J Immunol **180:**2531-2537.
179. **Shahangian, A., E. K. Chow, X. Tian, J. R. Kang, A. Ghaffari, S. Y. Liu, J. A. Belperio, G. Cheng, and J. C. Deng.** 2009. Type I IFNs mediate development of postinfluenza bacterial pneumonia in mice. J Clin Invest **119:**1910-1920.
180. **Shao, F., P. O. Vacratsis, Z. Bao, K. E. Bowers, C. A. Fierke, and J. E. Dixon.** 2003. Biochemical characterization of the Yersinia YopT protease: cleavage site and recognition elements in Rho GTPases. Proc Natl Acad Sci U S A **100:**904-909.
181. **Shao, W., G. Yeretssian, K. Doiron, S. N. Hussain, and M. Saleh.** 2007. The caspase-1 digestome identifies the glycolysis pathway as a target during infection and septic shock. J Biol Chem **282:**36321-36329.
182. **Shin, H., and G. R. Cornelis.** 2007. Type III secretion translocation pores of Yersinia enterocolitica trigger maturation and release of pro-inflammatory IL-1beta. Cell Microbiol **9:**2893-2902.
183. **Silva, M. T.** 2010. Bacteria-induced phagocyte secondary necrosis as a pathogenicity mechanism. J Leukoc Biol **88:**885-896.
184. **Sjoholm, A.** 1998. Aspects of the involvement of interleukin-1 and nitric oxide in the pathogenesis of insulin-dependent diabetes mellitus. Cell Death Differ **5:**461-468.
185. **Sodeinde, O. A., A. K. Sample, R. R. Brubaker, and J. D. Goguen.** 1988. Plasminogen activator/coagulase gene of Yersinia pestis is responsible for degradation of plasmid-encoded outer membrane proteins. Infect Immun **56:**2749-2752.
186. **Stehlik, C., and A. Dorfleutner.** 2007. COPs and POPs: modulators of inflammasome activity. J Immunol **179:**7993-7998.
187. **Stehlik, C., M. Krajewska, K. Welsh, S. Krajewski, A. Godzik, and J. C. Reed.** 2003. The PAAD/PYRIN-only protein POP1/ASC2 is a modulator of ASC-mediated nuclear-factor-kappa B and pro-caspase-1 regulation. Biochem J **373:**101-113.
188. **Stoll, S., G. Muller, M. Kurimoto, J. Saloga, T. Tanimoto, H. Yamauchi, H. Okamura, J. Knop, and A. H. Enk.** 1997. Production of IL-18 (IFN-gamma-inducing factor) messenger RNA and functional protein by murine keratinocytes. J Immunol **159:**298-302.

189. **Sutterwala, F. S., Y. Ogura, M. Szczepanik, M. Lara-Tejero, G. S. Lichtenberger, E. P. Grant, J. Bertin, A. J. Coyle, J. E. Galan, P. W. Askenase, and R. A. Flavell.** 2006. Critical role for NALP3/CIAS1/Cryopyrin in innate and adaptive immunity through its regulation of caspase-1. Immunity **24:**317-327.
190. **Suzuki, T., L. Franchi, C. Toma, H. Ashida, M. Ogawa, Y. Yoshikawa, H. Mimuro, N. Inohara, C. Sasakawa, and G. Nunez.** 2007. Differential regulation of caspase-1 activation, pyroptosis, and autophagy via Ipaf and ASC in Shigella-infected macrophages. PLoS Pathog **3:**e111.
191. **Takeuchi, M., Y. Nishizaki, O. Sano, T. Ohta, M. Ikeda, and M. Kurimoto.** 1997. Immunohistochemical and immuno-electron-microscopic detection of interferon-gamma-inducing factor ("interleukin-18") in mouse intestinal epithelial cells. Cell Tissue Res **289:**499-503.
192. **Tao, H., W. Liu, B. N. Simmons, H. K. Harris, T. C. Cox, and M. A. Massiah.** 2010. Purifying natively folded proteins from inclusion bodies using sarkosyl, Triton X-100, and CHAPS. Biotechniques **48:**61-64.
193. **Thomas, L. R., A. Henson, J. C. Reed, F. R. Salsbury, and A. Thorburn.** 2004. Direct binding of Fas-associated death domain (FADD) to the tumor necrosis factor-related apoptosis-inducing ligand receptor DR5 is regulated by the death effector domain of FADD. J Biol Chem **279:**32780-32785.
194. **Ting, J. P., S. B. Willingham, and D. T. Bergstralh.** 2008. NLRs at the intersection of cell death and immunity. Nat Rev Immunol **8:**372-379.
195. **Tominaga, K., T. Yoshimoto, K. Torigoe, M. Kurimoto, K. Matsui, T. Hada, H. Okamura, and K. Nakanishi.** 2000. IL-12 synergizes with IL-18 or IL-1beta for IFN-gamma production from human T cells. Int Immunol **12:**151-160.
196. **Trosky, J. E., A. D. Liverman, and K. Orth.** 2008. Yersinia outer proteins: Yops. Cell Microbiol **10:**557-565.
197. **Tschopp, J., and K. Schroder.** 2010. NLRP3 inflammasome activation: The convergence of multiple signalling pathways on ROS production? Nat Rev Immunol **10:**210-215.
198. **Upton, J. W., W. J. Kaiser, and E. S. Mocarski.** Virus inhibition of RIP3-dependent necrosis. Cell Host Microbe **7:**302-313.
199. **van de Veerdonk, F. L., S. P. Smeekens, L. A. Joosten, B. J. Kullberg, C. A. Dinarello, J. W. van der Meer, and M. G. Netea.** 2010. Reactive oxygen species-independent activation of the IL-1beta inflammasome in cells from patients with chronic granulomatous disease. Proc Natl Acad Sci U S A **107:**3030-3033.
200. **van der Velden, A. W., M. Velasquez, and M. N. Starnbach.** 2003. Salmonella rapidly kill dendritic cells via a caspase-1-dependent mechanism. J Immunol **171:**6742-6749.
201. **van der Zee, E., V. Everts, and W. Beertsen.** 1997. Cytokines modulate routes of collagen breakdown. Review with special emphasis on mechanisms of collagen degradation in the periodontium and the burst hypothesis of periodontal disease progression. J Clin Periodontol **24:**297-305.
202. **van Dissel, J. T., P. van Langevelde, R. G. Westendorp, K. Kwappenberg, and M. Frolich.** 1998. Anti-inflammatory cytokine profile and mortality in febrile patients. Lancet **351:**950-953.

203. **Vanden Berghe, T., M. Kalai, G. Denecker, A. Meeus, X. Saelens, and P. Vandenabeele.** 2006. Necrosis is associated with IL-6 production but apoptosis is not. Cell Signal **18:**328-335.
204. **Vanden Berghe, T., G. van Loo, X. Saelens, M. Van Gurp, G. Brouckaert, M. Kalai, W. Declercq, and P. Vandenabeele.** 2004. Differential signaling to apoptotic and necrotic cell death by Fas-associated death domain protein FADD. J Biol Chem **279:**7925-7933.
205. **Vercammen, D., R. Beyaert, G. Denecker, V. Goossens, G. Van Loo, W. Declercq, J. Grooten, W. Fiers, and P. Vandenabeele.** 1998. Inhibition of caspases increases the sensitivity of L929 cells to necrosis mediated by tumor necrosis factor. J Exp Med **187:**1477-1485.
206. **Viboud, G. I., and J. B. Bliska.** 2005. Yersinia outer proteins: role in modulation of host cell signaling responses and pathogenesis. Annu Rev Microbiol **59:**69-89.
207. **Wang, S., M. Miura, Y. K. Jung, H. Zhu, E. Li, and J. Yuan.** 1998. Murine caspase-11, an ICE-interacting protease, is essential for the activation of ICE. Cell **92:**501-509.
208. **Watson, P. R., A. V. Gautier, S. M. Paulin, A. P. Bland, P. W. Jones, and T. S. Wallis.** 2000. Salmonella enterica serovars Typhimurium and Dublin can lyse macrophages by a mechanism distinct from apoptosis. Infect Immun **68:**3744-3747.
209. **Wei, M. C., W. X. Zong, E. H. Cheng, T. Lindsten, V. Panoutsakopoulou, A. J. Ross, K. A. Roth, G. R. MacGregor, C. B. Thompson, and S. J. Korsmeyer.** 2001. Proapoptotic BAX and BAK: a requisite gateway to mitochondrial dysfunction and death. Science **292:**727-730.
210. **Willingham, S. B., D. T. Bergstralh, W. O'Connor, A. C. Morrison, D. J. Taxman, J. A. Duncan, S. Barnoy, M. M. Venkatesan, R. A. Flavell, M. Deshmukh, H. M. Hoffman, and J. P. Ting.** 2007. Microbial pathogen-induced necrotic cell death mediated by the inflammasome components CIAS1/cryopyrin/NLRP3 and ASC. Cell Host Microbe **2:**147-159.
211. **Winau, F., S. Weber, S. Sad, J. de Diego, S. L. Hoops, B. Breiden, K. Sandhoff, V. Brinkmann, S. H. Kaufmann, and U. E. Schaible.** 2006. Apoptotic vesicles crossprime CD8 T cells and protect against tuberculosis. Immunity **24:**105-117.
212. **Wong, F. S., B. N. Dittel, and C. A. Janeway, Jr.** 1999. Transgenes and knockout mutations in animal models of type 1 diabetes and multiple sclerosis. Immunol Rev **169:**93-104.
213. **Yamamoto, M., K. Yaginuma, H. Tsutsui, J. Sagara, X. Guan, E. Seki, K. Yasuda, S. Akira, K. Nakanishi, T. Noda, and S. Taniguchi.** 2004. ASC is essential for LPS-induced activation of procaspase-1 independently of TLR-associated signal adaptor molecules. Genes Cells **9:**1055-1067.
214. **Yamashima, T., A. B. Tonchev, T. Tsukada, T. C. Saido, S. Imajoh-Ohmi, T. Momoi, and E. Kominami.** 2003. Sustained calpain activation associated with lysosomal rupture executes necrosis of the postischemic CA1 neurons in primates. Hippocampus **13:**791-800.
215. **Yoshimoto, T., H. Okamura, Y. I. Tagawa, Y. Iwakura, and K. Nakanishi.** 1997. Interleukin 18 together with interleukin 12 inhibits IgE production by induction of interferon-gamma production from activated B cells. Proc Natl Acad Sci U S A **94:**3948-3953.

216. **Yoshimoto, T., K. Takeda, T. Tanaka, K. Ohkusu, S. Kashiwamura, H. Okamura, S. Akira, and K. Nakanishi.** 1998. IL-12 up-regulates IL-18 receptor expression on T cells, Th1 cells, and B cells: synergism with IL-18 for IFN-gamma production. J Immunol **161:**3400-3407.
217. **Yrlid, U., and M. J. Wick.** 2000. Salmonella-induced apoptosis of infected macrophages results in presentation of a bacteria-encoded antigen after uptake by bystander dendritic cells. J Exp Med **191:**613-624.
218. **Zamboni, D. S., K. S. Kobayashi, T. Kohlsdorf, Y. Ogura, E. M. Long, R. E. Vance, K. Kuida, S. Mariathasan, V. M. Dixit, R. A. Flavell, W. F. Dietrich, and C. R. Roy.** 2006. The Birc1e cytosolic pattern-recognition receptor contributes to the detection and control of Legionella pneumophila infection. Nat Immunol **7:**318-325.
219. **Zauberman, A., S. Cohen, E. Mamroud, Y. Flashner, A. Tidhar, R. Ber, E. Elhanany, A. Shafferman, and B. Velan.** 2006. Interaction of Yersinia pestis with macrophages: limitations in YopJ-dependent apoptosis. Infect Immun **74:**3239-3250.
220. **Zauberman, A., A. Tidhar, Y. Levy, E. Bar-Haim, G. Halperin, Y. Flashner, S. Cohen, A. Shafferman, and E. Mamroud.** 2009. Yersinia pestis endowed with increased cytotoxicity is avirulent in a bubonic plague model and induces rapid protection against pneumonic plague. PLoS ONE **4:**e5938.
221. **Zhang, D. W., J. Shao, J. Lin, N. Zhang, B. J. Lu, S. C. Lin, M. Q. Dong, and J. Han.** 2009. RIP3, an energy metabolism regulator that switches TNF-induced cell death from apoptosis to necrosis. Science **325:**332-336.
222. **Zhang, Y., and J. B. Bliska.** 2005. Role of macrophage apoptosis in the pathogenesis of Yersinia. Curr Top Microbiol Immunol **289:**151-173.
223. **Zhang, Y., and J. B. Bliska.** 2003. Role of Toll-like receptor signaling in the apoptotic response of macrophages to Yersinia infection. Infect Immun **71:**1513-1519.
224. **Zhang, Y., J. Murtha, M. A. Roberts, R. M. Siegel, and J. B. Bliska.** 2008. Type III secretion decreases bacterial and host survival following phagocytosis of Yersinia pseudotuberculosis by macrophages. Infect Immun **76:**4299-4310.
225. **Zhang, Y., A. T. Ting, K. B. Marcu, and J. B. Bliska.** 2005. Inhibition of MAPK and NF-kappa B pathways is necessary for rapid apoptosis in macrophages infected with Yersinia. J Immunol **174:**7939-7949.
226. **Zheng, L., N. Bidere, D. Staudt, A. Cubre, J. Orenstein, F. K. Chan, and M. Lenardo.** 2006. Competitive control of independent programs of tumor necrosis factor receptor-induced cell death by TRADD and RIP1. Mol Cell Biol **26:**3505-3513.
227. **Zheng, Y., S. Lilo, I. E. Brodsky, Y. Zhang, R. Medzhitov, K. B. Marcu, and J. B. Bliska.** 2011. A Yersinia effector with enhanced inhibitory activity on the NF-kappaB pathway activates the NLRP3/ASC/caspase-1 inflammasome in macrophages. PLoS Pathog **7:**e1002026.
228. **Zhou, D., Y. Han, and R. Yang.** 2006. Molecular and physiological insights into plague transmission, virulence and etiology. Microbes Infect **8:**273-284.
229. **Zhou, R., A. Tardivel, B. Thorens, I. Choi, and J. Tschopp.** 2010. Thioredoxin-interacting protein links oxidative stress to inflammasome activation. Nat Immunol **11:**136-140.
230. **Zong, W. X., and C. B. Thompson.** 2006. Necrotic death as a cell fate. Genes Dev **20:**1-15.